2021

ELUCIDATING PEATLAND DISTURBANCE ECOLOGY AND CARBON DYNAMICS THROUGH THE LENS OF SOIL USING INFRARED SPECTROMETRY

Dominic Uhelski
Michigan Technological University, dmuhelsk@mtu.edu

ELUCIDATING PEATLAND DISTURBANCE ECOLOGY AND CARBON DYNAMICS THROUGH THE LENS OF SOIL USING INFRARED SPECTROMETRY

By

Dominic M. Uhelski

A DISSERTATION

Submitted in partial fulfillment of the requirements for the degree of

DOCTOR OF PHILOSOPHY

In Forest Science

MICHIGAN TECHNOLOGICAL UNIVERSITY

2021

This dissertation has been approved in partial fulfillment of the requirements for the Degree of DOCTOR OF PHILOSOPHY in Forest Science.

College of Forest Resources and Environmental Science

Dissertation Co-Advisor:	*Evan S. Kane*
Dissertation Co-Advisor:	*Rodney A. Chimner*
Committee Member:	*Andrew J. Burton*
Committee Member:	*Katherine Heckman*
Committee Member:	*Noel Urban*
College Dean:	*Andrew J. Storer*

Table of Contents

Author Contribution Statement

This body of work includes multi-authored papers in various stages of publishing. Details regarding publish status, copyright, and author contributions are detailed below for each chapter.

Chapter 1, *FTIR Spectrometry Estimates Pyrogenic Carbon Content of Peat Soils*, is in review for publication in the Soil Science Society of America Journal. The manuscript ID is S-2021-05-0159-OR.

Co-author contributions: Dominic Uhelski, Evan Kane, and Rod Chimner conceived and designed the study. Katherine Heckman provided advice on experimental design and expertise in FTIR spectrometry. Dominic Uhelski performed the experiments. Li Xie performed NMR experiments. Jessica Miesel analyzed NMR data. Dominic Uhelski analyzed the data, created figures, and wrote the manuscript; other authors provided editorial advice.

Acknowledgements

I want to thank my co-advisors, Evan Kane and Rod Chimner, for their constant support and guidance throughout my time as a graduate student at Michigan Tech. Thanks to my committee members, Katherine Heckman, Andrew Burton, and Noel Urban, for their service and valuable input. I thank the US Forest Service, for their funding and workspace, the Ecosystem Science Center, for their graduate research grant, and the Michigan Technological University graduate school, for their doctoral finishing fellowship award. Special thanks to the undergraduate research assistants for their help in the lab, particularly Andrew Robertson and Sam Kurkowski, without whom this research would not have been possible. Thanks to fellow graduate students, Sean Westley, Jennifer Klemm, Colleen Sutheimer, and Stefan Hupperts for companionship and assistance in the field.

Finally, I want to thank my partner, Sara Cloft, for her unconditional love, support, insights, and wits, and my family for their support, encouragement, and faith in me.

List of Abbreviations and Definitions

FTIR, Fourier-transform infra-red, a type of spectrometry

DRIFT, a method of diffuse reflectance FTIR spectrometry

^{13}C NMR, nuclear magnetic resonance spectrometry

DP, direct polarization, a method of NMR spectra acquisition

CPTOSS or CP, cross polarization (with total spinning sideband suppression), another method of NMR spectra acquisition

PyC, pyrogenic carbon, AKA char, charcoal, or black carbon

OM, organic matter

RMSE, root mean square error, a measure of model accuracy

PRESS, predicted residual sum of squared error, a measure of model predictive accuracy

VIF, variance inflation factor, a measure of multicollinearity

FF, fire frequency

LARCA, Long-term apparent rate of carbon accumulation

OPF, open poor fen, a peatland ecotype

TPF, treed poor fen, a peatland ecotype

FPF, forested poor fen, a peatland ecotype

FRF, forested rich fen, a peatland ecotype

Abstract

We sought to quantify the fire regimes of peatlands in the hemi-boreal zone of North America, and to understand the qualities of their peat. We used infrared spectrometry to accomplish both goals by gathering spectral information about the organic matter in each sample. We used a series of mixtures of natural peat and natural peat charcoal to isolate the spectral components associated with charcoal concentration. We built a multiple linear regression model which predicts the charcoal concentration in peat samples. We validated our data using nuclear magnetic resonance spectrometry. As a result, we can accurately predict the charcoal concentration of peat samples using only their infrared spectra. Applying this method, we analyzed the charcoal concentration throughout the peat profile in 29 sites in the hemi-boreal region of North America. These sites fell into four peatland ecotypes common in the hemi-boreal region, three types of poor fens, differing by tree cover, and forested rich fens. We found that the poor fen ecotypes had a mean fire return interval of 480 years, while the forested rich fens usually had no evidence of fire. We also found that fire frequency was negatively correlated with carbon accumulation in the poor fen ecotypes. These findings indicate that fire is a normal part of poor fen ecosystems but is rare in forested rich fens. Significant changes to these norms could have deleterious consequences for these ecosystems. We also performed analyses to compare the peat quality of these same ecotypes to one another. Peat quality refers to molecular lability. We were able to consider peat quality throughout each core. We identified that forested peatlands had more consistent, lower peat quality than open fens, which had high quality surface peat that declined in quality rapidly.

Overall open poor fens had the highest peat quality, followed by forested poor fens, and finally forested rich fens. This implies that open poor fens are more vulnerable to both short- and long-term disturbances to temperature or water levels. Our research contributes knowledge that equips ecologists, managers, and policy makers to better understand, plan for, and conserve peatlands in our changing world.

1 Dissertation Introduction

1.1 Overview

This dissertation is composed of 3 chapters concerning methods applicable to peatland research and characteristics of peatlands in the hemi-boreal region of North America. Chapter 1 describes novel method development for estimation of peat charcoal content through infrared spectrometry. Chapter 2 describes the application of this method to define historical fire occurrence in hemi-boreal North American peatlands and the associated long-term carbon cycle effects of peatland fire. Chapter 3 describes the peat chemical properties in hemi-boreal peatlands, elaborating on their trends with depth and across some of the ecotypes prevalent in this region.

1.2 Background

Fire is an important abiotic disturbance feature of virtually all terrestrial ecosystems. The frequency, intensity, and duration of fire are defining characteristics to which ecosystems and species adapt over varying timescales. These characteristics are encompassed by the term “fire regime.” Because ecosystems adapt to fire regimes, maintenance of this regime is a part of maintaining ecosystem resilience. However, peatland fire regimes are relatively understudied, and methods of determining aspects of fire regimes in peatlands are underdeveloped.

The fire frequency aspect of a fire regime can be determined by direct observation of fires on the landscape over time, historical accounts, or fire scar dendrochronology. These options are limited by the capacity to monitor landscapes, and the period of record

keeping provided by historical documents or tree relics. The nature of peatlands as wetland systems precludes these options due to long fire intervals, limited records, and lack of suitable tree species for dendrochronology. However, as carbon-accumulating systems, peatlands provide possibility of direct observation of evidence of past fires in the form of charcoal trapped within the peat profile. However, charcoal detection and isolation methods have been developed primarily for mineral soil ecosystems, and the high organic matter content of peat soil interferes with many of the more economical methods.

The typical method of charcoal detection in peat cores is optical microscopy and direct observation and counting of charcoal particles. This method is labor-intensive, as cores must be cut into thin slices and each one manually inspected. Studies utilizing this method are typically limited to between 1 to 5 peat cores, and/or are limited in depth considered. While this method also allows identification of additional properties, such as histological information relevant to the history of the neighboring or immediate ecosystems, the limitation on sample size reduces confidence and limits the development of peatland historical knowledge.

1.3 Research

We sought to free ourselves and our peers from the limitations imposed by the microscopic method by developing a new one. Chapter 1 describes the development of an infrared spectrometric method for estimating charcoal concentration in peat. Using this method, charcoal concentration can be estimated rapidly. We estimate that conservatively, each sample takes only 10 minutes of work to process from core to

completion, including cutting, determination of bulk density, grinding, determination of organic content, preparation for spectroscopy, and scanning. Of this processing time, only about 3 minutes are required per sample for spectroscopy only. The only requirements are the spectrometer and accessories, a balance, mortar and pestle for preparation, sample containers, and about ½ gram of potassium bromide (KBr) per sample. We paid about $0.64 per g of KBr. Ignoring equipment and validation costs associated with setting up the lab and verifying the model, and the minimal cost for sample containers, the marginal cost of each sample processed with infrared spectroscopy is $1.07, $0.32 for KBr and $0.75 for labor at $15 per hour.

Due to the efficiency of this method, we were able to analyze over 2,000 samples for char content for chapter 2. This allowed us to study 29 sites instead of the 1-5 typical for peatland fire history work. This makes chapter 2 a comprehensive analysis of peatland fire history in the hemi-boreal region. In combination with traditional bulk density, organic matter content, and radiocarbon data, we were also able to evaluate the net long-term effect of fire on carbon cycling.

While using spectrometry does not allow for histological identifications to be made, as traditional microscopy does, auxiliary data beyond the charcoal concentration can be derived from the infrared spectrum of each sample. This data formed the basis for chapter 3. Using spectral indices, we were able to extensively evaluate peat properties in 3 different peatland ecotypes throughout the depth profile.

1.4 Summary

Collectively, these 3 chapters each represent important steps forward in the understanding of peatland ecosystems. Chapter 1 paves the way for more plentiful and thorough fire history studies through the application of the method described there. Chapter 2 describes the fire history of 29 peatland sites in the hemi-boreal region and may be the most extensive single primary study of peatland fire history produced thus far. Furthermore, the effects of fire on peatland carbon services are quantified. Chapter 3 describes the peat properties in the same hemi-boreal peatland sites with a resolution and depth span that stand out in the field.

2 FTIR Spectrometry Estimates Pyrogenic Carbon Content of Peat Soils

2.1 Abstract

Quantifying historical patterns of fire regimes in peatlands can help contextualize current fire behavior and aid in planning on multiple scales. However, current methods for detecting the evidence of past fires in peat soils are laborious or expensive. Our goal was to develop an effective and inexpensive method for detecting pyrogenic carbon (PyC) concentration in peat, which could be used to estimate the occurrence of fires by analysis of discrete soil samples. We correlated Fourier-transform infrared spectrometry (FTIR) measurements of peat, and admixtures of peat and PyC to nuclear magnetic resonance spectrometry (NMR) estimates of PyC concentrations. Analyses of FTIR spectra isolated 15 unique spectral features within the peat matrices, of which 5 were statistically relevant to PyC detection. Models incorporating FTIR components reliably predicted peat sample PyC concentrations, and therefore could be used to detect the presence of past fire events within peat soil profiles with relatively low cost and time investment.

2.2 Introduction

Peatlands represent a globally significant carbon (C) stock containing 545 to 1055 Pg C (Nichols and Peteet, 2019). While these stores generally accumulate over long periods of time, changes in climate and disturbance regimes, including increases in the extent and severity of wildfires, threaten the stability of peatland C stocks (Turetsky et al., 2015; Goldstein et al., 2020). Wildfires are also important in structuring plant communities in peatlands and fires have been used as a management tool in these ecosystems (Farage et al., 2009). Despite the importance of fire in peatlands there is little information available due to the difficulties of discerning fire frequencies in peatlands (cf., Kasin et al., 2013). Therefore, a quick and affordable method of quantifying historical fire patterns in peatlands would be beneficial to expand the depth and scope of fire research in these ecosystems.

The basic method for discerning fire frequencies in peatlands is to identify the occurrence of pyrogenic carbon (PyC), also called char or black carbon (BC), in accumulated strata within a peat soil profile or nearby sediments (cf., Clark and Hussey, 1995). Pyrogenic C encompasses a range of organic compounds which range from barely altered organic matter to completely condensed graphitic carbon (Goldberg, 1985; Masiello, 2004). There are many techniques that have been used for identifying PyC, with varying degrees of specificity and resource requirements (Schmidt et al., 2001; Hammes et al., 2007). Organic soils offer a particular challenge in PyC detection because of chemical similarities between peat and the products of burning (Hedges et al., 2000), though some

chemo-oxidative methods such as the modified weak nitric acid and peroxide method and the dichromate oxidation + Soxhlet extraction methods have had success in isolating PyC in organic horizons (Kaal et al., 2007; Knicker et al., 2007; Hatten and Zabowski, 2009; Maestrini and Miesel, 2017). However, it is difficult to quantify artifacts from chemically and/or thermally oxidizing methods for PyC detection in organic matrices (Hammes et al., 2007), and time-consuming laboratory procedures with toxic or otherwise dangerous reagents are still required. Microscopy is often used in paleoecology to identify pollen and PyC particles in organic soils, but such studies are typically limited to only a few cores due to the time it takes to use this technique (Markgraf and Huber, 2010; Gałka et al., 2015; Crausbay et al., 2017). Microscopic methods have limited potential for analysis beyond evaluating particle morphology and color, neither of which are exclusive to, nor necessarily consistent in PyC (but see Crausbay et al., 2017). Nuclear magnetic resonance (NMR) spectrometry is a useful method for identifying and quantifying PyC in organic matrixes, such as peat (Baldock et al., 2004; Kaal et al., 2007; Ding and Rice, 2012; Leifeld et al., 2018). However, NMR is expensive and time-consuming, which greatly limits the number of samples that can be processed. Benzene polycarboxylic acid (BPCA) and hydrogen pyrolysis (hypy) both have potential to work in peat soils, but, like NMR and microscopy, have limited application due to long processing times (Cotrufo et al., 2016, and references within).

In contrast to these methods, Fourier-transform infra-red (FTIR) spectrometry is relatively inexpensive to run, does not involve caustic reagents or complex laboratory procedures and can have higher sample throughput. FTIR has been used to study a

variety of organic materials and processes including wood decay (Pandey and Pitman, 2003), soil organic matter (Chen et al., 2002; Demyan et al., 2012; Margenot et al., 2017; Matamala et al., 2017), peat decomposition, humification, and recalcitrance (Prasad et al., 2000; Artz et al., 2006, 2008; Hodgkins et al., 2018), pyrolysis (Guo and Bustin, 1998; Merino et al., 2015), and PyC in upland soils (Nocentini et al., 2010; Cotrufo et al., 2016; Hardy et al., 2017). FTIR was recently used to detect PyC in wetland lagoon sediments (Cadd et al., 2020), which has promise for employing this method in other matrices. Despite these advancements, to our knowledge FTIR has not yet been applied to identifying PyC in peat. In this study, we evaluated the efficacy of FTIR spectrometry to quantify admixtures of PyC generated in peatland wildfires and hemic and sapric peat, as validated with NMR spectrometry.

2.3 Methods

2.3.1 Admixture Preparation

We produced six sets of admixtures using three different sources of naturally produced PyC (to capture real-world PyC variability) and two peat sources representing shallow (recently living and senescent moss, 0-40 cm) and deep (humified peat, >40 cm) depth classes taken from *Sphagnum* peatlands. Both types of peat were composites made from *Sphagnum* peat of the appropriate depth. The surface peat was a composite of surficial *Sphagnum* that was harvested from peatlands in central Alberta (Bourgeau-Chavez et al., 2020). The deep peat was a composite of hemic to sapric *Sphagnum* peat that was

harvested from peatlands in the Upper Peninsula of Michigan (Chimner et al., 2014). We dried the peat samples at 60º C before grinding them in a Wiley mill. We then ground subsamples of the peat in a ball mill until the peat was pulverized. We acquired the three samples of naturally produced PyC from peat using forceps and a dissecting microscope to obtain material visually apparent as PyC from recent fire events. We did not further isolate the PyC. The three PyC samples come from evident char layers found in northwestern Canadian peatlands (Bourgeau-Chavez et al., 2020), Minnesota (Potvin et al., 2014), and Michigan (Bess and Chimner, 2014) peatland sites. We ground the PyC using a mortar and pestle and mixed it with the previously ball-milled peat to make admixture series with every combination of PyC and peat matrix. The admixture intervals were 0, 5, 15, 30, 50, 75, and 100% (visually) apparent PyC by mass fraction. We did not produce admixtures containing 75% PyC for the Canadian char due to lack of material. We did not duplicate endmembers of 0 or 100% PyC to avoid skewing the regression. Furthermore, we used 8 naturally occurring char layers from three different field sites in the Upper Peninsula of Michigan. The total number of samples we have is (2 peats (shallow, deep)) x (3 PyC sources) x (5 rates (5, 15, 30, 50, 75)) + (5 analyses, (2 for peat depths and 3 PyC) - (2 analyses for the two peats with no 75% PyC Canadian char) = 31 admixtures + 8 field samples = n = 41.

We analyzed all 3 natural char endmembers and 6 of the additional naturally occurring char layers for C, H, N, and O using a Costech 4010 Elemental Analyzer calibrated to atropine standard. Only 6 of the 8 natural char layer samples had sufficient sample mass for elemental analysis. The values presented reflect the elemental composition of these

samples as mixtures of char and peat. The elemental composition is intermediate between condensed hydrocarbon and lignin-like biomolecules (Kim et al., 2003), which reflects the products of smoldering combustion in a peat matrix (Figure 1). These values are similar to those of macroscopic char particles found in the mineral/organic soil interface of boreal spruce forest sites in interior Alaska (Kane et al., 2007).

2.3.2 FTIR Spectra Handling

We prepared all samples for FTIR by mixing with FTIR-grade KBr to 10% sample by mass. We mixed samples using a small agate mortar and pestle to further break down the KBr crystals and mix them with the sample. We dried samples at 60º C for >24 hours before subjecting them to diffuse reflectance FTIR (DRIFT) using a Thermo Scientific Nicolet iS5 spectrometer, equipped with a standard fast recovery deuterated triglycine sulfate (DTGS) detector, and an iD Foundation – Diffuse accessory (Thermo Fisher Scientific, Ann Arbor, MI). We chose the DRIFT method due to the ease of sample preparation and its effectiveness on heterogenous samples such as peat (Niemeyer et al., 1992). The DRIFT method allows the beam to contact more of the sample than attenuated total reflectance (ATR), which is beneficial for increasing the probability of detecting PyC particles. We produced spectra of the 4000-400 cm^{-1} range with resolution of 4 cm^{-1} and a data interval of 0.5 cm^{-1} by averaging 64 scans. We used ultrapure N_2 purge to further reduce the interference of humidity and to improve spectral fidelity. Automatic background correction built into the software further eliminated remaining atmospheric effects. We acquired background spectra by scanning KBr blank samples, at least once

every two hours when running samples to account for changing atmospheric ([CO_2], relative humidity) conditions.

We used custom code written in Python to baseline correct and standardize the spectra to compare relative peak areas, rather than absolute data, which was variable due to sample properties, dilution factors, and atmospheric conditions during testing. Recognizing that peaks often overlap, we used the peak fitting function in Origin (Origin 2019b 64-bit, OriginLab Corporation, Northampton, MA) to condense the volume of data per sample by fitting 15 gaussian peaks to the spectral features, summarizing those peak areas for use in modeling. This is an elaboration of the peak derivative measurement methods used by Pandey and Pitman (2003). Whereas that method measures peaks by drawing a line connecting the "bottom" sides of each peak and integrating the area between the line and the peak, in contrast, peak fitting allows overlapping of peaks. Identification of overlapping peaks has been identified as particularly important (see Heller et al., 2015) in the densely packed "fingerprint region" of the spectra (850-1875 cm^{-1}). Peak fitting also reduces the number of factors that must be considered in model building, allowing more parsimonious statistical methods to be used.

Peak fitting has been used to good effect for FTIR in multiple applications (Zhang et al., 2013; Gaffney et al., 2015; Belton et al., 2018; Gardegaront et al., 2018; Sadat and Joye, 2020). Reggente et al. (2019) have also shown excellent agreement between peak fitting and partial least squares models for FTIR data on atmospheric aerosols. We achieved stability by carefully controlling both the number of peaks to fit and the allowed range of variation in peak location, area, and width. This limitation ensured repeatability and

stability but sacrificed perfect line fitting in the region between 3800 and 2000 cm^{-1} where the shape of the spectrum was skewed with few distinct peaks (Figure 2). The 3 peak areas fitted in the 3800 to 2000 cm^{-1} region correlated well with their respective peak heights, despite the imperfect line fitting.

2.3.3 NMR

We used NMR data to ensure accurate PyC estimates for model fitting and to validate our FTIR models. The molecular mixing model developed by Baldock et al. (2004) is a widely accepted method of PyC quantification based on NMR spectrometry (Miesel et al., 2015; Leifeld et al., 2018). We selected the three "pure" char and two "pure" peat admixture endmembers, and a series of 8 putative no char to putative high char unknown samples taken from 3 peat cores harvested from peatlands in the Upper Peninsula of Michigan for NMR analysis. In reality, all 8 unknown samples were determined by NMR to contain some amount of naturally produced char. ^{13}C solid state NMR experiments were performed on a Varian Infinity-Plus NMR spectrometer equipped with a 6 mm MAS broadband probe operating at 399.75 MHz for ^{1}H to determine the mass fraction of each sample that was composed of PyC. For each sample, both cross polarization with total sideband suppression (CPTOSS, or CP for brevity) and direct polarization (DP) were acquired under 6 kHz magic angle spinning. The CPTOSS data were acquired with 16,000 scans and a recycle delay of 3 s while the DP data were acquired with 3000 scans and a recycle delay of 100 s using a standard one-pulse experiment with ^{1}H decoupling during acquisition. All data were processed with a 100 Hz Gaussian line broadening and

baseline correction. The ^{13}C chemical shifts were referenced against an external standard of adamantane. Background signal subtraction was performed to remove the signal from the rotor for the DP spectra (there was no background signal from the rotor for the CPTOSS spectra). We determined total organic C and total N content via dry combustion on an elemental analyzer (EHS 4010 gas chromatograph, Costech, Valencia, CA). The NMR spectra and C and N results were used to calculate the composition of each sample using the modified Baldock molecular mixing model (Baldock et al., 2004). The output of this regression includes a char (PyC) fraction, which we used to validate the accuracy of our model estimates. The admixture PyC contents were corrected based on the original mixing ratio and the NMR-determined PyC contents of the admixture endmembers.

The direct polarization NMR method requires long recycle delays due to the slow relaxation of ^{13}C, as opposed to the CPTOSS method which uses a much shorter recycle delay since the relaxation is dependent on ^{1}H and the relaxation time of ^{1}H is much shorter than that of ^{13}C (Mao et al., 2000). Another advantage of CPTOSS over DP is that the ^{13}C signals in CPTOSS are enhanced by ^{1}H via ^{1}H-^{13}C dipolar couplings and the enhancement is different for each ^{13}C since the dipolar coupling is different for each ^{13}C, as a result, the ^{13}C signals in CPTOSS are not quantitative (Smernik et al., 2002a). As opposed to CPTOSS, DP is a more quantitative method to detect the more condensed PyC, routinely detecting >90% of PyC (Skjemstad et al., 1999; Baldock and Smernik, 2002; Smernik et al., 2002b). Both the CPTOSS and DP methods have been employed to produce different perspectives on the continuum of PyC, with CPTOSS measurements

being considered representative of less condensed material and DP measurements representative of more condensed material (Kane et al., 2010). To facilitate this potential use, we evaluated the correlations of both methods to our FTIR data through independent models.

2.3.4 Model Building

Initial modeling attempts indicated heteroscedasticity within the data, so a base 10 logarithmic transformation was applied to our known PyC values given by NMR. Using the NMR-validated PyC contents for our 33 admixtures and 8 field samples, (n=41), six final models were fit to all combinations of conditions, predicting both DP and CP NMR estimates, and integrating either all matrices, only surface peat matrices (depth interval 0-40 cm, n=18, surface admixtures only), or only deep peat matrices (depths > 40 cm, n=26, deep admixtures + field samples). We first evaluated a partial least squares regression (PLSR) approach for FTIR peak assessments, as was used in a similar approach for mineral soils (Sanderman et al., 2020), but determined that the limitations of sample size imposed by the expense of NMR spectrometry made PLSR unsuitable. Future work to increase sample size to be suitable for PLSR could yield a more broadly applicable model. Instead, we used mixed direction, stepwise parameter selection in JMP (JMP Pro 14, *SAS,* Cary, NC), to determine the peaks of greatest importance to predicting PyC. The selected parameters were fit to the data using standard least squares regression. We used variance inflation factors (VIFS) to eliminate parameters that exhibited multicollinearity. We used PRESS statistics to evaluate a model's suitability for

prediction by testing the model accuracy using leave-one-out cross-validation. Having PRESS values similar to their corresponding normal values indicates the model is not overfit to the training data.

2.4 Results

2.4.1 Correlation between FTIR and both DP and CP NMR methods

While some characteristics (R^2, RMSE, PRESS RMSE) of the depth-specific models were in some cases better than the generalized models, their slopes were similar (Table 1 and Figure 3). We therefore focused on the two overall models correlating FTIR spectra with NMR measures of peat PyC content, one for DP NMR, and one for CP NMR. Using overall models also removes the need to differentiate between deep and surface peat, a boundary that can be difficult to locate in practice, simplifying future application. The overall DP predicting model had similar or better PRESS values to depth-specific models predicting DP; given the difference in matrix composition this is remarkable (Table 1). In comparison, the CP predicting overall model was similar in PRESS statistics to the deep peat-specific model but explained less of the variance than the surface peat-specific model (Table 1).

DP NMR measures were consistently higher than CP NMR measures of PyC, which is reflected by the difference in model slopes between the two (Table 1 and Figures 3 and 4). Both DP and CP models tended to overestimate PyC when PyC concentration was

low and underestimate it when PyC concentration was high (Figure 4). The DP model positively correlated PyC mass fraction with peak 12 (mean peak location ± standard deviation) (1720 cm^{-1} ± <0.01) and peak 3 (1160 cm^{-1} ± 1). These peaks are associated with a wide variety of organic moieties, notably for peak 3, aromatics, and for peak 12, anhydrides (Table 2). The DP model negatively correlated PyC mass fraction with three other peaks, peak 14 (2921 ± 2), peak 7 (1381 ± 0.02), and peak 4 (1229 ± 2.77 cm^{-1}). These peaks correlated with other, mostly non-aromatic organic moieties not strongly associated with PyC (Table 2). The predictive equation for this model is presented in equation 1:

[1]

$$Y = 0.0009601 + P3 * 0.0184174 - P4 * 0.002144676 - P7 * 0.02146913 + P12 * 0.0124995933 - P14 * 0.007019469$$

The CP model positively correlated PyC mass fraction with the same two peaks, 12 (1720 cm^{-1} ± <0.01) and 3 (1160 cm^{-1} ± 1), which are associated with a wide variety of organic moieties, notably for peak 3, aromatics, and for peak 12, anhydrides (Table 2). It negatively correlated PyC mass fraction with two other peaks, peak 4 (1229 ± 2.77 cm^{-1}) and peak 7 (1381 ± 0.02 cm^{-1}). These peaks were related to other, mostly non-aromatic organic moieties not strongly associated with PyC (Table 2). The predictive model for this is reflected in equation 2:

[2]

$$Y = 0.775340741 + P3 * 0.0279113645 - P4 * 0.003161707 - P7 * 0.022494595 + P12 * 0.007968334$$

In both equations 1 and 2, predicted sample PyC mass percent equals 10^{Y+1}, and PX refers to the area under the peak with the given identification number.

2.5 Discussion

2.5.1 Model Components

We determined that FTIR can be used to make useful predictions of the PyC content of peat soil. The aromatic structures of char may not interact as strongly with infrared light as other, more polar, non-char moieties, but we were still able to predict the char content of peat samples with accuracy (Table 1). Ultimately, model associations were chosen statistically rather than *a priori* based on their actual correlation in our sample set with the PyC concentrations of 11 different naturally produced peatland chars.

Both the DP and CP models correlated positively with peaks 3 and 12. Peak 3 is associated with C-O and R-O-R bonds (Skoog, 2014), and -C-OH bonds (Niemeyer et al., 1992), though contributions may also come from aromatic moieties (Colthup, 1950), which are common in PyC. Colthup (1950) associates the region around peak 12 with anhydrides, a class of molecules which can be formed through pyrolysis of cellulose and hemicellulose (Simoneit et al., 1999; Nolte et al., 2001). Another possibility is that the peak 12 signal represents aged PyC, which becomes "enriched in oxygen-containing functional groups such as carboxylic acid, **esters, aldehydes and ketones**," [emphasis added] eventually causing reversion of PyC to humic OM or mineralization (Preston and Schmidt, 2006). The latter three moieties are all represented under peak 12, and could

explain its strong relationship to PyC, particularly to aged PyC. Whether this results in overrepresentation of PyC that is older or was more oxidized is unclear and warrants further study.

Both models negatively correlated PyC with peaks representing more common moieties, particularly alkanes. The negative relationship of our models with alkanes and other uncondensed moieties likely has less to do with these moieties being unable to coexist with PyC, and more to do with the fact that the predictions are measured in mass fraction. Therefore, any increase in the mass percent contribution from other moieties must result in a decrease in percent PyC. These other moieties represent other constituents of peat, with which PyC, if present, must share space, including aliphatics, lignin, cellulose, and others. Comparison of our PyC – component relationships to those of a similar study investigating lagoon sediments (Cadd et al., 2020) show little agreement. These differences could be explained by differences in site characteristics; their site was an emergent marsh which introduces differences in fuels and burn characteristics. Moreover, the sediment matrix for their study was mineral lacustrine deposits, which could change the spectral representation of the components relative to PyC.

2.5.2 Model Application

For determination of historical fire regimes of peat soil profiles, the FTIR method must be applied to small enough depth intervals to capture PyC layers with minimal dilution by unaltered peat. Changes in the patterns of burning with fuel type (surficial vegetation vs. peat burning) or wildfire intensity may not produce a detectable PyC layer, either due to

most C being combusted rather than pyrolyzed, or due to little C being affected. Such a scenario is unlikely in a peat wildfire but may be possible in a vegetation fire where fuel can be finer and drier, and thus more susceptible to flaming vs. smoldering. The threshold for detectability largely depends on the thickness of each sample and the calibration of the model. Layers of PyC may overlap one another, or an antecedent layer could be consumed by one or more succeeding fires, so estimates of fire regimes must consider these complications. Moreover, in wetlands with lateral flow (such as fens), recent PyC may simply be translocated (cf., Masiello and Berhe, 2020), but this is less likely in more ombrotrophic peatlands. We suggest that PyC layers could be distinguished when a spike in predicted PyC exists within the profile, where the lower prediction interval(s) of the sample(s) composing the spike deviate from a baseline minimum PyC content determined by the researchers. Layers of PyC may bridge multiple samples in a vertical sequence if the sampling increment is thick enough or if there is vertical movement of PyC, so we recommend that spikes in the profile be counted rather than individual samples within the spike with significant PyC, to avoid overestimating fire occurrence. Using these methods and keeping in mind these considerations should help produce conservative minimum fire return intervals for a given peat profile. These techniques in combination with radiocarbon dating should be useful tools in deriving minimum fire frequencies or maximum average fire return intervals in peatlands.

2.5.3 Model Limitations

While the models shown here show promise for evaluating the fire histories of peatlands, they were fit to a limited range of real PyC contents, so samples exceeding this range may not be accurately predicted by the models. Notwithstanding, we highlight here that our models identified natural PyC with likely variable burn conditions and time since fire, which suggests our models are robust within this ecosystem type. We chose this approach over one including "pure" graphitic PyC because this would not be representative of natural chars, particularly in peatlands. We fit our models on peat representative of *Sphagnum*-dominated northern peatlands, so different peat sources (and changes in burn conditions) may reduce the accuracy of the model in other ecosystems. However, the peaks used in each model are related to moieties present in a broad range of peat types (cf., Hodgkins et al., 2018), suggesting our models may be broadly applicable within this ecosystem type. Applying this model would require accepting the assumptions that the peat and char being measured fall within the range of variation of the samples used to fit this model. In which case, the PRESS statistics for the models would give the best indication of the appropriate level of certainty. Therefore, we recommend validation measures be taken for individual studies, particularly on peats that are significantly different, such as those from tropical peatlands. We invite further study of this method to validate the method and broaden the peat, char, and instrumental datasets available to the research community.

2.6 Conclusion

Fourier-transform infra-red spectrometry has shown to be an effective and relatively inexpensive method for detecting char in peat soils. We suggest this method can be used to detect the presence of past fire events in discrete samples within a peat soil profile. This enables researchers and land managers to interpret peatland-specific fire history data, something previously not possible without great investment. We suggest that the procedures and equations provided herein are broadly suitable for northern poor-fen or bog ecosystems but recommend calibration for other ecosystems (such as those with different parent materials or climates).

2.7 Acknowledgments

We acknowledge support and funding received from the USDA Forest Service, Hiawatha National Forest, and in-kind support from the USDA Forest Service, Northern Research Station. Funding from the National Institute of Food and Agriculture, USDA, McIntire-Stennis program, Michigan Tech graduate school, and the Ecosystem Science Center (Michigan Tech) also supported this study.

2.8 Conflict of Interest

The authors declare no conflict of interest.

2.9 Tables and Figures

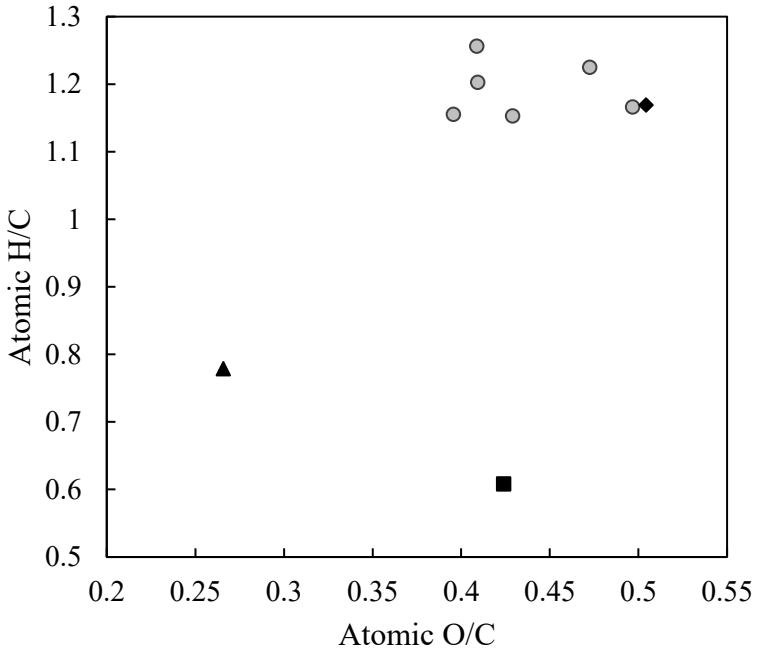

Figure 1. The van Krevelen diagram of 9 of the 11 total natural char samples used to fit our models. Gray circles are natural char layers, the black symbols represent the three char endmembers used in making the admixtures. The diamond is the Michigan char, the triangle is the Minnesota char, and the square is the Canadian char.

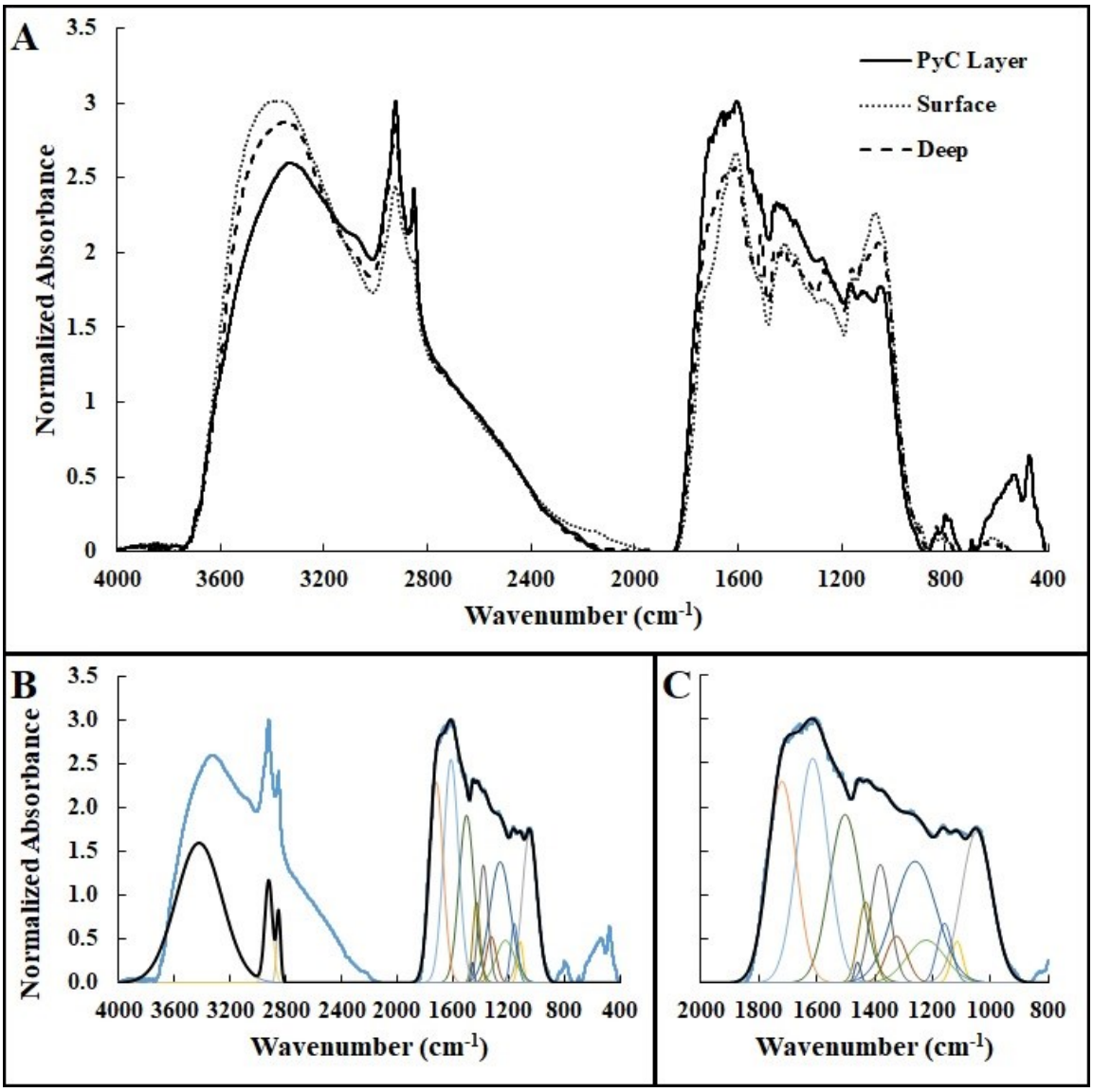

Figure 2. Plot A shows the FTIR spectra of three prototypical samples. The PyC layer is from the Sleeper Lake peatland fire in Michigan, USA. The surface and deep samples are without added PyC; their origins are explained in the admixture preparation subsection of the methods. Plots B and C show the peak fitting results for the PyC sample. Plot B shows the whole spectrum. Plot C shows a detail view of the fingerprint region. In both B

and C, the blue line is the original spectrum and the black line is the best fit line built by summing the values of all gaussian peaks (colored peaks) fitted to the original.

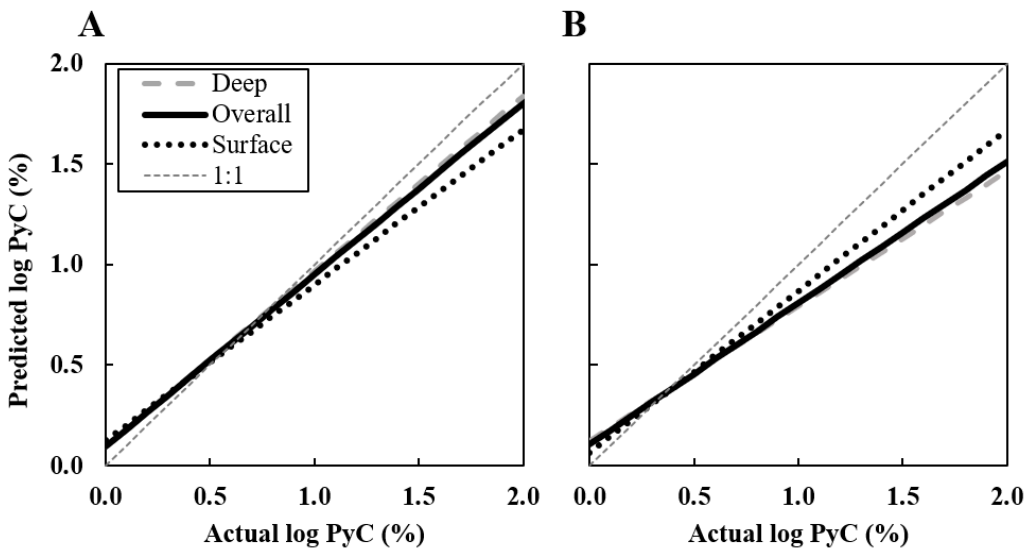

Figure 3. Plots showing the predicted vs. actual slopes of all models on the log scale, with 1:1 (y = x) line in dotted gray line, for direct polarization (A) and cross polarization (B) models. Model statistics are as presented in Table 1.

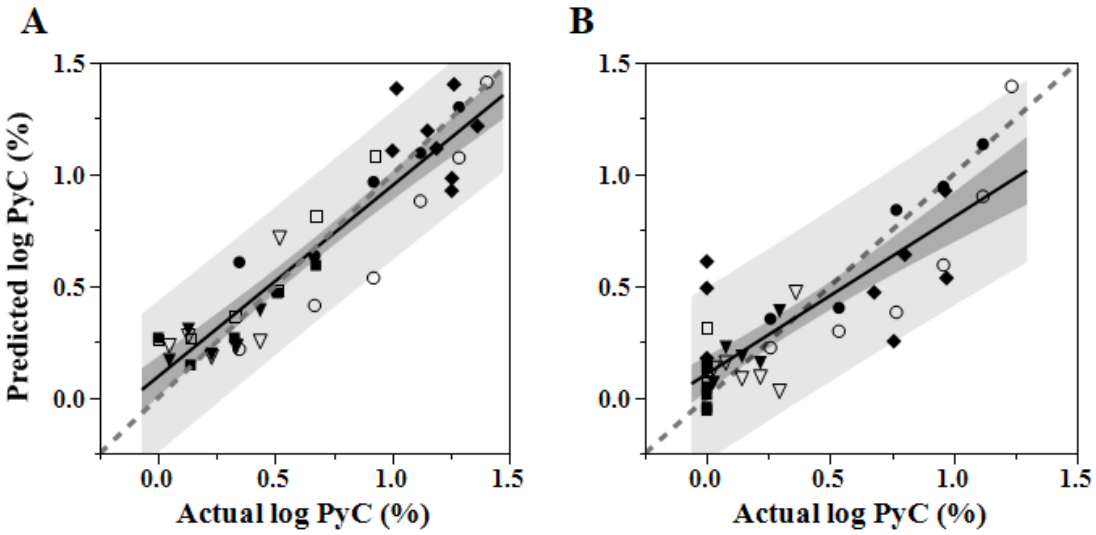

Figure 4. A plot showing the predicted v. actual values for the overall direct polarization (A) and overall cross polarization (B) models. Depicted are sample points, mean (solid black line), confidence interval (dark gray zone), prediction interval (light gray zone), and 1:1 (y = x) line (dotted gray line). Filled symbols are deep samples, open symbols are surface samples. Squares are Canadian char admixtures, triangles are Minnesota char admixtures, circles are Michigan char admixtures, and diamonds are NMR-validated natural char layers.

Table 1. Summary data for direct polarization and cross polarization models incorporating different depth intervals (0-40 cm, > 40 cm). The models predict the mass percent of PyC in a sample on the log 10 scale, therefore RMSE values are given in the log 10 transformed scale. Bolded rows indicate the overall models that are the focus of analysis.

MODEL DATA		STANDARD TERMS					PRESS STATS	
Matrix	Predicting	n	Slope	R2	Adj. R2	RMSE	PRESS RMSE	PRESS R2
Overall	**DP**	**41**	**0.85**	**0.855**	**0.834**	**0.185**	**0.209**	**0.781**
Surface	DP	18	0.773	0.773	0.743	0.215	0.241	0.658
Deep	DP	26	0.873	0.883	0.861	0.173	0.199	0.808
Overall	**CP**	**41**	**0.7**	**0.703**	**0.669**	**0.233**	**0.259**	**0.583**
Surface	CP	18	0.804	0.804	0.778	0.196	0.204	0.745
Deep	CP	26	0.672	0.725	0.673	0.243	0.280	0.548

Table 2. Depicted are the roster of peaks fit to each sample spectrum, their identifier (Peak), wavenumber (WN), associated moieties and bonds, according to (Colthup, 1950; Sekiguchi et al., 1983; Niemeyer et al., 1992; Cocozza et al., 2003; Skoog, 2014), and how they were considered by models fit for both DP and CP estimations. Superscripts indicate bonds and moieties supported by Niemeyer et al., 1992 (1) and Cocozza et al., 2003 (2), which concern themselves specifically with peat samples. Gray cells indicate when a peak was used as a parameter in an overall model. P values and LogWorths are indicated in the context of the overall models. Relationships between peaks not included in the model selection procedure and sample PyC concentrations are available in supplemental materials.

Peak	Peak WN (cm^{-1})	Relation w/ PyC (DP)	Relation w/ PyC (CP)	P value (Log Worth) (DP)	P value (Log Worth) (CP)	Associated Moieties	Associated Bonds
1	1054 ± 1.84	0	0			Aromatics, Ethyl & propyl alkanes, Primary alcohols, Aliphatic aldehydes, Polysaccharides[2]	C-C, C-O[2], C-N,
2	1116 ± 1.29	0	0			Aromatics, Anhydrides, Isopropyl alkanes, Aliphatic ethers, Secondary alcohols, Amides, Amines, Benzoate / phyhalate esters	C-C, C-O, C-N,
3	1160 ± 0.94	+	+	0.0016 (2.796)	<0.0001 (5.959)	Aromatics, Aliphatics[1], Amides, Amines, Esters, Ketones, Iso-propyl and Tertiary butyl alkanes	C-C, C-O, C-N, -C-OH[1]
4	1229 ± 2.77	-	-	0.0065 (2.185)	0.0009 (3.048)	Acetate, Cyclic anhydrides, Aromatic alcohols, Aromatic ketones, ethers[2], carboxyls[1,2]	C-O[1,2], C-N, O-H, -CH[1]
5	1267 ± 1.45	0	0			Cyclic anhydrides, Aromatic ethers, Aromatic alcohols, Aromatic ketones, Esters, Tertiary butyl alkanes, Phenolic OH[1], ethers[2], carboxyls[2]	C-O[2], C-N, O-H,-C-OH[1]
6	1326 ± 0.77	0	0			Alkanes, Alkenes, Alcohols, Amines	C-H, O-H

7	1381 ± 0.02	-	-	<0.0001 (5.956)	<0.0001 (4.700)	Alkanes, Tertiary alcohols, Aromatic alcohols, Aldehydes, Phenolic OH[2], Aliphatic OH[2]	C=S, C-H, O-H[2]
8	1431 ± 0.76	0	0			Alkanes, Alkenes, Carboxylic acids, Alcohols, Phenolic OH[2], Aliphatic OH[2]	C-H, O-H[2]
9	1460 ± 0.68	0	0			Alkanes, Primary Alcohols, Vicinal trisubstituted aromatics, Methyl[1], Methylene[1]	C-H[1]
10	1512 ± 3.30	0	0			Aromatics[2], Amides[2], Amines[2], Imines[2]	N-H, C=C[1,2], C=N[2]
11	1615 ± 1.19	0	0			Alkenes, Aromatics[2], Ionized carboxyl[2], Amides, Amines, HCl, Covalent nitrate, Covalent nitrite	C=N, C=C[2], N-H, -COO[-1,2]
12	1720 ± 9.10E-13	+	+	<0.0001 (14.953)	<0.0001 (8.200)	Anhydrides, Esters, Aldehydes[2], Ketones[2], Covalent carbonates, Carboxyl[2], Carbonyl[2]	C=O[1,2]
13	2852 ± 1.78	0	0			Alkanes, Aldehydes, Aliphatic CH[2]	C-H[1,2]
14	2921 ± 1.65	-	0	0.0004 (3.405)		Alkanes, Alkenes, Carboxylic acids, Aliphatic CH[2]	C-H[2]
15	3425 ± 2.27E-12	0	0			Alcohols, Amines, Amides	O-H[2], N-H

2.10 References

Artz, R.R.E., S.J. Chapman, and C.D. Campbell. 2006. Substrate utilisation profiles of microbial communities in peat are depth dependent and correlate with whole soil FTIR profiles. Soil Biol. Biochem. 38(9): 2958–2962. doi: 10.1016/j.soilbio.2006.04.017.

Artz, R.R.E., S.J. Chapman, J. Robertson, and J.M. Potts. 2008. FTIR Spectroscopy Can be Used as a Screening Tool for Organic Matter Quality in Regenerating Cutover Peatlands. Soil Biol. Biochem. 42(2): 515-527. DOI: 10.1016/j.soilbio.2007.09.019.

Baldock, J.A., C.A. Masiello, Y. Gélinas, and J.I. Hedges. 2004. Cycling and composition of organic matter in terrestrial and marine ecosystems. Mar. Chem. 92(1-4 SPEC. ISS.): 39–64. doi: 10.1016/j.marchem.2004.06.016.

Baldock, J.A., and R.J. Smernik. 2002. Chemical composition and bioavailability of thermally altered Pinus resinosa (Red pine) wood. Org. Geochem. 33(9): 1093–1109. doi: 10.1016/S0146-6380(02)00062-1.

Belton, D.J., R. Plowright, D.L. Kaplan, and C.C. Perry. 2018. A robust spectroscopic method for the determination of protein conformational composition – Application to the annealing of silk. Acta Biomater. 73: 355–364. doi: 10.1016/j.actbio.2018.03.058.

Bess, J.A. and R.A. Chimner. 2014. Ditch Restoration in a Large Northern Michigan Fen. Ecological Restoration 32:260-274. doi: 10.3368/er.32.3.260

Bourgeau-Chavez, L.L., S.L. Grelik, M. Billmire, L.K. Jenkins, E.S. Kasischke, et al.

2020. Assessing Boreal Peat Fire Severity and Vulnerability of Peatlands to Early Season Wildland Fire. Front. For. Glob. Chang. 3(February): 1–13. doi: 10.3389/ffgc.2020.00020.

Cadd, H.R., J. Tyler, J. Tibby, J. Baldock, B. Hawke, et al. 2020. The potential for rapid determination of charcoal from wetland sediments using infrared spectroscopy. Palaeogeogr. Palaeoclimatol. Palaeoecol. 542(December 2019). doi: 10.1016/j.palaeo.2019.109562.

Chen, J., B. Gu, E.J. LeBoeuf, H. Pan, and S. Dai. 2002. Spectroscopic characterization of the structural and functional properties of natural organic matter fractions. Chemosphere 48(1): 59–68. doi: 10.1016/S0045-6535(02)00041-3.

Chimner, R. A., Ott, C. A., Perry, C. H., & Kolka, R. K. 2014. Developing and Evaluating Rapid Field Methods to Estimate Peat Carbon. Wetlands, 34(6), 1241–1246. https://doi.org/10.1007/s13157-014-0574-6

Clark, J.S., and T.C. Hussey. 1995. Estimating the mass flux of charcoal from sedimentary records: effects of particle size, morphology, and orientation. The Holocene 6.

Cocozza, C., V. D'Orazio, T.M. Miano, and W. Shotyk. 2003. Characterization of solid and aqueous phases of a peat bog profile using molecular fluorescence spectroscopy, ESR and FT-IR, and comparison with physical properties. Org. Geochem. 34(1): 49–60. doi: 10.1016/S0146-6380(02)00208-5.

Colthup, N.B. 1950. Spectra-Structure Correlation in the Infra-Red Region. J. Opt. Soc. Am. 40(6).

Cotrufo, M.F., C. Boot, S. Abiven, E.J. Foster, M. Haddix, et al. 2016. Quantification of pyrogenic carbon in the environment: An integration of analytical approaches. Org. Geochem. 100: 42–50. doi: 10.1016/j.orggeochem.2016.07.007.

Crausbay, S.D., P.E. Higuera, D.G. Sprugel, and L.B. Brubaker. 2017. Fire catalyzed rapid ecological change in lowland coniferous forests of the Pacific Northwest over the past 14,000 years. Ecology 98(9): 2356–2369. doi: 10.1002/ecy.1897.

Demyan, M.S., F. Rasche, E. Schulz, M. Breulmann, T. Müller, et al. 2012. Use of specific peaks obtained by diffuse reflectance Fourier transform mid-infrared spectroscopy to study the composition of organic matter in a Haplic Chernozem. Eur. J. Soil Sci. 63(2): 189–199. doi: 10.1111/j.1365-2389.2011.01420.x.

Ding, G., and J.A. Rice. 2012. Black carbon evaluation in natural organic matter samples using recoupled long-range dipolar dephasing solid-state 13C NMR. Geoderma 189–190: 381–387. doi: 10.1016/j.geoderma.2012.04.020.

Farage, P., A. Ball, T.J. McGenity, C. Whitby, and J. Pretty. 2009. Burning management and carbon sequestration of upland heather moorland in the UK. Aust. J. Soil Res. 47(4): 351–361. doi: 10.1071/SR08095.

Gaffney, J.S., N.A. Marley, and K.J. Smith. 2015. Characterization of fine mode atmospheric aerosols by Raman microscopy and diffuse reflectance FTIR. J. Phys. Chem. A 119(19): 4524–4532. doi: 10.1021/jp510361s.

Gałka, M., G. Miotk-Szpiganowicz, M. Marczewska, J. Barabach, W.O. van der Knaap, et al. 2015. Palaeoenvironmental changes in Central Europe (NE Poland) during the last 6200 years reconstructed from a high-resolution multi-proxy peat archive.

Holocene 25(3): 421–434. doi: 10.1177/0959683614561887.

Gardegaront, M., D. Farlay, O. Peyruchaud, and H. Follet. 2018. Automation of the Peak Fitting Method in Bone FTIR Microspectroscopy Spectrum Analysis: Human and Mice Bone Study. J. Spectrosc. 2018(Figure 1). doi: 10.1155/2018/4131029.

Goldberg, E.D. 1985. Black Carbon in the Envrionment: Properties and Distribution. John Wiley and Sons, New York.

Goldstein, A., W.R. Turner, S.A. Spawn, K.J. Anderson-teixeira, S. Cook-patton, et al. 2020. Protecting irrecoverable carbon in Earth's ecosystems. Nat. Clim. Chang. 10(April): 287–295. doi: 10.1038/s41558-020-0738-8.

Guo, Y., and R.M. Bustin. 1998. FTIR spectroscopy and reflectance of modern charcoals and fungal decayed woods: implications for studies of inertinite in coals. Int. J. Coal Geol. 37(1–2): 29–53. doi: 10.1016/S0166-5162(98)00019-6.

Hammes, K., M.W.I. Schmidt, R.J. Smernik, L.A. Currie, W.P. Ball, et al. 2007. Comparison of quantification methods to measure fire-derived (black-elemental) carbon in soils and sediments using reference materials from soil, water, sediment and the atmosphere. Global Biogeochem. Cycles 21(3). doi: 10.1029/2006GB002914.

Hardy, B., J. Leifeld, H. Knicker, J.E. Dufey, K. Deforce, et al. 2017. Long term change in chemical properties of preindustrial charcoal particles aged in forest and agricultural temperate soil. Org. Geochem. 107: 33–45. doi: 10.1016/j.orggeochem.2017.02.008.

Hatten, J.A., Zabowski, D. 2009. Changes in Soil Organic Matter Pools and Carbon

Mineralization as Infl uenced by Fire Severity. Soil Science Society of America. 73: 262-273. doi:10.2136/sssaj2007.0304.

Hedges, J.I., G. Eglinton, P.G. Hatcher, D.L. Kirchman, C. Arnosti, S. Derenne, R.P. Evershed, I. Kogel-Knabner, J.W. de Leeuw, R. Littke, W. Michaelis, J. Rullkotter. 2000. The molecularly-uncharacterized component of nonliving organic matter in natural environments. Org Geochem. 31:945–958.

Heller, C., R.H. Ellerbrock, N. Roßkopf, C. Klingenfuß, and J. Zeitz. 2015. Soil organic matter characterization of temperate peatland soil with FTIR-spectroscopy: Effects of mire type and drainage intensity. Eur. J. Soil Sci. 66(5): 847–858. doi: 10.1111/ejss.12279.

Hodgkins, S.B., C.J. Richardson, R. Dommain, H. Wang, P.H. Glaser, et al. 2018. Tropical peatland carbon storage linked to global latitudinal trends in peat recalcitrance. Nat. Commun. 9(1): 1–13. doi: 10.1038/s41467-018-06050-2.

Hribljan, J.A., E.S. Kane, and R.A. Chimner. 2017. Implications of Altered Hydrology for Substrate Quality and Trace Gas Production in a Poor Fen Peatland. Soil Sci. Soc. Am. J. 81(3): 633. doi: 10.2136/sssaj2016.10.0322.

Kaal, J., J.A. Baldock, P. Buurman, K.G.J. Nierop, X. Pontevedra-Pombal, et al. 2007. Evaluating pyrolysis-GC/MS and 13C CPMAS NMR in conjunction with a molecular mixing model of the Penido Vello peat deposit, NW Spain. Org. Geochem. 38(7): 1097–1111. doi: 10.1016/j.orggeochem.2007.02.008.

Kane, E.S., E.S. Kasischke, D.W. Valentine, M.R. Turetsky, and A.D. McGuire. 2007. Topographic influences on wildfire consumption of soil organic carbon in interior

Alaska: Implications for black carbon accumulation. J. Geophys. Res. Biogeosciences 112(3): 1–11. doi: 10.1029/2007JG000458.

Kane, E.S., W.C. Hockaday, M.R. Turetsky, C.A. Masiello, D.W. Valentine, et al. 2010. Topographic controls on black carbon accumulation in Alaskan black spruce forest soils: Implications for organic matter dynamics. Biogeochemistry 100(1): 39–56. doi: 10.1007/s10533-009-9403-z.

Kasin, I., Y-I, Blanck, K.O. Storaunet, J. Rolstad, M. Ohlson. 2013. The charcoal record in peat and mineral soil across a boreal landscape and possible linkages to climate change and recent fire history. The Holocene. 23(7): 1052-1065. DOI: 10.1177/0959683613479678.

Kim, S., R.W. Kramer, and P.G. Hatcher. 2003. Graphical Method for Analysis of Ultrahigh-Resolution Broadband Mass Spectra of Natural Organic Matter, the Van Krevelen Diagram. Anal. Chem. 75(20): 5336–5344. doi: 10.1021/ac034415p.

Knicker, H., Müller, P., & Hilscher, A. 2007. How useful is chemical oxidation with dichromate for the determination of "Black Carbon" in fire-affected soils? Geoderma, 142(1–2), 178–196. https://doi.org/10.1016/j.geoderma.2007.08.010

Leifeld, J., C. Alewell, C. Bader, J.P. Krüger, C.W. Mueller, et al. 2018. Pyrogenic Carbon Contributes Substantially to Carbon Storage in Intact and Degraded Northern Peatlands. L. Degrad. Dev. 29(7): 2082–2091. doi: 10.1002/ldr.2812.

Maestrini, B., and J.R. Miesel. 2017. Modification of the weak nitric acid digestion method for the quantification of black carbon in organic matrices. Org. Geochem. 103: 136–139. doi: 10.1016/j.orggeochem.2016.10.010.

Mao, J.-D., W.-G. Hu, K. Schmidt-Rohr, G. Davies, E.A. Ghabbour, et al. 2000. Quantitative Characterization of Humic Substances by Solid-State Carbon-13 Nuclear Magnetic Resonance. Soil Sci. Soc. Am. J. 64(3): 873–884. doi: 10.2136/sssaj2000.643873x.

Margenot, A.J., F.J. Calderón, K.A. Magrini, and R.J. Evans. 2017. Application of DRIFTS, 13C NMR, and py-MBMS to Characterize the Effects of Soil Science Oxidation Assays on Soil Organic Matter Composition in a Mollic Xerofluvent. Appl. Spectrosc. 71(7): 1506–1518. doi: 10.1177/0003702817691776.

Markgraf, V., and U.M. Huber. 2010. Late and postglacial vegetation and fire history in Southern Patagonia and Tierra del Fuego. Palaeogeogr. Palaeoclimatol. Palaeoecol. 297(2): 351–366. doi: 10.1016/j.palaeo.2010.08.013.

Masiello, C.A. 2004. New directions in black carbon organic geochemistry. Mar. Chem. 92: 201–213. doi: 10.1016/j.marchem.2004.06.043.

Masiello, C.A., A.A. Berhe. 2020. First interactions with the hydrologic cycle determine pyrogenic carbon's fate in the Earth system. Earth Surf. Process. Landforms. 45: 2394–2398. DOI: 10.1002/esp.4925.

Matamala, R., F.J. Calderón, J.D. Jastrow, Z. Fan, S.M. Hofmann, et al. 2017. Influence of site and soil properties on the DRIFT spectra of northern cold-region soils. Geoderma 305(December 2016): 80–91. doi: 10.1016/j.geoderma.2017.05.014.

Merino, A., B. Chávez-Vergara, J. Salgado, M.T. Fonturbel, F. García-Oliva, et al. 2015. Variability in the composition of charred litter generated by wildfire in different ecosystems. Catena 133: 52–63. doi: 10.1016/j.catena.2015.04.016.

Miesel, J.R., W.C. Hockaday, R.K. Kolka, and P.A. Townsend. 2015. Soil organic matter composition and quality across fire severity gradients in coniferous and deciduous forests of the southern boreal region. J. Geophys. Res. G Biogeosciences 120(6): 1124–1141. doi: 10.1002/2015JG002959.

Nichols, J.E., and D.M. Peteet. 2019. Rapid expansion of northern peatlands and doubled estimate of carbon storage. Nat. Geosci. 12(November): 917–922. doi: 10.1038/s41561-019-0454-z.

Niemeyer, J., Y. Chen, and J.-M. Bollag. 1992. Characterization of Humic Acids, Composts, and Peat by Diffuse Reflectance Fourier-Transform Infrared Spectroscopy. Soil Sci. Soc. Am. J. 56(1): 135–140. doi: 10.2136/sssaj1992.03615995005600010021x.

Nocentini, C., G. Certini, H. Knicker, O. Francioso, and C. Rumpel. 2010. Nature and reactivity of charcoal produced and added to soil during wildfire are particle-size dependent. Org. Geochem. 41(7): 682–689. doi: 10.1016/j.orggeochem.2010.03.010.

Nolte, C.G., J.J. Schauer, G.R. Cass, and B.R.T. Simoneit. 2001. Highly polar organic compounds present in wood smoke and in the ambient atmosphere. Environ. Sci. Technol. 35(10): 1912–1919. doi: 10.1021/es001420r.

Pandey, K.K., and A.J. Pitman. 2003. FTIR studies of the changes in wood chemistry following decay by brown-rot and white-rot fungi. Int. Biodeterior. Biodegrad. 52(3): 151–160. doi: 10.1016/S0964-8305(03)00052-0.

Prasad, M., J.B.G.M. Verhagen, and T.G.L. Aendekerk. 2000. Effect of peat type and pH on breakdown of peat using fourier transform infrared spectroscopy. Commun. Soil

Sci. Plant Anal. 31(17–18): 2881–2889. doi: 10.1080/00103620009370635.

Preston, C.M., and M.W.I. Schmidt. 2006. Black (pyrogenic) carbon: a synthesis of current knowledge and uncertainties with special consideration of boreal regions. Biogeosciences 3(C): 397–420. doi: 10.5194/bg-3-397-2006.

Reggente, M., A.M. Dillner, and S. Takahama. 2019. Analysis of functional groups in atmospheric aerosols by infrared spectroscopy: Systematic intercomparison of calibration methods for US measurement network samples. Atmos. Meas. Tech. 12(4): 2287–2312. doi: 10.5194/amt-12-2287-2019.

Sadat, A., and I.J. Joye. 2020. Peak fitting applied to fourier transform infrared and raman spectroscopic analysis of proteins. Appl. Sci. 10(17). doi: 10.3390/app10175918.

Sanderman, J., K. Savage, S.R.S. Dangal. 2020. Mid-infrared spectroscopy for prediction of soil health indicators in the United States. Soil Science Society of America Journal. 84: 251-261. DOI: 10.1002/saj2.20009.

Sekiguchi, Y., J.S. Frye, and F. Shafizadeh. 1983. Structure and formation of cellulosic chars. J. Appl. Polym. Sci. 28: 3513–3525.

Simoneit, B.R.T., J.J. Schauer, C.G. Nolte, D.R. Oros, V.O. Elias, et al. 1999. Levoglucosan, a tracer for cellulose in biomass burning and atmospheric particles. Atmos. Environ. 33(2): 173–182. papers3://publication/uuid/3E935E2F-ED96-40DC-8374-344125150073.

Skjemstad, J.O., J.A. Taylor, and R.J. Smernik. 1999. Estimation of charcoal (char) in soils. Commun. Soil Sci. Plant Anal. 30(15–16): 2283–2298. doi:

10.1080/00103629909370372.

Skoog, D.A. 2014. Fundamentals of analytical chemistry. 9th ed. Thomson-Brooks/Cole, Belmont, California.

Smernik, R.J., J.A. Baldock, and J.M. Oades. 2002a. Impact of remote protonation on 13C CPMAS NMR quantitation of charred and uncharred wood. Solid State Nucl. Magn. Reson. 22(1): 71–82. doi: 10.1006/snmr.2002.0065.

Smernik, R.J., J.A. Baldock, J.M. Oades, and A.K. Whittaker. 2002b. Determination of T1ρH relaxation rates in charred and uncharred wood and consequences for NMR quantitation. Solid State Nucl. Magn. Reson. 22(1): 50–70. doi: 10.1006/snmr.2002.0064.

Schmidt, M.W.I., J.O. Skjemstad, C.I. Czimczik, B. Glaser, K.M. Prentice, et al. 2001. Comparative analysis of black carbon in soils. Global Biogeochem. Cycles 15(1): 163–167. doi: 10.1029/2000GB001284.

Turetsky, M.R., B. Benscoter, S. Page, G. Rein, G.R. van der Werf, et al. 2015. Global vulnerability of peatlands to fire and carbon loss. Nat. Geosci. 8(1): 11–14. doi: 10.1038/NGEO2325.

Zhang, Y., J. Maxted, A. Barber, C. Lowe, and R. Smith. 2013. The durability of clear polyurethane coil coatings studied by FTIR peak fitting. Polym. Degrad. Stab. 98(2): 527–534. doi: 10.1016/j.polymdegradstab.2012.12.003.

3 Reconstructing Fire History in Hemi-boreal Peatlands: Implications for Long-term Carbon Accumulation

3.1 Abstract

Peatlands are crucial carbon storing ecosystems, but this function is vulnerable to changes to disturbance regimes. Baseline disturbance data on fire history is lacking in the hemi-boreal region. We use peat core records, radiocarbon dating, and infrared spectrometry to identify and date past fire events from 29 peatlands in 4 major hemi-boreal peatland ecotypes including: open poor fens, treed poor fens, forested poor fens, and forested rich fens AKA rich conifer swamps, in the hemi-boreal region. In this region poor fens experienced 2.1 fires ka^{-1} or once every 480 years on average, and the rich fens experienced almost no fire. We found a significant negative relationship between fire frequency and long-term apparent rate of carbon accumulation. This work indicates that fire is a natural occurrence in poor fen peatlands in the hemi-boreal region of North America, a context important to land managers and ecologists working in these systems.

3.2 Introduction

Peatlands have been recognized for decades to be important long-term carbon (C) sinks, containing vast amounts of C, between 545 to 1055 Pg C globally (Nichols and Peteet, 2019). However, there is concern that this C sink has or will soon weaken or

reverse primarily due to climate change, land conversion, or change to disturbance regimes, such as fire (Goldstein et al., 2020). Most threats to peatland stability will come from perturbations of established regimes, either in climate, land use, or disturbance regimes (Loisel et al., 2021).

Fire is a significant disturbance driver in peatlands globally. However, due to difficulty in detecting peat fires, it is difficult to estimate the extent of peat burning (Turetsky et al., 2015). These fires can burn down meters deep into peat soils depending on hydrologic conditions, but boreal peatlands typically burn ~13 cm, releasing ~3.4-3.6 kg of C per m^2 (Turetsky et al., 2011). This naturally has at least a transient negative impact on C storage which is multiplied by each fire, so frequency is important. Estimates of fire frequencies (FF) for peatlands can range widely from 5 to 12.5 fires ka^{-1}, or 0.59 to 2.2 fires ka^{-1}, and fire regimes can vary significantly between regions (Wieder and Vitt, 2010; Walker et al., 2020).

Changes in the fire frequency in boreal ecosystems exert considerable control over many ecosystem processes, which ultimately govern carbon storage (Johnstone et al., 2010; Walker et al., 2019, 2020). While fire regimes are comparatively well quantified in uplands, much less is known of FF in peatlands (Johnstone et al., 2010; Larson and Green, 2017). Only a few studies in other, nearby regions have estimated peatland FF, one in Quebec (7.7 fires ka^{-1}) (Cogbill, 1985), and one in Western Canada (range from 0-5.3 fires ka^{-1}) (Kuhry, 1994). With so little available data, the effects of peatland fire on C are also poorly understood. The long-term apparent rate of carbon accumulation (LARCA) in peatlands generally ranges from 0 to 60 $g*m^{-2}*yr^{-1}$ (Clymo et

al., 1998; Pitkänen et al., 1999). Pitkänen et al. noted a relationship between the spacing of char layers (implicitly related to FF) and LARCA in Finland (Pitkänen et al., 1999). A similar finding relating FF to LARCA was also shown in a discontinuous permafrost region in Northwest Territories, Canada (Robinson and Moore, 2000). Together, these findings agree with research in upland boreal systems suggesting that an increased fire return interval reduces long-term C accumulation, but to our knowledge this has not been replicated in the hemi-boreal peatlands of North America.

There are several types of peatlands present in the hemi-boreal zone, each of which, due to differences in hydrology, vegetation, or other factors, could have distinct fire regimes. Our goal was to quantify the fire regimes of some of the most plentiful hemi-boreal peatland ecotypes, poor fens and rich conifer swamps. We hypothesized that peatland ecotypes would be susceptible to wildfire to different degrees, specifically, we suspected that the rich conifer swamps would experience significantly less wildfire than other peatland ecotypes, due to a fire-resistant overstory, relative lack of understory, and consistent water table. This is supported by multiple studies which describe a negative association between northern white cedar and wildfire disturbance (Fenton and Bergeron, 2008; Taylor and Chen, 2011; Apfelbaum et al., 2017; Jules et al., 2018; Rayfield et al., 2021). We hypothesized that LARCA would be negatively related to fire frequency, as hinted at by Pitkänen et al., because of the consumption of sequestered carbon during combustion. Robinson and Moore compared recent apparent C accumulation rates in Northwestern Canada, finding that rich fens accumulated C significantly slower than poor fens (Robinson and Moore, 1999); we hypothesized that we would find that when using

LARCA as our measure we would be able to confirm this observation of greater C accumulation in poor fens than rich fens.

3.3 Methods

3.3.1 Sample Locations

We analyzed 29 soil cores from peatlands across the Upper Peninsula of Michigan, northern Wisconsin, and northern Minnesota (Fig. 1). The boreal zone of North America is typically considered to reach its southernmost extent along the north shore of Lake Superior, with a hemi-boreal zone that encompasses the Upper Peninsula, a small part of northern Wisconsin, and much of northern Minnesota (Langor et al., 2014, see Fig. 13). Our sampling locations were all within this hemi-boreal zone. All sites also fell within the Northern Forests (I) > Mixed Wood Shield (II) > Northern Lakes and Forests (III) Ecoregion as defined by the US EPA (U.S. Environmental Protection Agency, 2013). This ecoregion is described as "humid continental, marked by warm summers and severe winters, with no pronounced dry season," with a mean annual temperature ranging from ~2°C to ~6°C, and mean annual precipitation ranging from 500 to 960 mm (Wiken et al., 2011).

The hemi-boreal peatlands that we sampled can be described as fens. Both the poor fens and rich conifer swamps sampled are peat bearing and groundwater fed. We therefore refer to the rich conifer swamps as forested rich fens (FRFs) for here on to avoid confusion with mineral wetlands. These fen ecotypes are common and may be

isolated, coastal, or part of large upland-peatland complexes (Bourgeau-Chavez et al., 2017, see Fig. 10). The poor fens are dominated by typical vegetation such as *Sphagnum* (L.) mosses, black spruce (*Picea mariana* (Mill.) Britton, Sterns & Poggenb.), tamarack (*Larix laricina* (Du Roi) K. Koch), sedges (*Carex spp.* L.), Labrador tea (*Rhododendron groenlandicum* (Oeder) Kron & Judd), bog rosemary (*Andromeda polifolia* L.), leatherleaf (*Chamaedaphne calyculata* L.), etc. (Kost et al., 2007). The FRFs that we sampled were silvic and dominated by northern white cedar (*Thuja occidentalis* L.) with presence of balsam fir (*Abies balsamea* (L.) Mill.), white spruce (*Picea glauca* (Moench) Voss), hemlock (*Tsuga canadensis* L.) with a sparse understory due to heavy shading and deer herbivory (Kost et al., 2007).

3.3.2 Sampling

We avoided coring in laggs or ecotones which have variable hydrology. At each site where a moss layer was present, we inserted PVC tubes into the peat to a depth of 50 cm to collect the low bulk density surficial moss and peat. The surficial sample was carefully removed and cut into 10 cm depth increments. We then used a Russian peat corer to sample the peat profile down to the mineral soil. We immediately froze all samples upon return to the lab. We logged location data on a per site basis, using a Garmin eTrex 20. We classified our sample sites by peatland ecotype following the Kudray method used in the Hiawatha National Forest where many of our core samples were taken (Kudray, 2019). This resulted in 4 classes, open poor fens (OPF) (<10% tree cover, acidic) (n=16), treed poor fens (TPF) (>10% tree cover with mean height <10 m,

acidic) (n=6), forested poor fens (FPF) (>10% tree cover with mean height >10 m, acidic) (n=1), and forested rich fens (FRF) (>10% tree cover, circumneutral) (n=6).

3.3.3 Sample Processing

In the lab, we cut the still-frozen peat into 2 cm increments before drying at 60° C to constant mass, and then weighed the samples to determine bulk density. We ground and homogenized the samples using a Wiley mill equipped with a 40 mesh screen. This resulted in a powdered sample with a maximum particle size of 425 microns. We combusted a subsample of each peat sample at 500° C for at least 12 hours to establish the fraction organic matter (OM) by mass. We then diluted a subsample with potassium bromide (KBr) salt to 10% peat by mass in preparation for FTIR spectrometry.

3.3.4 Spectrometry

We followed the methodology outlined in section 2 to prepare our peat samples for FTIR. In brief, we collected the FTIR spectra of the samples using a Thermo Scientific Nicolet iS5 spectrometer, equipped with a standard fast recovery deuterated triglycine sulfate (DTGS) detector, and an iD Foundation – Diffuse accessory (Thermo Fisher Scientific, Ann Arbor, MI). We baseline corrected and standardized each spectrum before using the peak fitting function in Origin (Origin 2019b 64-bit, OriginLab Corporation, Northhampton, MA) to condense the volume of data per sample by fitting 15 gaussian peaks to the spectral features. We used the peak areas fitted using this method as inputs to the char prediction model outlined in section 2.

The model outlined in section 2 was optimally suited for the samples in this study because we developed them in parallel using peats and chars from the same region and even some of the same cores. In brief, the model predicts the mass fraction of char in each sample from the peak areas identified from its unique FTIR spectrum. The char concentration was validated by direct polarization NMR using the Nelson and Baldock molecular mixing model. Using this model, we can make good estimates of char concentration throughout the peat column and use those estimates to detect fire events.

3.3.5 Fire counting

For each core, individual fire events were inferred from char concentrations determined by FTIR spectrometry (Section 2). When char content exceeded 11.37% we concluded that this likely reflected a fire event. We chose this threshold because it was the average of the 3 NMR-validated char endmembers used to build the model (Section 2). In addition, we only indicated the presence of fire on the local maximum, so each spike was only counted once, even when it spanned multiple samples. Furthermore, each spike in char concentration had to be 5% higher than the local minima both above and below it to avoid minor fluctuations being considered separate events. The only exceptions to these rules were in cases where there were no samples either above or below the sample in question due to coinciding with the top or bottom of a core. These rules ensure that our estimates are conservative, uniform, and repeatable. We know that fire evidence can be erased by subsequent fires burning antecedent char layers, and low-severity fires may only burn vegetation without leaving detectable traces. As a result, our

estimates of fire frequency (FF) are minima and likely represent the more severe, impactful fires.

We determined the approximate age of each sample within our cores by using linear depth-age interpolation between samples with verified ages. Ages were verified by radiocarbon dating or assumption of modernity for surface samples. For OPF and TPF cores with surface samples present, the surficial moss layer samples were assigned ages incrementally from the top down, using observed surface peat accumulation rates for poor fens in the hemi-boreal region (Potvin et al., 2015, see Fig. 7). We determined the location of the boundary between surficial (acrotelmic) and deeper (catotelmic) peat by interpreting bulk density; we defined the border to be above the sample that displayed a sudden relative increase in BD, sensu. (Malmer and Wallén, 1993).

We calculated the C content of our peat using LOI to determine %OM and applied a conversion factor of 0.53 to estimate C mass from BD and %OM. We calculated the long-term rate of carbon accumulation (LARCA) for each core by integrating the carbon content of each sample between the top and bottom of each FRF and FPF core and the age range of those samples. For OPF and TPF, we used the same procedure, but limited minimum depth to 50 cm to avoid surficial bias due to more rapid and variable accumulation of undecomposed C in surficial moss (Clymo et al., 1998; Young et al., 2021).

3.3.6 Radiocarbon Dating

Samples were graphitized in preparation for ^{14}C abundance measurement at the Carbon, Water & Soils Research Lab in Houghton, Michigan. Peat samples were dried, weighed into quartz tubes, and sealed under vacuum. Samples were combusted at 900°C for 6 hours with cupric oxide (CuO) and silver (Ag) in sealed quartz test tubes to form CO2 gas. The CO2 was then reduced to graphite through heating at 570°C in the presence of hydrogen (H2) gas and an iron (Fe) catalyst (Vogel et al., 1987). Graphite targets were then analyzed for radiocarbon abundance by Accelerator Mass Spectrometry at either the Keck Carbon Cycle AMS Facility, Earth System Science Dept., University of California Irvine or at the DirectAMS facility in Bothell, WA (Zoppi et al., 2007) (Supplementary Table 1). Radiocarbon measurements were corrected for mass-dependent fractionation using AMS inline measurements of δ13C following Stuiver and Polach, 1977. Sample preparation backgrounds were subtracted, based on measurements of ^{14}C-free wood. Calibrated ages were calculated with OxCal v.4.4 (Bronk Ramsey, 2009) using the IntCal20 calibration curve. Calibrated median ages were used to determine peat initiation date and calculate LARCA and FF (Table 2). Basal peat was differentiated from mineral substrate by sample %OM. In some cases, the peat–mineral boundary was not captured so initiation dates may be more recent than reality.

3.3.7 Statistics

We used mean separation on FF and LARCA to test our hypotheses about variance across peatland ecotypes, and linear regression to test our last hypothesis about the relationship between LARCA and FF. For any analysis relating to LARCA two samples, from the Sleeper Lake location (Table 2), were excluded due to insufficient depth to integrate over. For data analysis we used JMP Pro 14.0.0 (SAS Institute Inc.). We used non-parametric tests because of data heteroscedasticity. We began by running Levine's unequal variance test to determine whether to use Wilconxin or Welch's test for significance testing, if significant, we proceeded to use Steel-Dwass for mean separation (Fujiwara et al., 2014). Before modeling the relationship between fire and LARCA, we limited our cores to those younger 4000 years (see Fig. 2)) based on peatland age to avoid the known issues related to peatland age affecting LARCA results (Clymo et al., 1998; Yu, 2012; Young et al., 2021). We checked for normality in our data before modeling and used linear regression.

3.4 Results

It is notable that there are a few waves of nearly simultaneous peatland establishment, which can be perceived clearly in Figure 2. These coincidences occur ca. 7000-8000, 5000-6000, 2000-3000, and 1000-1500 years before 2021. The time span from 2500 to 3500 years before 2021 was particularly active. There is no discernable relationship between initiation date and ecotype.

We can observe that there are distinctly fewer fire observations in FRF peatlands compared to the poor fen peatlands (Fig. 3). There is considerable heterogeneity in fire occurrence within ecotypes, and even within cores. Poor fen sites do not have significantly different fire frequencies from one another. The mean FF of FRFs is 0.18 fires ka^{-1}, with 4 out of 6 cores having no fire observations, and the most frequently burning core having 0.37 fires ka^{-1} (Table 1). This is significantly lower than the mean FF of the OPFs, which was 2.0 fires ka^{-1} (Table 1, Fig. 4). Interestingly, the mean FF of the OPFs did not differ significantly from that of the TPFs (2.6 fires ka^{-1}) or the FPF (1.9 fire ka^{-1}) (Table 1, Fig. 4). The three poor fen classes did not differ significantly from one another, and their medians and ranges were notably similar (Fig. 4).

Despite the differences in FF between the rich and poor fen ecotypes, we observed no significant LARCA differences between any of the four ecotypes (Fig. 5). All peatland types with sufficient sample size (OPF, TPF, and FRF) had wide ranges (~10 to ~45 g m^{-2} yr^{-1}). In descending order of LARCA the order is TPF, OPF, and FRF (notably medians, quartiles, minima, and maxima all follow the same trend).

We also found support for a negative relationship between fire frequency and C accumulation. Our model (based on a subsample of sites younger than 4000 yrs to avoid previously-mentioned issues with LARCA, and excluding the largely non-burning FRFs) showed a significant ($p=0.013$, $r^2=0.41$, $n=14$) negative relationship between FF and LARCA (Figs. 6 & 7). The modelled relationship is presented in (Eq. 1).

Equation 1:

$$LARCA\ (g\ m^{-2}yr^{-1}) = 44.84 - (7.31\ \times FF(fires\ ka^{-1}))$$

3.5 Discussion

3.5.1 Peatland initiation patterns

The majority of peatlands in this study initiated between 2500 to 3500 years before 2021. This notable pulse of peatland initiation coincides with a marked decrease in both North American and global temperature anomalies (Viau et al., 2006; Marcott et al., 2013). This period of global cooling is the likely cause for this pulse of peatland initiation. The fact that we are now experiencing an opposite, increasing, rapid, anthropogenic trend in global temperature anomaly is therefore alarming with regard to hemi-boreal peatlands.

3.5.2 Fire frequency of different hemi-boreal peatland types

We were able to produce fire histories for 29 sites in the hemi-boreal zone of North America. This represents the first comprehensive evaluation of regional peatland fire frequency. Our data suggest that, within this region, rich forested fen peatlands dominated by northern white cedar experience very little fire, with only 3 total fires observed in over 18,000 collective recorded years. In comparison, the *Sphagnum* dominated poor fen peatlands shows evidence of 2.1 fires ka^{-1}. This is less frequent than the 7.7 fires ka^{-1} estimated in Quebec (Cogbill, 1985), but the range of our observations (0-5.8 fires ka^{-1}) fell nearly exactly in into the range of observations published for peatlands in western Canada (0-5.3 fires ka^{-1}) (Kuhry, 1994). This supports our hypothesis that forested rich fens experience fire significantly less than poor fens in the

same region. Though we have not established the cause, we suspect this to be due to a combination of stable water tables and a closed canopy reducing ground cover capable of carrying a fire.

The poor fens are represented in this study by 3 ecotypes, OPFs, TPFs, and the FPF. The OPFs and TPFs do not differ significantly in FF. While we do not have the sample size to draw conclusions about the fire regime of FPFs broadly, the FPF site that we sampled appears to follow this same broad pattern of poor fen FF homogeneity. The implication of this finding is that poor fen ecotypes have comparable fire regimes regardless of tree cover, which was the main differentiator between these 3 ecotypes. The large ranges observed in OPF and TPF FF imply that within the poor fen group, and even within ecotype, the fire regime of each peatland is unique and one or more unaccounted-for variables is responsible for explaining FF with greater accuracy. Since tree cover can change and is not expected to stay constant through millennia, the lack of differentiation in fire history by tree cover is unsurprising.

There is considerable heterogeneity in the timing of fires within a given core (Fig. 3). Some cores appear to have relatively uniform fire histories, while others have notable "boom and bust" periods. Some cores have long time spans post initiation without fire observations, while others burned frequently from the start. Synchronization of fire events, presumably due to regional drought, appears to have occurred at least once, around 1500 years ago, but this has not been verified by radiocarbon dating of all relevant char layers. For reasons explained below, in the Methodological Considerations subsection, we were unfortunately unable to compare recent fire history to the fire history

of the deep past. Due to this, and the aforementioned heterogeneities, we are unable to discern any consistent pattern of fire through time.

3.5.3 Fire frequency and carbon accumulation in hemi-boreal peatlands

We were able to support our hypothesis and Kuhry's and Robinson and Moore's observation of a negative relationship between fire and carbon accumulation (Kuhry, 1994; Robinson and Moore, 2000). This indicates that the fire can lower peatland C stocks. Based on our model, LARCA approaches 0 when the FF approaches 6.15 fires ka^{-1}, implying more frequent large fires would result in extirpation of the peatland. More likely, hydrology begins to limit fire before reaching this point. We have already seen the result of severe hydrological disturbance on peatland fire regimes and C cycling in Indonesia (Sazawa et al., 2018; Vetrita and Cochrane, 2020).

While we found a significant negative relationship between fire frequency and LARCA, we were not able to support our hypothesis that FRFs would have lower LARCAs than other peatland ecotypes. This is counterintuitive to our findings of higher FF in poor fen ecotypes compared to the FRFs. While we found no significant difference in LARCA between ecotypes, the weak trend was for FRFs to have slightly lower LARCA than the poor fens despite having much fewer fire observations, which does agree with Robinson and Moore's findings (Robinson and Moore, 1999). The great variability that we found in LARCA within ecotypes rather than across them leads us to conclude that LARCA values are mostly unique to each specific peatland. The range of

LARCAs we observed span the range of observations in the literature (Pitkänen et al., 1999; Robinson and Moore, 1999, 2000).

3.5.4 Methodological Considerations

The model that we developed in section 2 was fit to admixtures composed of *Sphagnum* peat. As such, the model predictions are not necessarily accurate in cedar peat matrices. This may account for the paucity of char detections in cedar peat, and therefore this research should not be construed as evidence that cedar-dominated FRFs do not experience wildfire.

It is important to note that we took a conservative approach to our fire counts. We set a high bar for char content to even consider a fire may be present, and additionally required that there be a prescribed decline in char content in surrounding samples to count a spike in concentration as a fire event. It is possible that fires could have occurred without being counted by our method for several reasons. Fires may burn only surficial material like shrubs or sedges, resulting in little char production, smoldering peat fires may consume much of the char produced, peatland fires are known to be spatially heterogeneous on a microtopographic scale (Benscoter and Vitt, 2008; Benscoter et al., 2015). Furthermore, subsequent fires could consume antecedent char layers, erasing them from the record, or the char layers of two or more fires could merge by proximity. These occurrences would result in either too little or no char left to detect or, in the latter case, result in multiple fires being counted as one.

Additionally, the resolution of our sampling (in 2 or 10 cm depth increments) could have implications for fire detection. Since the entire sample for a given increment was homogenized, the char concentration of any assumed discrete char layer is diluted by the mass of the surrounding sample. In 2 cm depth increments, this is not much, perhaps enough to miss subtle char signatures, such as those produced from low severity fires. Unfortunately, our method does not allow for fire severity to be quantified, but we most likely identify the most severe and C-relevant fires. In the 10 cm surficial samples from OPF and TPF sites, the dilution effect would be much stronger. Therefore, we cannot confidently say that a lack of fire observations in these samples represents a real absence, and we cannot draw conclusions about fire from the time periods integrated in these samples. For example, figure 2 may imply that there has been a lack of fire in near present times, but this conclusion is neither supported nor refuted by our methods, we simply cannot say. These considerations mean that our fire counts and fire frequencies are best considered as minima. Furthermore, the relationship of our model of fire frequency to LARCA is fit based on these minima, so the true slope of the relationship may in fact be shallower than we observed here, which could explain the difference in slope between our model and that of (Kuhry, 1994).

Our methods are conservative when it comes to identifying fire events, so we are unlikely to identify introduction of allogenic char, such as from atmospheric deposition, and we avoided coring in peatland margins to minimize the chances of capturing allogenic char that was transported from uplands. Taking the totality of these

methodological considerations into account, we believe that our records, while conservative, do accurately represent the presence of fire within the peatland itself.

3.5.5 Implications for Fire in Hemi-boreal peatlands

Our findings show that poor fens in this hemi-boreal region experience around 2.1 fires ka^{-1}, or approximately once every 480 years. As outlined above, these data are most likely based upon severe peat fires, so more frequent, less severe fire is a possible feature of these poor fen systems. In contrast, we found very little evidence of fire in the cedar dominated FRFs, implying that fire is rare or even abnormal in this ecotype. However, low-severity fires may be a feature which we were simply unable to detect.

The black spruce present, if not dominant, in many poor fens in the hemi-boreal region are fire-dependent species, which indicates that fire is ecologically necessary for maintenance of treed poor fen ecotypes. However, established fire regimes for boreal black spruce dominated forests indicate more frequent fire (2.5-20 fires ka^{-1} (Zackrisson, 1977; Carcaillet et al., 2007; Brown and Giesecke, 2014; Drobyshev et al., 2014)) than we found for our peatlands. One readily available explanation is that the nature of the hydric peatland environment acts to both slow the growth of trees and reduce fire frequency in comparison to upland or mesic black spruce forests.

One study modeling climate change in North America predicted moderate 2-4° C increase in both summer and winter temperatures in our study region and 0-40% change in winter precipitation and ±20% change in summer precipitation from 2071 to 2100 compared to early 2000s (Šeparović et al., 2013). Another study on relative regional

climate change vulnerability showed our region straddling two of their regions, both of which had moderate vulnerability based on temperature and precipitation change and interannual variation (Giorgi, 2006). In comparison to late 20th century climate, interannual variability in precipitation was predicted to be much higher in summer and elevated to a lesser degree in winter. Interannual variability in temperature was predicted to be higher in summer and lower in winter.

Higher summer temperatures would increase evapotranspiration while higher winter temperatures would have a negative impact on snowpack, which is important to water provisioning in this region. More winter precipitation could have a positive impact on snowpack; however, the risk of fires is highest during the summer, particularly in drought years, and the prediction for slight increase or decrease in precipitation during summer is inconclusive. Severe peat fires are dependent on drought conditions to occur, so the predicted increases to interannual variation in summer are concerning. More frequent and/or more severe drought in this region would increase the vulnerability of peatlands to severe fire, with consequent impacts on the C cycle within them.

3.6 Conclusion

We established conservative fire frequencies for peatlands in the Upper Peninsula and hemi-boreal region, with the median poor fen experiencing 2.1 fires ka^{-1}, and the median rich fen experiencing no fire. We found a significant negative relationship between fire frequency and long-term apparent rate of carbon accumulation. Within our regional focus, we observed a wide range of LARCAs. Despite the difference in

vegetation and fire regimes between poor and rich fen classes, their LARCAs did not differ significantly from one another. Our work provides vital context to land managers and ecologists working in the hemi-boreal region of North America. Our findings imply that fire is a natural part of poor fen peatlands in the hemi-boreal region, but that severe fire is infrequent. Further work to confirm or expand upon these findings would benefit from consideration of fire heterogeneity, increased depth resolution, particularly near the surface, and measurement of hydrology.

3.7 Tables and Figures

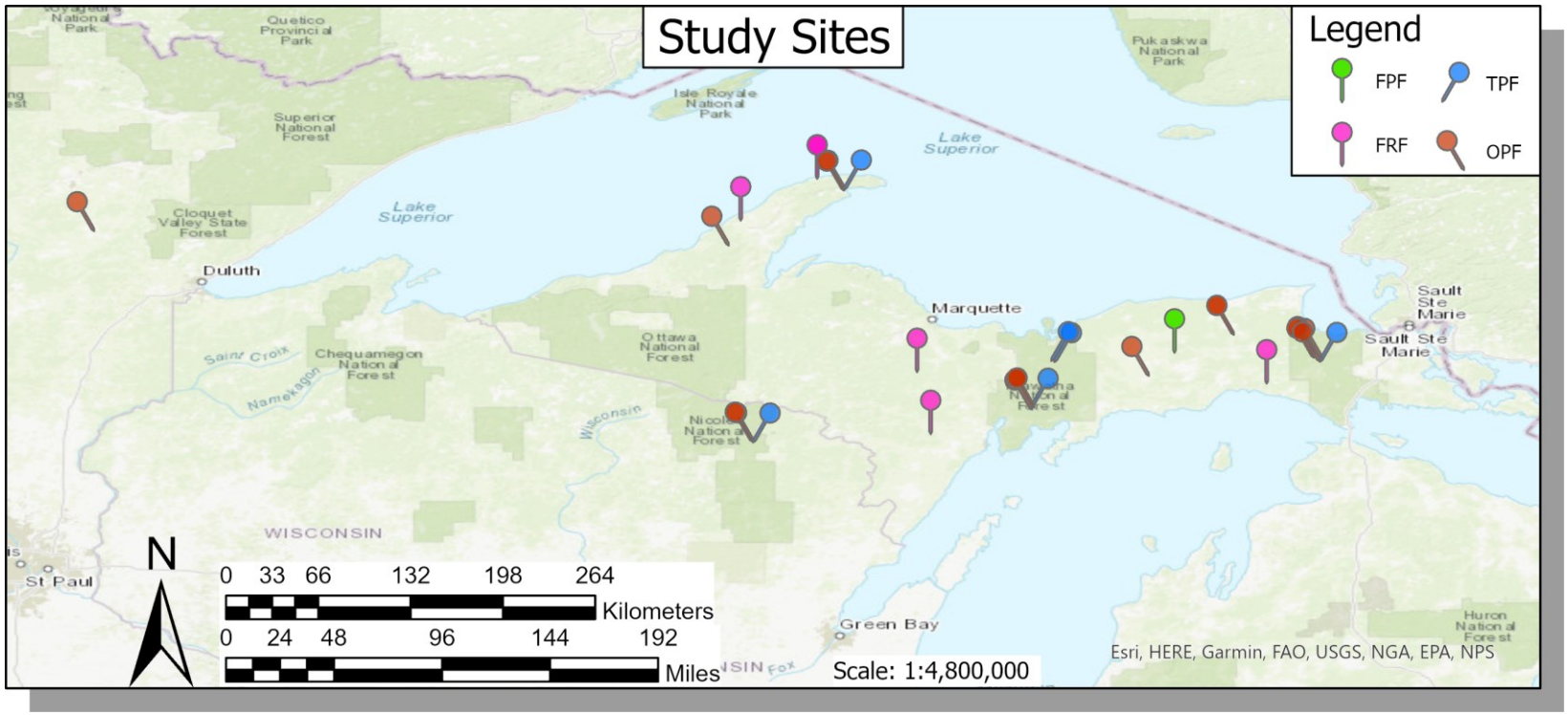

Figure 1: This map indicates the locations and ecotypes of all sampling locations used in this study.

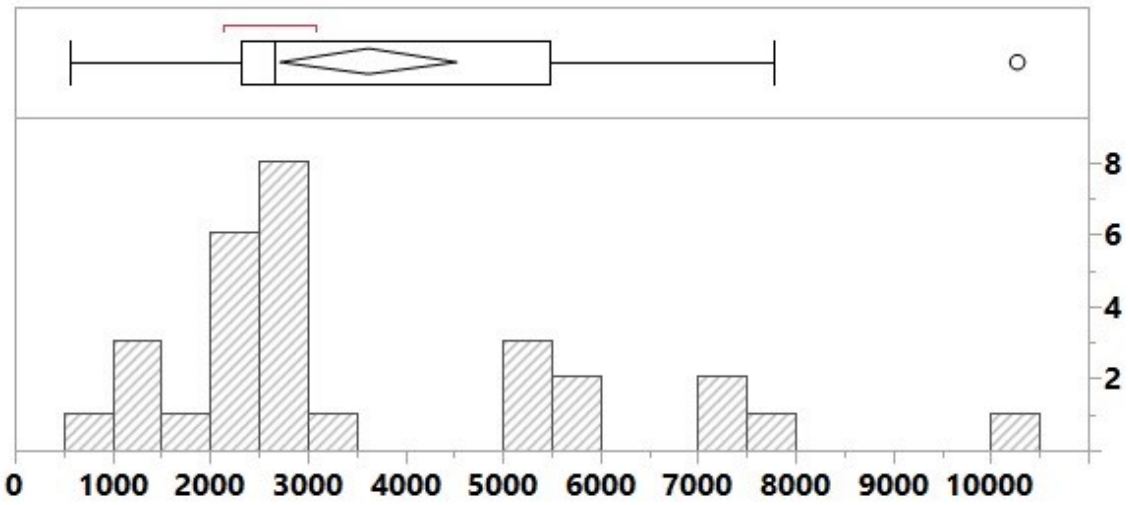

Figure 2: This histogram indicates the time since 2021 of peatland initiation for each core. The box and whisker plot depicts quartiles.

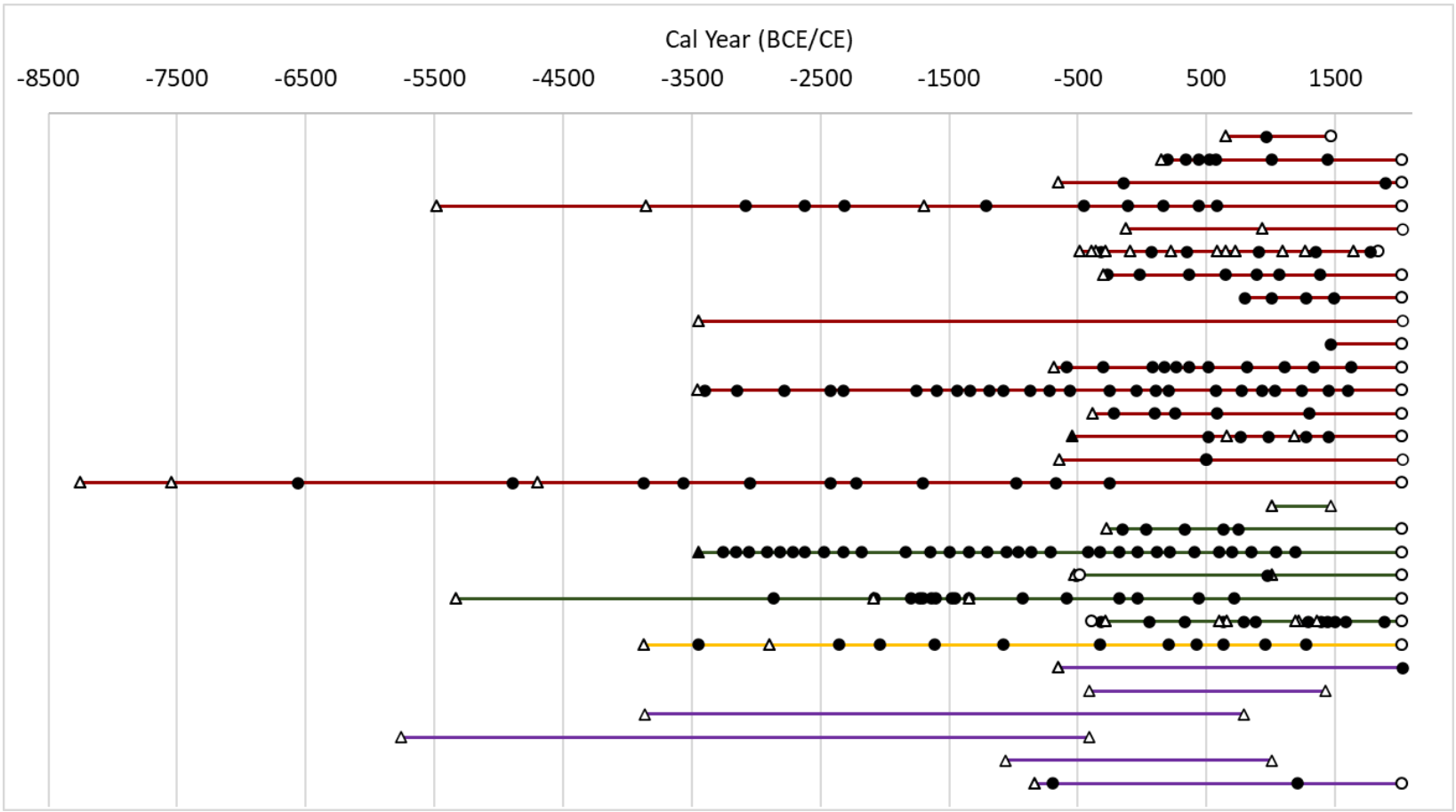
Cal Year (BCE/CE)
-8500
-7500
-6500
-5500
-4500
-3500
-2500
-1500
-500
500
1500

Figure 3: This chart indicates the estimated age of each fire identified in each core. Cores are represented by colored lines, red, OPF = open poor fens, green, TPF = treed poor fens, yellow, FPF = forested poor fen, purple, FRF = forested rich fens. Open circles represent tops of cores with modern material present, triangles represent radiocarbon dated samples between which dates are interpolated, filled symbols indicate fires. Note section 3.5.4: Methodological Considerations contains relevant details, most importantly that FRF data is uncertain.

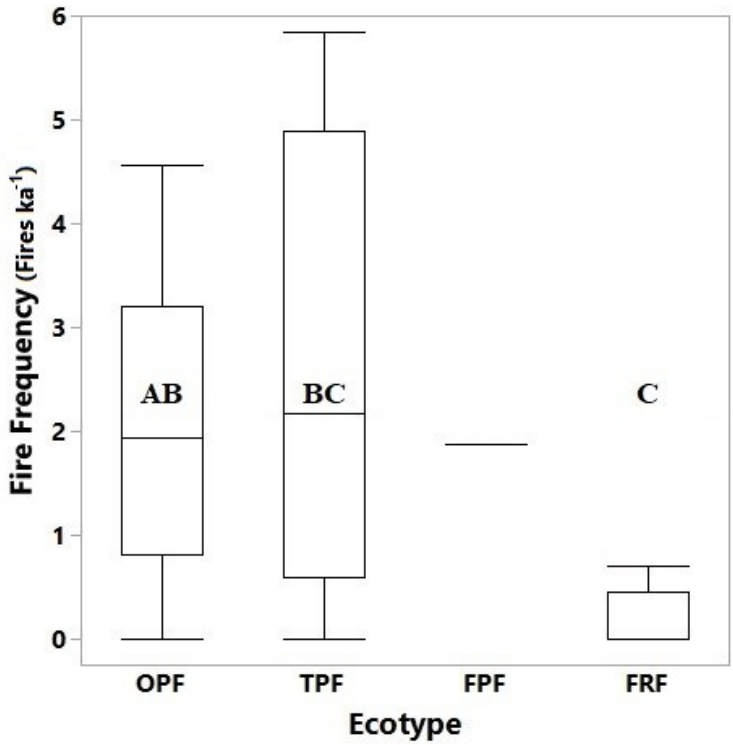

Figure 4: These box-and-whisker charts show the quartiles of the mean fire frequency estimates for the 4 ecotype classes examined. OPF = open poor fens, TPF = treed poor fens, FPF = forested poor fen, FRF = forested rich fens. Note section 3.5.4: Methodological Considerations contains relevant details, most importantly that FRF data is uncertain.

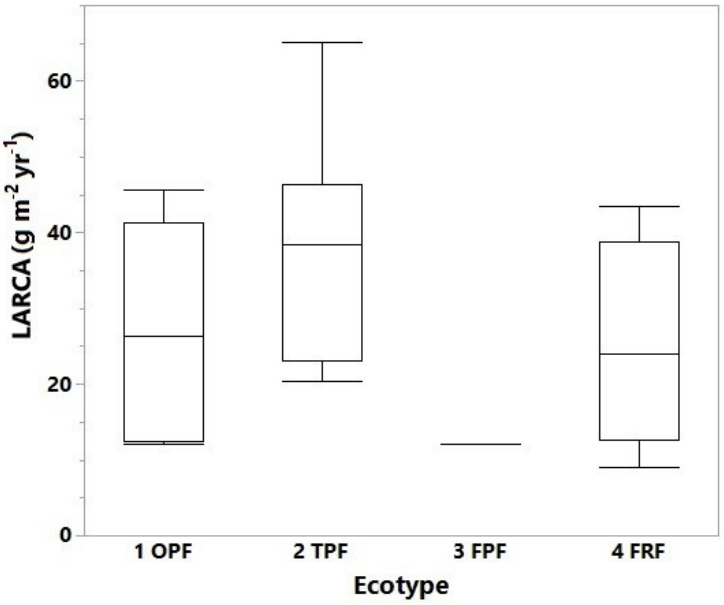

Figure 5: This box-and-whisker plot indicates the quartiles for the LARCA of the ecotypes. They vary widely within ecotypes, but we found no significant difference between classes (p=0.298). OPF = open poor fens, TPF = treed poor fens, FPF = forested poor fen, FRF = forested rich fens.

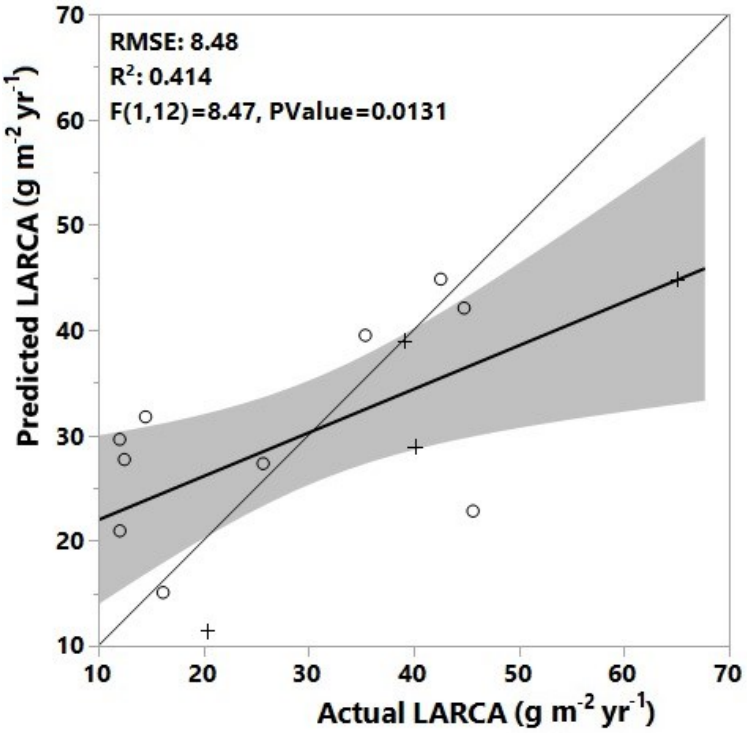

Figure 6: The predicted v actual plot for the linear regression model of LARCA and fire frequency for peatlands younger than 4000 years old. o symbols are open poor fens (OPFs) and + symbols are treed poor fens (TPFs). Forested rich fen (FRF) sites are omitted due to lack certainty.

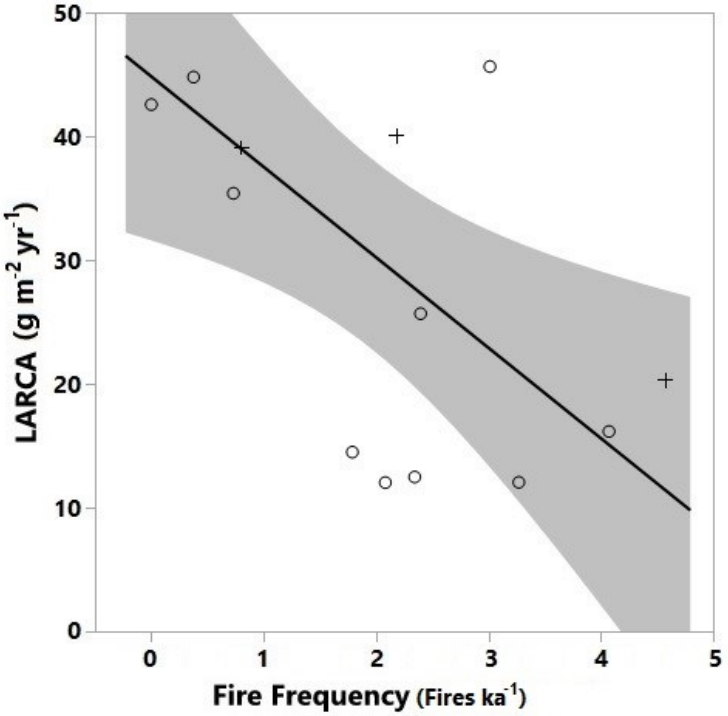

Figure 7: This plot shows the fitted relationship between LARCA and FF for peatlands younger than 4000 years old. o symbols are open poor fens (OPFs) and + symbols are treed poor fens (TPFs). Forested rich fen (FRF) sites are omitted due to lack of fire.

Table 1: This table summarizes our findings regarding FF and LARCA. OPF = open poor fens, green, TPF = treed poor fens, yellow, FPF = forested poor fen, purple, FRF = forested rich fens.

	OVERALL (N=29)		**OPF (N=16)**		**FRF (N=6)**		**TPF (N=6)**		**FPF (N=1)**	
	FF (Fires ka^{-1})	**LARCA (g m^{-2} yr^{-1})**	**FF (Fires ka^{-1})**	**LARCA (g m^{-2} yr^{-1})**	**FF (Fires ka^{-1})**	**LARCA (g m^{-2} yr^{-1})**	**FF (Fires ka^{-1})**	**LARCA (g m^{-2} yr^{-1})**	**FF (Fires ka^{-1})**	**LARCA (g m^{-2} yr^{-1})**
Maximum	5.9	43.0	4.6	43.0	5.9	35.4	1.9	9.0	0.7	37.1
3rd Quartile	2.4	29.5	3.1	24.0	4.0	32.2	1.9	9.0	0.3	32.6
Mean	1.7	20.1	2.0	17.6	2.6	26.0	1.9	9.0	0.2	22.7
Median	1.2	19.5	1.9	16.2	2.2	24.8	1.9	9.0	0.0	21.0
1st Quartile	0.4	10.8	1.0	8.8	1.1	20.0	1.9	9.0	0.0	13.9
Minimum	0.0	0.8	0.0	0.8	0.0	18.2	1.9	9.0	0.0	9.1

Table 2: Summary data for the 29 peat cores evaluated in this study. OPF = open poor fens, green, TPF = treed poor fens, yellow, FPF = forested poor fen, purple, FRF = forested rich fens. Names go by the convention Location.Core#. This is useful when cross-referencing with Appendix 2

Ecot ype	Name	Lat (dd) (WGS84)	Long (dd) (WGS84)	Depth (cm)	Calibrated Age (Cal yr BCE/CE)	Lower 95.7% CI (Cal yr BCE/CE)	Upper 95.7% CI (Cal yr BCE/CE)	# Fires	FF (Fires ka^{-1})	Mean Peat Acc. (g m^{-2} yr^{-1})	LARCA (g m^{-2} yr^{-1})	Mean BD (g cm^{-3})	Mean %OM	Mean %C
OPF	Betchler Lake.2001	46.302510	-84.910710	71	798	688	878	4	3.3	9.8	12.0	0.1	88.6	47.0
OPF	Betchler Lake.2011	46.314020	-84.955690	247	-3444	-3519	-3372	0	0.0	43.2	27.1	0.1	88.3	46.8
OPF	Betchler Lake.2021	46.303450	-84.960460	55	1462	1422	1621	1	1.8	3.6	14.5	0.0	84.5	44.8
OPF	Betchler Lake.2031	46.279850	-84.924260	149	-680	-789	-568	11	4.1	26.0	16.2	0.1	94.4	50.0
OPF	Bete Grise.1	47.381900	-87.973601	71	652	610	666	1	0.7	27.8	35.4	0.2	92.4	49.0
OPF	Bete Grise.14	47.376510	-87.979389	93	-122	-193	-50	0	0.0	37.4	42.6	0.2	93.0	49.3

OPF	Elmer, MN.1001	47.116033	-92.796300	147	-302	-354	-168	7	3.0	62.6	45.6	0.1	90.3	47.9
OPF	Hedmark Pines, WI.4001	45.761210	-88.560040	447	-637	-786	-541	1	0.4	81.1	44.8	0.1	92.0	48.8
OPF	Hedmark Pines, WI.4021	45.765060	-88.568460	223	-8254	-8284	-8225	11	1.1	18.9	12.2	0.1	88.2	46.7
OPF	Painesdale .12	47.022795	-88.719401	238	-5476	-5535	-5380	9	1.2	51.7	33.9	0.2	93.7	49.7
OPF	Ramsey Lake.3011	45.970990	-86.771700	247	-3454	-3516	-3365	25	4.6	71.2	40.8	0.1	95.4	50.6
OPF	Ramsey Lake.3021	45.983670	-86.759490	95	-380	-401	-232	5	2.1	33.2	12.0	0.1	92.0	48.7
OPF	Ramsey Lake.3031	45.984300	-86.758090	99	-539	-750	-412	6	2.3	20.3	12.5	0.1	92.2	48.8
OPF	Seney.16	46.186584	-86.020793	86	-483	-734	-403	6	2.4	36.8	25.7	0.3	89.7	47.6
OPF	Sleeper Lake.3	46.449698	-85.474701	53	152	81	210	7	3.7	-	-	0.2	91.8	48.7

OPF	Sleeper Lake.4	46.450797	-85.475000	51	-652	-753	-423	3	1.1	-	-	0.2	79.4	42.1
TPF	Alt Sph Lake.8001	46.275058	-86.627725	489	-5334	-5376	-5224	16	2.2	37.7	24.0	0.1	92.9	49.2
TPF	Betchler Lake.2041	46.276960	-84.922150	91	-275	-388	-206	5	2.2	37.8	40.1	0.1	92.4	49.0
TPF	Bete Grise.2	47.383634	-87.977336	84	1007	977	1025	0	0.0	55.7	65.0	0.2	92.7	49.1
TPF	Hedmark Pines, WI.4011	45.759110	-88.563520	413	-485	-746	-397	2	0.8	66.8	39.1	0.1	93.8	49.7
TPF	Peck Lake.8002	46.281630	-86.647683	167	-387	-401	-235	11	4.6	34.4	20.3	0.1	95.4	50.6
TPF	Ramsey Lake.3001	45.982170	-86.777370	249	-3448	-3622	-3371	32	5.9	62.5	37.9	0.1	94.8	50.3
FPF	Seney Forested. 7000	46.334880	-85.855840	184	-3869	-3951	-3797	11	1.9	17.1	12.2	0.1	87.5	46.3
FRF	Bob's Lake.21	46.210278	-87.509721	94	-3868	-3978	-3794	0	0.0	26.3	13.9	0.3	83.4	44.2

FRF	Eagle Harbor.10	47.452501	-88.151389	140	-652	-758	-416	1	0.4	52.8	43.6	0.2	88.1	46.7
FRF	Eagle Harbor.26	47.451385	-88.151669	144	-1059	-1197	-933	0	0.0	70.1	37.1	0.2	87.5	46.4
FRF	Marsin Core.19	47.183333	-88.642780	74	-413	-513	-396	0	0.0	64.5	34.2	0.3	83.3	44.1
FRF	Rexton. 5001	46.137160	-85.263730	49	-831	-900	-807	2	0.7	17.2	9.1	0.2	72.8	38.6
FRF	Whitney. 22	45.811943	-87.422222	99	-5756	-5829	-5721	0	0.0	26.4	14.0	0.4	77.9	41.3

3.8 References

Apfelbaum, S.I., A. Haney, F. Wang, J. Burris, and J. Carlson. 2017. Old-Growth Southern Boreal Forest Stability and Response to a Stand-Replacing Wildfire. Nat. Areas J. 37(4): 474–488. doi: 10.3375/043.037.0404.

Belton, D.J., R. Plowright, D.L. Kaplan, and C.C. Perry. 2018. A robust spectroscopic method for the determination of protein conformational composition – Application to the annealing of silk. Acta Biomater. 73: 355–364. doi: 10.1016/j.actbio.2018.03.058.

Benscoter, B.W., D. Greenacre, and M.R. Turetsky. 2015. Wildfire as a key determinant of peatland microtopography. Can. J. For. Res. 45(April): 1132–1136. doi: 10.1139/cjfr-2015-0028.

Benscoter, B.W., and D.H. Vitt. 2008. Spatial patterns and temporal trajectories of the bog ground layer along a post-fire chronosequence. Ecosystems 11(7): 1054–1064. doi: 10.1007/s10021-008-9178-4.

Blodau, C., N.T. Roulet, T. Heitmann, H. Stewart, J. Beer, et al. 2007. Belowground carbon turnover in a temperate ombrotrophic bog. Global Biogeochem. Cycles 21(1): 1–12. doi: 10.1029/2005GB002659.

Bourgeau-Chavez, L.L., S. Endres, R. Powell, M.J. Battaglia, B. Benscoter, et al. 2017. Mapping boreal peatland ecosystem types from multitemporal radar and optical satellite imagery. Can. J. For. Res. 47(4): 545–559. doi: 10.1139/cjfr-2016-0192.

Bridgham, S.D., J. Pastor, B. Dewey, J.F. Weltzin, and K. Updegraff. 2008. Rapid carbon response of peatlands to climate change. Ecology 89(11): 3041–3048. doi: 10.1890/08-0279.1.

Bridgham, S.D., K. Updegraff, and J. Pastor. 1998. Carbon, nitrogen, and phosphorus mineralization in northern wetlands. Ecology 79(5): 1545–1561. doi: 10.1890/0012-9658(1998)079[1545:CNAPMI]2.0.CO;2.

Broder, T., C. Blodau, H. Biester, and K.H. Knorr. 2012. Peat decomposition records in three pristine ombrotrophic bogs in southern Patagonia. Biogeosciences 9(4): 1479–1491. doi: 10.5194/bg-9-1479-2012.

Bronk Ramsey, C. 2009. Bayesian analysis of radiocarbon dates. Radiocarbon 51(1): 337–360. doi: 10.1017/S0033822200033865.

Brown, K.J., and T. Giesecke. 2014. Holocene fire disturbance in the boreal forest of central Sweden. Boreas 43(3): 639–651. doi: 10.1111/bor.12056.

Carcaillet, C., I. Bergman, S. Delorme, G. Hornberg, and O. Zackrisson. 2007. Long-term fire frequency not linked to prehistoric occupations in northern Swedish boreal forest. Ecology 88(2): 465–477. doi: 10.1890/0012-9658(2007)88[465:LFFNLT]2.0.CO;2.

Chimner, R.A., C.A. Ott, C.H. Perry, and R.K. Kolka. 2014. Developing and Evaluating Rapid Field Methods to Estimate Peat Carbon. Wetlands 34(6): 1241–1246. doi: 10.1007/s13157-014-0574-6.

Clymo, R.S., J. Turunen, and K. Tolonen. 1998. Carbon Accumulation in Peatland. Oikos

81(2): 368–388.

Cogbill, C. V. 1985. Dynamics of the boreal forests of the Laurentian Highlands, Canada. Can. J. For. Res. 15(1): 252–261. doi: https://doi-org.services.lib.mtu.edu/10.1139/x85-043.

Drobyshev, I., A. Granström, H.W. Linderholm, E. Hellberg, Y. Bergeron, et al. 2014. Multi-century reconstruction of fire activity in northern European boreal forest suggests differences in regional fire regimes and their sensitivity to climate. J. Ecol. 102(3): 738–748. doi: 10.1111/1365-2745.12235.

Fenton, N.J., and Y. Bergeron. 2008. Does time or habitat make old-growth forests species rich? Bryophyte richness in boreal Picea mariana forests. Biol. Conserv. 141(5): 1389–1399. doi: 10.1016/j.biocon.2008.03.019.

Flanagan, N.E., H. Wang, S. Winton, and C.J. Richardson. 2020. Low-severity fire as a mechanism of organic matter protection in global peatlands: Thermal alteration slows decomposition. Glob. Chang. Biol. 26(March): 3930–3946. doi: 10.1111/gcb.15102.

Fujiwara, A., T. Hirawake, K. Suzuki, I. Imai, and S.I. Saitoh. 2014. Timing of sea ice retreat can alter phytoplankton community structure in the western Arctic Ocean. Biogeosciences 11(7): 1705–1716. doi: 10.5194/bg-11-1705-2014.

Gaffney, J.S., N.A. Marley, and K.J. Smith. 2015. Characterization of fine mode atmospheric aerosols by Raman microscopy and diffuse reflectance FTIR. J. Phys. Chem. A 119(19): 4524–4532. doi: 10.1021/jp510361s.

Gardegaront, M., D. Farlay, O. Peyruchaud, and H. Follet. 2018. Automation of the Peak Fitting Method in Bone FTIR Microspectroscopy Spectrum Analysis: Human and Mice Bone Study. J. Spectrosc. 2018(Figure 1). doi: 10.1155/2018/4131029.

Giorgi, F. 2006. Climate change hot-spots. Geophys. Res. Lett. 33(8): 1–4. doi: 10.1029/2006GL025734.

Goldstein, A., W.R. Turner, S.A. Spawn, K.J. Anderson-teixeira, S. Cook-patton, et al. 2020. Protecting irrecoverable carbon in Earth's ecosystems. Nat. Clim. Chang. 10(April): 287–295. doi: 10.1038/s41558-020-0738-8.

Hodgkins, S.B., C.J. Richardson, R. Dommain, H. Wang, P.H. Glaser, et al. 2018. Tropical peatland carbon storage linked to global latitudinal trends in peat recalcitrance. Nat. Commun. 9(1): 1–13. doi: 10.1038/s41467-018-06050-2.

Hribljan, J.A., E.S. Kane, and R.A. Chimner. 2017. Implications of Altered Hydrology for Substrate Quality and Trace Gas Production in a Poor Fen Peatland. Soil Sci. Soc. Am. J. 81(3): 633. doi: 10.2136/sssaj2016.10.0322.

Johnstone, J.F., T.N. Hollingsworth, F.S. Chapin, and M.C. Mack. 2010. Changes in fire regime break the legacy lock on successional trajectories in Alaskan boreal forest. Glob. Chang. Biol. 16(4): 1281–1295. doi: 10.1111/j.1365-2486.2009.02051.x.

Jules, A.N., H. Asselin, Y. Bergeron, and A.A. Ali. 2018. Are marginal balsam fir and eastern white cedar stands relics from once more extensive populations in north-eastern North America? Holocene 28(10): 1672–1679. doi: 10.1177/0959683618782601.

Kalbitz, K., W. Geyer, and S. Geyer. 1999. Spectroscopic properties of dissolved humic substances - A reflection of land use history in a fen area. Biogeochemistry 47(2): 219–238. doi: 10.1023/A:1006134214244.

Kane, E.S., E.S. Kasischke, D.W. Valentine, M.R. Turetsky, and A.D. McGuire. 2007. Topographic influences on wildfire consumption of soil organic carbon in interior Alaska: Implications for black carbon accumulation. J. Geophys. Res. Biogeosciences 112(3): 1–11. doi: 10.1029/2007JG000458.

Keller, J.K., A.K. Bauers, S.D. Bridgham, L.E. Kellogg, and C.M. Iversen. 2006. Nutrient control of microbial carbon cycling along an ombrotrophic-minerotrophic peatland gradient. J. Geophys. Res. Biogeosciences 111(3): 1–14. doi: 10.1029/2005JG000152.

Keller, J.K.., J.R. White, S.D. Bridgeham, and J. Paster. 2004. Climate change effects on carbon and nitrogen mineralization in peatlands through changes in soil quality. Glob. Chang. Biol.: 1053–1064. doi: 10.1111/j.1365-2486.2004.00785.x.

Kim, S., R.W. Kramer, and P.G. Hatcher. 2003. Graphical Method for Analysis of Ultrahigh-Resolution Broadband Mass Spectra of Natural Organic Matter, the Van Krevelen Diagram. Anal. Chem. 75(20): 5336–5344. doi: 10.1021/ac034415p.

Kolka, R., S.D. Bridgham, and C.L. Ping. 2016. Soils of peatlands: histosols and gelisols. In: Vepraskas, M.J. and Craft, C.L., editors, Wetlands soils: genesis, hydrology, landscapes and classification. Press/Lewis Publishing, Boca Raton, FL. p. 277–309

Kost, M.A., D.A. Albert, J.G. Cohen, B.S. Slaughter, R.K. Schillo, et al. 2007. Natural

Communities of Michigan: Classification and Description. Michigan Nat. Featur. Invent. Rep. No. 2007-21. https://mnfi.anr.msu.edu/communities/community.cfm?id=10652 (accessed 20 September 2016).

Kudray, G. 2019. Field Guide Hiawatha National Forest Ecological Classification System.

Kuhry, P. 1994. The role of fire in the development of Sphagnum-dominated peatlands in western boreal Canada. J. Ecol. 82(4): 899–910.

Laiho, R. 2006. Decomposition in peatlands: Reconciling seemingly contrasting results on the impacts of lowered water levels. Soil Biol. Biochem. 38(8): 2011–2024. doi: 10.1016/j.soilbio.2006.02.017.

Langor, D.W., E.K. Cameron, C.J.K. Macquarrie, A. Mcbeath, A. Mcclay, et al. 2014. Non-native species in Canada's boreal zone: diversity, impacts, and risk. Environ. Rev. 22(4): 372–420.

Larson, E.R., and M.A. Green. 2017. Fire History at the Confluence of the Driftless Area and Central Sand Plains of Wisconsin: A Case Study from Castle Mound Pine Forest State Natural Area. Nat. Areas J. 37(3): 309–321. doi: 10.3375/043.037.0306.

Loisel, J., A. V. Gallego-Sala, M.J. Amesbury, G. Magnan, G. Anshari, et al. 2021. Expert assessment of future vulnerability of the global peatland carbon sink. Nat. Clim. Chang. 11(1): 70–77. doi: 10.1038/s41558-020-00944-0.

Malmer, N., and B. Wallén. 1993. Accumulation and release of organic matter in

ombrotrophic bog hummocks - processes and regional variation. Ecography (Cop.). 16(3): 193–211.

Marcott, S.A., J.D. Shakun, P.U. Clark, and A.C. Mix. 2013. A reconstruction of regional and global temperature for the past 11,300 years. Science (80-.). 339(6124): 1198–1201. doi: 10.1126/science.1228026.

Nichols, J.E., and D.M. Peteet. 2019. Rapid expansion of northern peatlands and doubled estimate of carbon storage. Nat. Geosci. 12(November): 917–922. doi: 10.1038/s41561-019-0454-z.

Nolte, C.G., J.J. Schauer, G.R. Cass, and B.R.T. Simoneit. 2001. Highly polar organic compounds present in wood smoke and in the ambient atmosphere. Environ. Sci. Technol. 35(10): 1912–1919. doi: 10.1021/es001420r.

Pitkänen, A., J. Turunen, and K. Tolonen. 1999. The role of fire in the carbon dynamics of a mire, eastern Finland. Holocene 9(4): 453–462. doi: 10.1191/095968399674919303.

Potvin, L.R., E.S. Kane, R.A. Chimner, R.K. Kolka, and E.A. Lilleskov. 2015. Effects of water table position and plant functional group on plant community, aboveground production, and peat properties in a peatland mesocosm experiment (PEATcosm). Plant Soil 387(1–2): 277–294. doi: 10.1007/s11104-014-2301-8.

Rayfield, B., V. Paul, F. Tremblay, M.J. Fortin, C. Hély, et al. 2021. Influence of habitat availability and fire disturbance on a northern range boundary. J. Biogeogr. 48(2): 394–404. doi: 10.1111/jbi.14004.

Robinson, S.D., and T.R. Moore. 1999. Carbon and peat accumulation over the past 1200 years in a landscape with discontinuous permafrost, Northwestern Canada. Global Biogeochem. Cycles 13(2): 591–601. doi: 10.1002/(ISSN)1944-9224.

Robinson, S.D., and T.R. Moore. 2000. The influence of permafrost and fire upon carbon accumulation in high boreal peatlands, Northwest Territories, Canada. Arct. Antarct. Alp. Res. 32(2): 155–166. doi: 10.2307/1552447.

Sadat, A., and I.J. Joye. 2020. Peak fitting applied to fourier transform infrared and raman spectroscopic analysis of proteins. Appl. Sci. 10(17). doi: 10.3390/app10175918.

Sazawa, K., T. Wakimoto, M. Fukushima, Y. Yustiawati, M.S. Syawal, et al. 2018. Impact of Peat Fire on the Soil and Export of Dissolved Organic Carbon in Tropical Peat Soil, Central Kalimantan, Indonesia. ACS Earth Sp. Chem. 2(7): 692–701. doi: 10.1021/acsearthspacechem.8b00018.

Šeparović, L., A. Alexandru, R. Laprise, A. Martynov, L. Sushama, et al. 2013. Present climate and climate change over North America as simulated by the fifth-generation Canadian regional climate model.

Simoneit, B.R.T., J.J. Schauer, C.G. Nolte, D.R. Oros, V.O. Elias, et al. 1999. Levoglucosan, a tracer for cellulose in biomass burning and atmospheric particles. Atmos. Environ. 33(2): 173–182. papers3://publication/uuid/3E935E2F-ED96-40DC-8374-344125150073.

Skoog, D.A. 2014. Fundamentals of analytical chemistry. 9th ed. Thomson-Brooks/Cole,

Belmont, California.

Stuiver, M., and H.A. Polach. 1977. Discussion of Reporting of 14C Data. Radiocarbon 19(3): 355–363.

Taylor, A.R., and H.Y.H. Chen. 2011. Multiple successional pathways of boreal forest stands in central Canada. Ecography (Cop.). 34(2): 208–219. doi: 10.1111/j.1600-0587.2010.06455.x.

Turetsky, M.R., B. Benscoter, S. Page, G. Rein, G.R. van der Werf, et al. 2015. Global vulnerability of peatlands to fire and carbon loss. Nat. Geosci. 8(1): 11–14. doi: 10.1038/NGEO2325.

Turetsky, M.R., E.S. Kane, J.W. Harden, R.D. Ottmar, K.L. Manies, et al. 2011. Recent acceleration of biomass burning and carbon losses in Alaskan forests and peatlands. Nat. Geosci. 4(1): 27–31. doi: 10.1038/ngeo1027.

U.S. Environmental Protection Agency. 2013. Level III and IV Ecoregions of the Continental United States. https://www.epa.gov/eco-research/level-iii-and-iv-ecoregions-continental-united-states%0Ahttp://www.epa.gov/wed/pages/ecoregions/level_iii_iv.htm.

Updegraff, K., S.D. Bridgham, J. Pastor, P. Weishampel, and C. Harth. 2001. Response of CO2 and CH4 emissions from peatlands to warming and water table manipulation. Ecol. Appl. 11(2): 311–326. doi: 10.1890/1051-0761(2001)011[0311:rocace]2.0.co;2.

Updegraff, K., J. Pastor, S.D.. Bridgham, and C.A.. Johnston. 1995. Environmental and

Substrate Controls over Carbon and Nitrogen Mineralization in Northern Wetlands. Ecol. Appl. 5(1): 151–163.

Verbeke, B. 2018. Peatland Organic Matter Chemistry Trends Over A Global Latitudinal Gradient. Thesis. http://purl.flvc.org/fsu/fd/2018_Sp_Verbeke_fsu_0071N_14561.

Vetrita, Y., and M.A. Cochrane. 2020. Fire frequency and related land-use and land-cover changes in Indonesia's Peatlands. Remote Sens. 12(1). doi: 10.3390/RS12010005.

Viau, A.E., K. Gajewski, M.C. Sawada, and P. Fines. 2006. Millennial-scale temperature variations in North America during the Holocene. doi: 10.1029/2005JD006031.

Vogel, J.S., J.R. Southon, and D.E. Nelson. 1987. Catalyst and binder effects in the use of filamentous graphite for AMS. Nucl. Inst. Methods Phys. Res. B 29(1–2): 50–56. doi: 10.1016/0168-583X(87)90202-3.

Walker, X.J., J.L. Baltzer, L. Bourgeau-Chavez, N.J. Day, C.M. Dieleman, et al. 2020. Patterns of Ecosystem Structure and Wildfire Carbon Combustion Across Six Ecoregions of the North American Boreal Forest. Front. For. Glob. Chang. 3(July): 1–12. doi: 10.3389/ffgc.2020.00087.

Walker, X.J., J.L. Baltzer, S.G. Cumming, N.J. Day, C. Ebert, et al. 2019. Increasing wildfires threaten historic carbon sink of boreal forest soils. Nature 572(7770): 520–523. doi: 10.1038/s41586-019-1474-y.

Wieder, R.K., and D.H. Vitt, editors. 2010. Boreal Peatland Ecosystems. Springer.

Wiken, E., F.J. Nava, and G. Griffith. 2011. North American Terrestrial Ecoregions—

Level III. (April): 1–149.

Young, D.M., A.J. Baird, A. V. Gallego-Sala, and J. Loisel. 2021. A cautionary tale about using the apparent carbon accumulation rate (aCAR) obtained from peat cores. Sci. Rep. 11(1): 1–12. doi: 10.1038/s41598-021-88766-8.

Yu, Z.C. 2012. Northern peatland carbon stocks and dynamics: A review. Biogeosciences 9(10): 4071–4085. doi: 10.5194/bg-9-4071-2012.

Zackrisson, O. 1977. Influence of Forest Fires on the North Swedish Boreal Forest. Oikos 29: 22–32. https://www.jstor.org/stable/3543289.

Zhang, Y., J. Maxted, A. Barber, C. Lowe, and R. Smith. 2013. The durability of clear polyurethane coil coatings studied by FTIR peak fitting. Polym. Degrad. Stab. 98(2): 527–534. doi: 10.1016/j.polymdegradstab.2012.12.003.

Zoppi, U., J. Crye, Q. Song, and A. Arjomand. 2007. Performance evaluation of the new AMS system at Accium Biosciences. Radiocarbon 49(1): 173–182. doi: 10.1017/S0033822200041990.

4 Is Woody Peat More Recalcitrant than *Sphagnum* Peat?

4.1 Abstract

Peatlands contain enormous carbon stocks, but their peat quality, and therefore lability, is variable. Determining the drivers of variance in peat molecular quality helps us to understand the peat formation process and to predict how changes could affect the carbon balance of peatland systems. Like upland systems, peatlands can vary in tree cover from completely open to forested. We compared open peatlands dominated by *Sphagnum* mosses to forested, or silvic, peatlands dominated by black spruce and tamarack or northern white cedar to understand the effect of forestation on peat quality. We used FTIR spectrometry to semi-quantitatively analyze peat properties throughout the depth profile in silvic and *Sphagnum* moss fen peatlands across the hemi-boreal Upper Great Lakes region. We found that tree cover was associated with differences in both surficial peat, largely though exclusion of moss species, and deep peat. Silvic, or forested, rich fens had lower molecular lability peat than *Sphagnum* poor fens as shown by Fourier-transform infrared spectral indices. This research identifies key differences between silvic and *Sphagnum* peatlands with implications for future assessments, predictions, and conservation.

4.2 Introduction

Peatlands are critical long-term carbon (C) sinks, yet there is much uncertainty concerning global C stocks within peatlands, with estimates ranging from 545 to 1055 Pg C (Nichols and Peteet, 2019). The C storage function of peatlands primarily occurs through the production, accumulation, and storage of C-rich peat, in excess of decomposition. However, there is concern that the C sink provided by peatlands has or will soon weaken or reverse, releasing C stored in peat through decomposition driven by climate change and land conversion, among other drivers (Goldstein et al., 2020).

Peat differs in vulnerability to decomposition based on its biochemical composition (molecular lability/recalcitrance) and environment (environmental lability/recalcitrance). This inherent molecular potential for decomposition is referred to hereafter as peat quality, “lability,” and “recalcitrance” should be understood to refer to the concentration of labile (alkane, alcohol) or recalcitrant (phenolic, aromatic) molecular components of peat. Environmental lability/recalcitrance refers to the biophysical environment for decomposition. Because decomposition occurs on a molecular level, this environment includes the physical, chemical, and biological setting for the molecules in question from the nanoscopic level up. The peat quality is therefore just one small, but important, part required to understand organic matter decomposition. Having a higher composition of labile components means this peat is higher quality (best thought of from the perspective of decomposers), and therefore it is more susceptible to mineralization and consequent loss of C, given a conducive environment. The initial composition of

organic matter inputs dictates the materials available for decomposition and conversion to peat. A common input for peat formation in boreal and hemi-boreal peatlands are peat mosses in the *Sphagnum* genus. *Sphagnum* moss-dominated peatlands produce peat that is visibly different from the rarer (in the hemi-boreal region) tree-dominated peatlands, which produce silvic peat. However, these different initial producers of peat substrates are not the sole cause of differences in peat (Laiho, 2006). Labile components are preferentially consumed during decomposition, leaving behind waste products and more recalcitrant components, reducing peat quality, and increasing its resistance to degradation overall. In this way, past decomposition is a major driver of current peat quality. Differences in peat inputs likely result in peat with different peat qualities, even after significant decomposition has occurred. However, disentangling the effects of input type from covarying biophysical environmental constraints to decomposition, such as climate and hydrology, has not been well elucidated (Bridgham et al., 1998). However, the peatland environment is broadly unfavorable for decomposition, primarily due to inundation, and in northern peatlands low temperatures also reduce the rate of decomposition. Many peatlands also have low nutrient availability, due variously to unfavorable pH, low nutrient input, and/or high nutrient demand, which limits the effectiveness of decomposers because nutrients are required to carry out the work of decomposition.

Peatlands are often delineated by their vegetation communities and hydrology (pH) (Kudray, 2019), but it is not yet established how these factors delineate changes in peat biochemical properties. Numerous studies have used mesocosms or incubations to

compare the C cycling response of different peat types and sometimes depths (Blodau et al., 2007) to changes in environmental conditions, including temperature (Updegraff et al., 1995), hydrology (Updegraff et al., 2001; Keller et al., 2004), and nutrient loading (Keller et al., 2006). These studies generally refer to 2-pool methods for estimating C fluxes, with a small labile pool which is responsible for most of the mineralization potential, and a large recalcitrant pool which is reactive to a much lower degree. Collectively, these experiments paint a complex picture of decomposition in peatlands, with environmental factors including temperature, hydrology, aeration, and duration of incubation all having significant effects on peat C cycling. In particular, extensive study employing incubations to assess peat quality has shown *Sphagnum* peat to have more labile organic matter than forest peat derived from cedar trees (Bridgham et al., 1998). However, how these changes in inherent molecular quality vary with other wood-derived peat (such as spruce or tamarack), or with depth in the peat profile, has not been investigated for hemi-boreal peatlands.

We investigated changes in quality of silvic peat (cedar derived and spruce/tamarack derived) and *Sphagnum* moss peat across the entire depth profile. These ecotypes are directly comparable to the "cedar swamps" and "acidic fens," respectively, from Bridgham et al., 1998. While studies already exist comparing peat quality throughout depth across latitudes as a proxy for climate (Hodgkins et al., 2018; Verbeke, 2018), we elected to make our comparison within one region to reduce confounding effects relating to climate. We hypothesized that the silvic peat was significantly lower in quality than *Sphagnum* peat, containing a lower concentration of labile molecules, in

other words a smaller labile C pool, and therefore being more recalcitrant overall, following the findings of Bridgham et al., 1998. We expect that this difference will be most apparent near the surface and will decrease, but not disappear completely, with depth.

4.3 Methods

4.3.1 Sample Locations

We sampled peatlands across the Upper Peninsula of Michigan, northern Wisconsin, and northern Minnesota (Fig. 1). The boreal zone of North America is typically considered to reach its southernmost extent along the north shore of Lake Superior, with a hemi-boreal zone that encompasses the Upper Peninsula of Michigan, a small part of northern Wisconsin, and much of northern Minnesota (Langor et al., 2014). Our sampling locations were all within this hemi-boreal zone. All sites also fell within the Northern Forests (I) > Mixed Wood Shield (II) > Northern Lakes and Forests (III) Ecoregion as defined by the US EPA (U.S. Environmental Protection Agency, 2013). This ecoregion is described as “humid continental, marked by warm summers and severe winters, with no pronounced dry season,” with a mean annual temperature ranging from ~2°C to ~6°C, and mean annual precipitation ranging from 500 to 960 mm (Wiken et al., 2011).

The peatlands studied are best described as fens. Both poor fens and rich fens are common within the hemi-boreal region. These fens are extensive and may be isolated,

coastal, or part of large upland-peatland complexes (Bourgeau-Chavez et al., 2017, see Fig. 10). The poor fens sampled for this study are dominated by *Sphagnum* (L.) mosses with additional typical species being black spruce (*Picea mariana* (Mill.) Britton, Sterns & Poggenb.), tamarack (*Larix laricina* (Du Roi) K. Koch), sedges (*Carex spp.* L.), Labrador tea (*Rhododendron groenlandicum* (Oeder) Kron & Judd), bog rosemary (*Andromeda polifolia* L.), leatherleaf (*Chamaedaphne calyculata* L.), etc. (Kost et al., 2007). The forested rich fens that we sampled are silvic and dominated by northern white cedar (*Thuja occidentalis* L.) with presence of balsam fir (*Abies balsamea* (L.) Mill.), white spruce (*Picea glauca* (Moench) Voss), hemlock (*Tsuga canadensis* L.) with a sparse understory due to heavy shading and deer herbivory (Kost et al., 2007). The forested poor fen site is unique in that densely forested peatlands with low pH are not common in this region. It follows the same pattern of the poor fens but with much greater canopy cover dominated by black spruce and tamarack with additional bog birch (*Betula pumila* L.). This site was included as it offered a unique opportunity to investigate the effects of woody spruce vegetation in poor fens, which contrasts with the cedar dominating the forested rich fen sites.

4.3.2 Field Sampling

We collected 30 peat cores from across the Upper Peninsula of Michigan, northern Wisconsin, and northern Minnesota. Fourteen cores were collected in 2012 for a related study (Chimner et al. 2014) and were stored dried and ground until analyzed for this project. We collected 15 new peat cores the exact same way as the earlier peat cores

by using the following methods. At each poor fen site, a sharpened PVC tube was inserted into precut peat to a depth of 50 cm. The surficial peat was carefully removed from the tube, cut into 10 cm depth increments, and stored in sealed plastic bags. We then used a Russian peat corer (Aquatic Research Instruments, Hope, ID, USA) to core the remaining deeper peat in 50 cm segments. We avoided coring in laggs or ecotones to get the most representative samples possible. Peat samples were stored in a freezer immediately upon return to the lab, usually within hours of extraction. We logged location data using a Garmin eTrex 20.

4.3.3 Sample Processing

In the lab, we cut the still-frozen peat into ~2 cm increments with a hand saw and dried them to constant weight in an oven at 60°C. Samples were weighed to measure bulk density. Samples were then ground and homogenized using a Wiley mill equipped with a 40 mesh screen. This resulted in a powdered sample with a maximum particle size of 425 microns. A subsample of each ~2 cm peat increment was combusted at 500°C for 12 hours to obtain % organic matter by mass.

4.3.4 Spectrometry

We used Fourier-transform infrared spectrometry (FTIR) to analyze the peat quality throughout the depth profile for each core. Preparation and analyses were conducted as described in detail in section 2. Briefly, we prepared samples for FTIR by mixing milled peat with FTIR-grade KBr to 10% sample by mass. We dried samples at

60º C for >24 hours before subjecting them to diffuse reflectance FTIR (DRIFT) using a Thermo Scientific Nicolet iS5 spectrometer with an iD Foundation – Diffuse accessory (Thermo Fisher Scientific, Ann Arbor, MI). We produced spectra of the 400-4000 cm-1 range with resolution of 4 cm-1 and a data interval of 0.5 cm-1 by averaging 64 scans. We used ultrapure N2 purge and automatic background correction to minimize the interference of humidity and to improve spectral fidelity.

We used custom code written in Python to baseline correct and standardize the spectra to compare relative peak heights, rather than absolute data, which was variable due to sample properties, dilution factors, and atmospheric conditions during spectrometry. We used several indices previously applied to evaluating peat properties (Hribljan et al. 2017, Flanagan et al. 2020). These included two substrate quality indices, a lignin index, and a humification index (cf., Table 1). The carbonyl/lignin ratio (C/L index) (1725/1620) is an index of the humification of fulvic acids (Kalbitz et al., 1999). The lipid/polysaccharide ratio (L/P index) (2920/1060) measures the peat composition, representing mainly waxes vs cellulose and hemicellulose (Hribljan et al., 2017). The lignin index (1265, 1515, 1620) simply averages three lignin peaks on the FTIR spectra, and represents lignin concentration (Hribljan et al., 2017). The humification index (1630/1030) compares aromatics to carbohydrates, and indicates recalcitrance (Flanagan et al., 2020). It is important to note that all these FTIR indices are semi-quantitative (relative) measures. These FTIR indices represent the relative abundance of different biomolecules in peat, which relate to lability, and inversely recalcitrance, by the resistance of these biomolecules to degradation. For simplicity, we consider the C/L

index positively related to lability, the lignin and humification indices negatively related to lability, and the L/P index related to botanical origin. The Python script and further index details are available in the supplemental.

4.3.5 Statistics

We binned vertical profile data into 25-cm depth increments to average out fine-scale peat heterogeneity. Sample bins 0-25 and 25-50 cm were considered surface samples for our purposes and all deeper bins were considered deep. We did not require a depth bin to be fully populated by samples, we produced bins if there was one or more sample within the depth range of the bin. When samples would have crossed bin boundaries they were included only in the upper bin. Due to these considerations, bins were not entirely uniform in number of samples included or mean depth due to missing samples or imperfect division of subsamples.

We used principal components analysis (PCA) of index results to identify 3 groups of samples *a posteriori,* open poor fens, OPF, forested poor fens, FPF, and forested rich fens, FRF. Open sites were characterized by a lack of tree cover, either devoid of trees or with sparse, stunted trees. Open poor fens possess *Sphagnum* peat. Forested sites were characterized by dense stands of high stature trees. These were primarily black spruce (*Picea mariana*) and tamarack (*Larix laricina*) in the FPF and northern white cedar (*Thuja occidentalis*) in the FRFs. The FRFs possess silvic peat. The forested poor fen was an anomaly which is shown as an example of an intermediate between *Sphagum* and silvic peat. By using these group divisions, we focused on tree

cover as the most potentially impactful difference in vegetation. We produced separate surficial (0-50 cm) and full (0 cm - base) PCAs to focus on the differences in contemporary ecosystems (surface peat) and the properties of peat profiles overall.

For analysis of individual FTIR indices, we used nonparametric mean separation to compare across peat types but within peat depth categories, and within peat types but across peat depth categories. Initial analysis of each FTIR index indicated that some were not normally distributed. We elected to use nonparametric statistics in all cases for the sake of consistency and simplicity (Fujiwara et al., 2014). We used Welch's ANOVA for means testing before proceeding to perform all pairs comparisons via Steel-Dwass method in JMP v14. We considered means and pairs significantly different at $\alpha = 0.05$.

4.4 Results

4.4.1 Surficial PCA

Principal components analysis on surface peat samples (0-25 cm and 25-50 cm), which we expect to best reflect the contemporary ecosystem, resulted in principal component one explaining 80.8% of the variance (Figure 2). Component two explained 13.4%. Component one was driven by the humification, lignin, carbonyl/lignin (C/L) and lipid/polysaccharide (L/P) substrate quality indices, in order of importance (Table 1). Component two was mainly composed of the L/P substrate quality index, with lesser contributions from the C/L quality index and the lignin index.

The principal components analysis of surface peat samples delineated three distinct groups (Fig. 2, Table 1). There is a distinct separation between the OPFs, in one group, and the FPF and FRF sites, in two other groups, similarly positioned along the axis of component 1. Component 1 appears to be reflective of the relative degree of tree cover and is associated with both humification and lignin. Component 2 appears to separate sites by lignin concentration and other subtle variances in peat quality, namely lipid/polysaccharide ratio. The separation on this axis appears to distinguish the forested rich and the poor fens from one another.

4.4.2 Whole Core PCA

The PCA of all peat depths binned into 25 cm depth intervals produces a similar output to the surface peat analysis (Fig. 3, Table 2). The major loadings remain the same, but there is more of a balance between components 1 and 2, which explain 64.8 and 26.1 % of the variance, respectively. In this PCA there are only two groups that can be clearly interpreted, rich fens and poor fens, including the FPF. Notably, there is less separation in quality indices across peat types. The trend with depth is that near surface samples in the poor fen have negative loadings on component 1, while deeper peat samples cluster more around the center of the plot. Conversely, the position of cedar samples in the ordination space did not change much with depth.

4.4.3 Individual Indices

Our three groupings showed distinctive differences in peat qualities (Figure 4). Open poor fens showed significant differences between peat depth bins, with their

surface samples being significantly higher than their deep peat on the carbonyl/lignin index, and significantly lower than their deep peat on the lipid/polysaccharide, lignin, and humification indices. In comparison, the FPF and FRFs showed no significant difference with depth in any indices. Open poor fens also differed significantly within depth classes from the other peat types; they are significantly higher than FRFs in C/L index and lower in L/P, lignin, and humification indices. Open poor fens were significantly lower in L/P indices and humification indices than FPF at depth (Figure 4). These results are reiterated in a continuous, unbinned, manner in figure 5, which shows a continuous mean and confidence interval for each ecotype for each index (Figure 5). Notably, most changes with depth, when present, within ecotype and index, occur between 25 and 75 cm.

4.5 Discussion

We defined changes in peat chemistry that occurred with differences in tree cover and the role played by depth in two common types of hemi-boreal peatlands. We found that rich fens have silvic peat that is more recalcitrant by all metrics than open poor fens and remained more recalcitrant throughout the peat profile. Extensive tree cover was associated with low peat quality at the surface, and more homogeneity across the depth profile. As peat depth increased, peat became more humified, and the distinction between the open poor fens and the FPF was lessened, though they still differed in L/P and humification indices. These findings suggest that FRF peat is more recalcitrant both at the surface and at depth than poor fen peat, even in the FPF.

The PCA of all depth increments and comparison of individual indices reflected the tendency of peat to humify with age and depth, resulting in a concentration of

recalcitrant peat components and therefore a tendency toward chemical homogeneity and resistance to further degradation as substrates are processed down toward states of minimal accessible energy. The forested sites, FPF and FRF, both had little understory vegetation, due to shading from the canopy. As a result, they both had surface peats which were highly recalcitrant and not significantly different from their deep peat, in contrast to the OPFs. This observation of high surface humification confirms our hypotheses and matches observations of high surficial decomposition in cedar peatlands using the von Post decomposition scale (Bridgham et al., 1998; Kolka et al., 2016). This also agrees with the labile C pool estimates from Bridgham et al. 1998. The open poor fens showed equivalent or greater differences with depth as observed between peatland classes. This is reflective of the large difference in peat properties between the fibric to hemic surface samples of the poor fens and their hemic to sapric deeper peat samples. The gradual increase in humification with depth in OPFs, which never reaches parity with humification in other ecotypes implies that in OPFs the decomposition process is slower and lability higher.

4.5.1 Implications

We established that there are distinct differences in peat properties which vary with tree cover, even within the same region. The trends we found across peatland ecosystem biomarkers are similar to those found by (Hodgkins et al., 2018), who investigated peat properties across latitude. Their low latitude peatlands, particularly the American Pocosin sites, which were shrub-dominated, and Bruneian Mendaram sites, which were tree-dominated, resembled our FRF sites, with lower lability at the surface,

which decreased little with depth. Meanwhile, their high latitude peatlands were much like our poor fen peatlands, *Sphagnum*-dominated, with higher relative lability at the surface, which decreased to be similar to the more recalcitrant peatland at depth. These similarities make sense, as the sites selected by Hodgkins et al., had a covariance of vegetation with latitude: their high latitude peat was from sites similar to our poor fens, and their sites became increasingly tree dominated with decreasing latitude, similar to our FRFs. Another recent study by Verbeke et al. replicated the latitudinal gradient and explicitly attempted to separate the effect of latitude and vegetation (Verbeke, 2018). They claim to have found effects of latitude separate from those of vegetation. One implication of the similarity between our findings is that forested boreal peatlands and forested tropical peatlands are similar in peat humification trends, if not species composition. Treed peatlands producing silvic peat follow similar trends with depth in vastly different latitudes. Open *Sphagnum* and cushion plant peatlands of Patagonia also follow similar patterns of humification as our OPFs (Broder et al., 2012). This implies that in peatlands plant functional type (e.g. tree, shrub, or moss) may be more important to peat lability than species identity.

We established that FRF sites had more recalcitrant peat than poor fen sites, which indicates greater molecular resilience to decomposition. Temperature, hydrology, and chemistry have important roles in peat formation and C cycling along site vegetation, and these factors feed back on one another (Updegraff et al., 1995, 2001; Bridgham et al., 1998, 2008; Keller et al., 2004, 2006; Blodau et al., 2007). The stability of these peatlands depends not only on the recalcitrance of their peat but also on the environmental conditions in which it is stored. While poor fen peat may be more labile

than rich fen peat this difference will likely not be consequential unless the environmental factors limiting decomposition, namely inundation, acidity, and oligotrophy, are altered (Laiho, 2006). Bridgham et al. 2008 states that peat exhibits rapid homeostatic response to hydrological alterations, as exhibited with land subsidence following drainage. The above-mentioned studies described a rapid, labile pool-related decrease in C flux over the period of incubation. However, Bridgham et al. 1998 describes total C mineralization on a mass-mass basis over 59-week incubations as equivalent between OPF and FRF-equivalent ecotypes. The implication is that small labile pools are rapidly exhausted under ideal environmental conditions and subsequent decomposition occurs at lower, similar rates in peat from both ecotypes. Therefore, under sustained disruptions, both peatland ecotypes will find new, likely more recalcitrant and less C-negative, stable states. Since the lability of poor fen peat, and OPF peat in particular, is greater than that of FRF peat, the poor fens will experience greater change in peat properties under sustained drying. Furthermore, poor fens, with greater lability, will likely release more C to the atmosphere during brief, seasonal disruptions than FRFs. The depth data presented here indicate that deeper peat, in addition to being protected through insulation provided by overhead layers and requiring greater hydrological disruption to effect, also are more recalcitrant, making disruptions that do occur less impactful. However, OPFs lability is mostly present near the surface, and even at depth, OPFs are still more labile than FRFs. Disruptions that do occur to deep peat would likely still be relatively more impactful in OPFs than FRFs. One advantage that OPFs have over FRFs is that they are generally deeper, and therefore more of their C is protected from disruption simply by depth.

There was insufficient power to draw conclusions on surface differences in the FPF. The surface peat lignin index is apparently lower in the open poor fens than the FPF, implying a difference that cannot be verified presently. The deep peat found in the FPF had significantly higher L/P ratio, and a significantly lower lignin index than the deep peat found in FRFs. This, combined with the similarity in lignin concentration between OPF and FPF deep peat lignin content indicates that there may have been less forest cover at the FPF site in the past. This implies that FPF sites may be more labile than FRF sites, which are remarkably consistent in peat qualities with depth within their group.

4.6 Conclusion

We found silvic peat in FRFs to be generally more recalcitrant than *Sphagnum* peat in poor fens, particularly at the surface. Peat in all systems converges in quality at greater depths, or greater age, but FRFs were the most similar across depths while open poor fens were the most dissimilar across depths, indicating a slower degradation process in poor fens than rich fens. We found that the patterns in peat quality observations with depth were comparable to previously published patterns in equivalent peat types regardless of location; silvic peat followed the same pattern of high surface humification that does not change much with depth in Brunei as we observed in Michigan, and moss peat followed the same pattern of low surface humification with gradual increase with depth in Patagonia as in Michigan. Michigan OPFs will likely be more impacted by climate change perturbations to temperature and water table, particularly seasonal perturbations, because their surficial labile carbon stocks are higher than FRFs. Differences in the plant

functional types providing peat inputs, in this case trees and mosses, drive significant differences in peat quality throughout the peat column, with trees producing more recalcitrant peat than mosses, with implications for C cycling and resilience to disturbance.

4.7 Tables and Figures

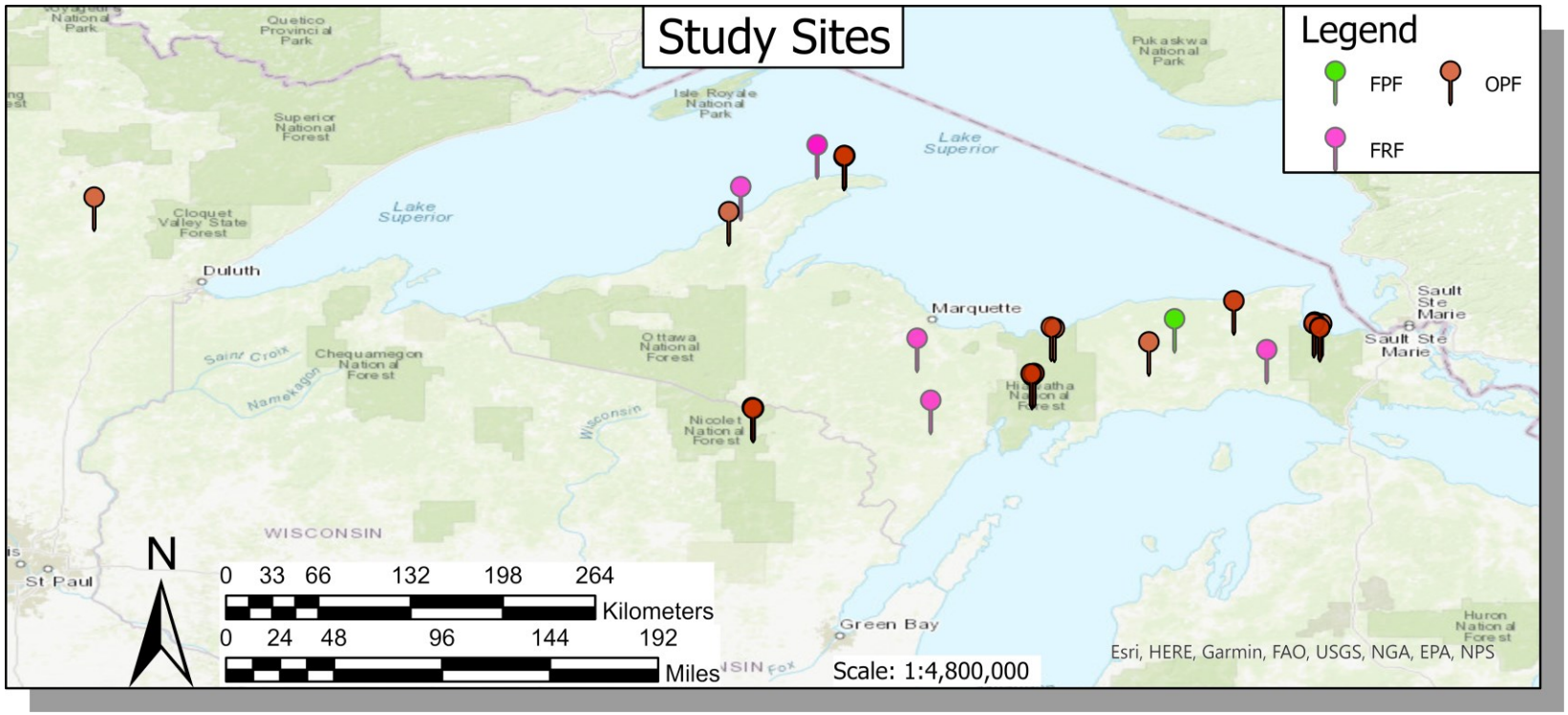

Figure 1: This map shows the location and ecotype of our sample sites.

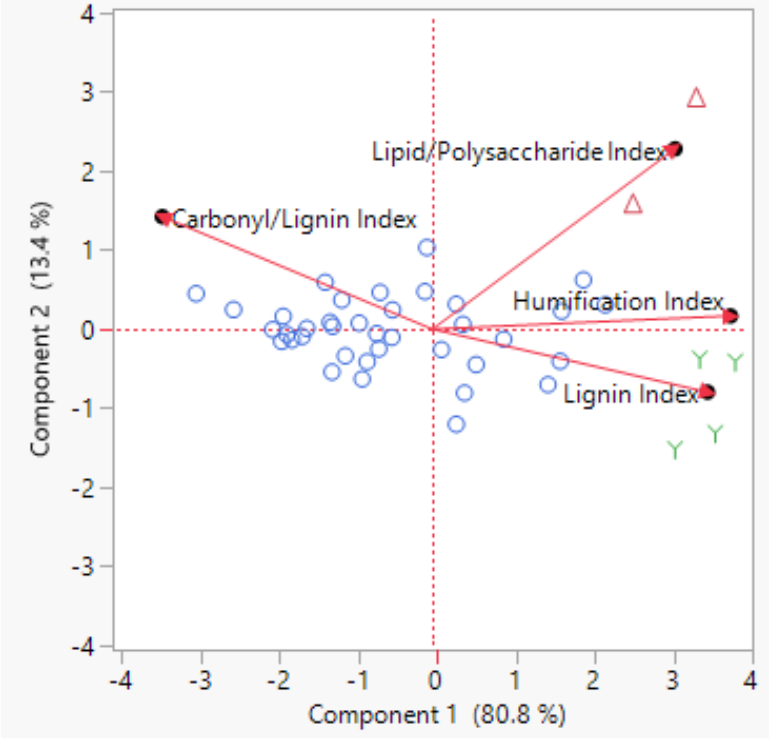

Figure 2: The PCA chart and loading vectors, indicating the distribution of peat types for the surface peat (0-25 cm and 25-50 cm). Colors indicate distinct groups of samples, circles indicate open poor fen (OPF) samples, triangles (Δ) indicate forested poor fen (FPF) samples, and Ys indicate forested rich fen (FRF) samples.

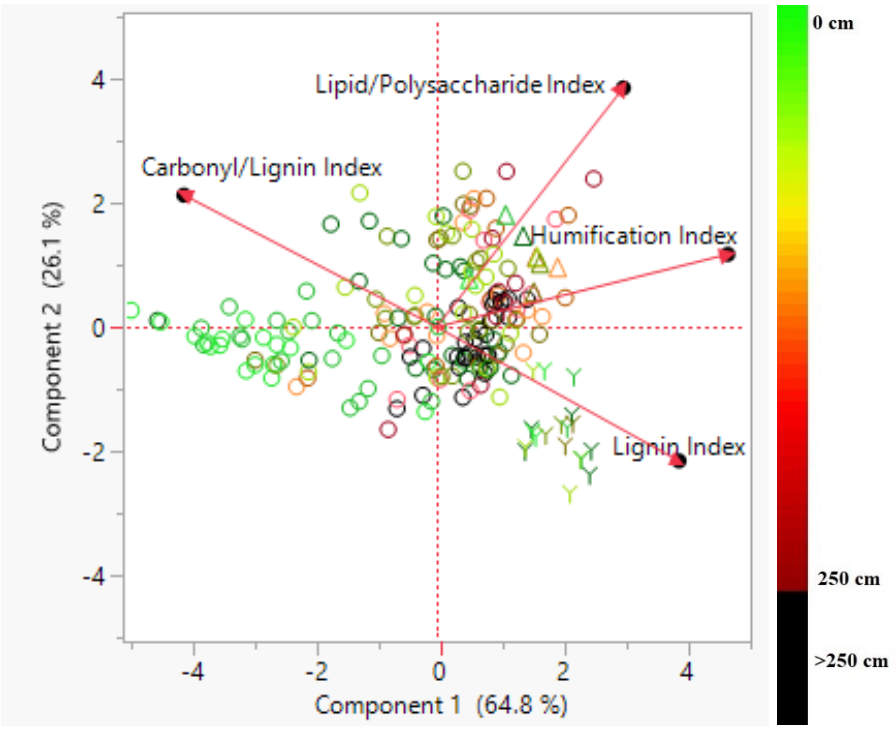

Figure 3: The PCA chart and loading vectors, indicating the distribution of peat types for all 25 cm peat depth bins. Colors indicate depth, surface samples being light green and transitioning with increasing depth to dark red at 225 cm bins while all bins 250 cm and deeper are black. Circles indicate open poor fen samples (OPF), triangles indicate forested poor fen (FPF) samples, and Ys indicate forested rich fen (FRF) samples.

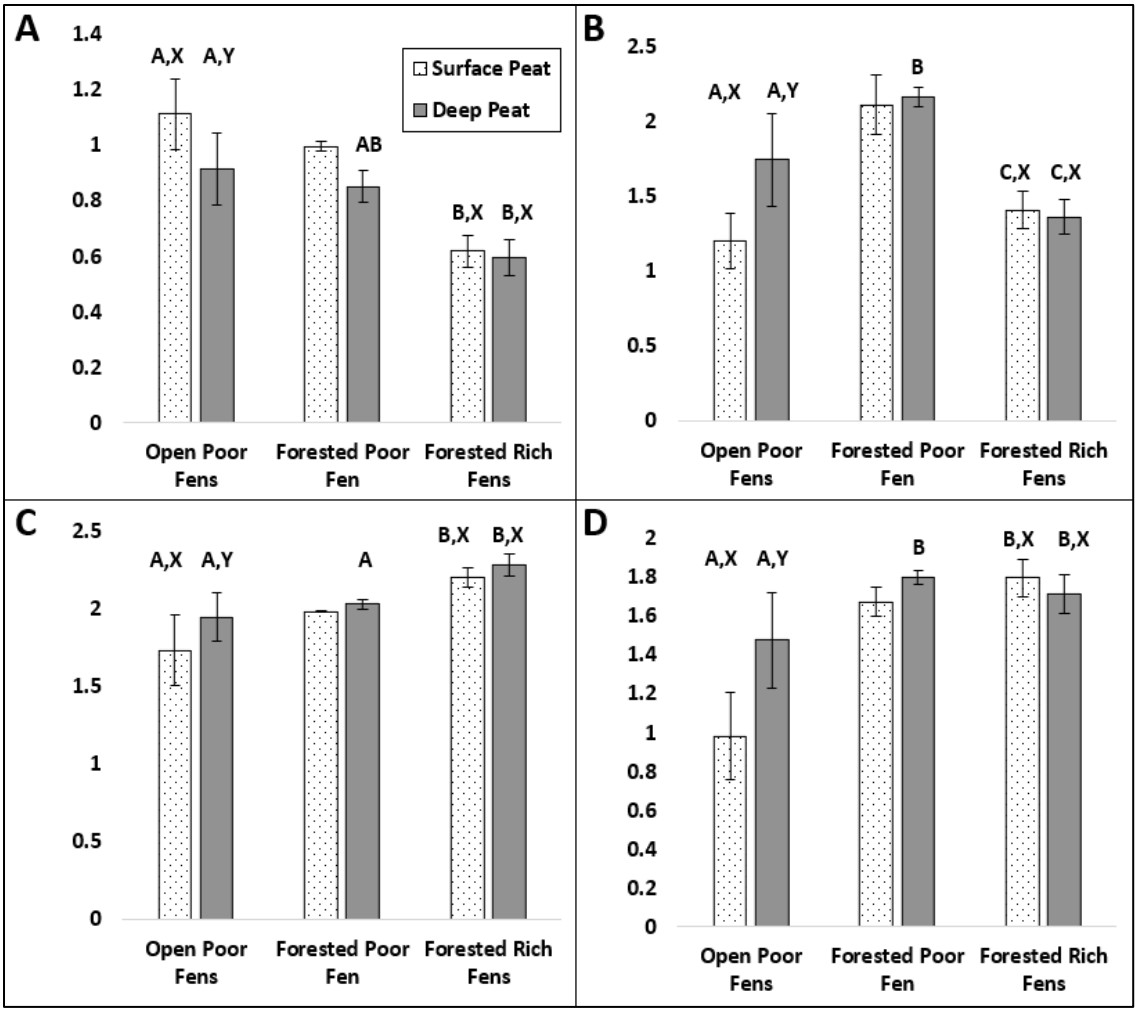

Figure 4: Bar charts indicating the significant differences in peat qualities between peat types within depth bins (A, B, C) and between surface and deep peat bins within the same peat type (X, Y, Z). Error bars indicate standard deviation. A. Carbonyl/Lignin Index B. Lipid/Polysaccharide Index C. Lignin Index D. Humification Index. Difference codes are not present between depths for the FPF or between peats for the FPF surface samples due to insufficient sample size.

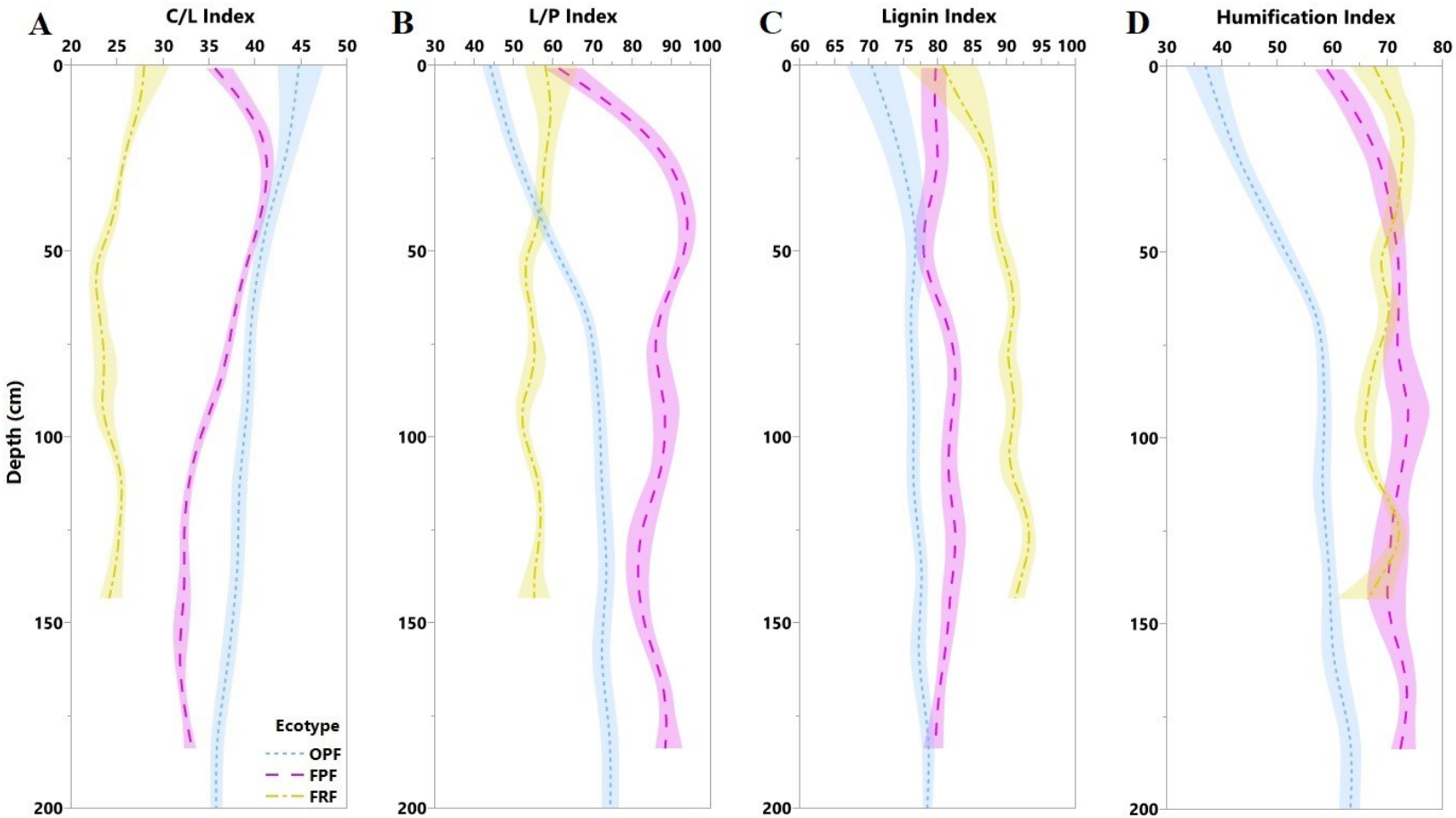
A
C/L Index
20 25 30 35 40 45 50
B
L/P Index
30 40 50 60 70 80 90 100
C
Lignin Index
60 65 70 75 80 85 90 95 100
D
Humification Index
30 40 50 60 70 80
Depth (cm)
0
50
100
150
200
Ecotype
OPF
FPF
FRF

Figure 5: This figure illustrates the relationship of each index with each ecotype and depth. All indices were multiplied by 40 for clarity. Trends for open poor fens (OPF; which extend to 500 cm) were truncated to 200 cm depth to highlight differences among the three sites. Dotted lines indicate means, colored zones indicate 95% confidence intervals. OPF = open poor fens, FPF = forested poor fen, FRF = forested rich fens.

Table 1: The PCA loading matrix for the surface two 25 cm peat depth bins (0-25 cm and 25-50 cm).

	PC1	PC2
CARBONYL/LIGNIN INDEX	-0.89264	0.37118
LIPID/POLYSACCHARIDE INDEX	0.80110	0.59471
LIGNIN INDEX	0.90839	-0.20728
HUMIFICATION INDEX	0.98427	0.04389

Table 2: The PCA loading matrix for all 25 cm peat depth bins.

	PC1	PC2
CARBONYL/LIGNIN INDEX	-0.82702	0.43058
LIPID/POLYSACCHARIDE INDEX	0.61040	0.78067
LIGNIN INDEX	0.79239	-0.43708
HUMIFICATION INDEX	0.95214	0.23727

4.8 References

Apfelbaum, S.I., A. Haney, F. Wang, J. Burris, and J. Carlson. 2017. Old-Growth Southern Boreal Forest Stability and Response to a Stand-Replacing Wildfire. Nat. Areas J. 37(4): 474–488. doi: 10.3375/043.037.0404.

Belton, D.J., R. Plowright, D.L. Kaplan, and C.C. Perry. 2018. A robust spectroscopic method for the determination of protein conformational composition – Application to the annealing of silk. Acta Biomater. 73: 355–364. doi: 10.1016/j.actbio.2018.03.058.

Benscoter, B.W., D. Greenacre, and M.R. Turetsky. 2015. Wildfire as a key determinant of peatland microtopography. Can. J. For. Res. 45(April): 1132–1136. doi: 10.1139/cjfr-2015-0028.

Benscoter, B.W., and D.H. Vitt. 2008. Spatial patterns and temporal trajectories of the bog ground layer along a post-fire chronosequence. Ecosystems 11(7): 1054–1064. doi: 10.1007/s10021-008-9178-4.

Blodau, C., N.T. Roulet, T. Heitmann, H. Stewart, J. Beer, et al. 2007. Belowground carbon turnover in a temperate ombrotrophic bog. Global Biogeochem. Cycles 21(1): 1–12. doi: 10.1029/2005GB002659.

Bourgeau-Chavez, L.L., S. Endres, R. Powell, M.J. Battaglia, B. Benscoter, et al. 2017. Mapping boreal peatland ecosystem types from multitemporal radar and optical satellite imagery. Can. J. For. Res. 47(4): 545–559. doi: 10.1139/cjfr-2016-0192.

Bridgham, S.D., J. Pastor, B. Dewey, J.F. Weltzin, and K. Updegraff. 2008. Rapid carbon

response of peatlands to climate change. Ecology 89(11): 3041–3048. doi: 10.1890/08-0279.1.

Bridgham, S.D., K. Updegraff, and J. Pastor. 1998. Carbon, nitrogen, and phosphorus mineralization in northern wetlands. Ecology 79(5): 1545–1561. doi: 10.1890/0012-9658(1998)079[1545:CNAPMI]2.0.CO;2.

Broder, T., C. Blodau, H. Biester, and K.H. Knorr. 2012. Peat decomposition records in three pristine ombrotrophic bogs in southern Patagonia. Biogeosciences 9(4): 1479–1491. doi: 10.5194/bg-9-1479-2012.

Bronk Ramsey, C. 2009. Bayesian analysis of radiocarbon dates. Radiocarbon 51(1): 337–360. doi: 10.1017/S0033822200033865.

Brown, K.J., and T. Giesecke. 2014. Holocene fire disturbance in the boreal forest of central Sweden. Boreas 43(3): 639–651. doi: 10.1111/bor.12056.

Carcaillet, C., I. Bergman, S. Delorme, G. Hornberg, and O. Zackrisson. 2007. Long-term fire frequency not linked to prehistoric occupations in northern Swedish boreal forest. Ecology 88(2): 465–477. doi: 10.1890/0012-9658(2007)88[465:LFFNLT]2.0.CO;2.

Chimner, R.A., C.A. Ott, C.H. Perry, and R.K. Kolka. 2014. Developing and Evaluating Rapid Field Methods to Estimate Peat Carbon. Wetlands 34(6): 1241–1246. doi: 10.1007/s13157-014-0574-6.

Clymo, R.S., J. Turunen, and K. Tolonen. 1998. Carbon Accumulation in Peatland. Oikos 81(2): 368–388.

Cogbill, C. V. 1985. Dynamics of the boreal forests of the Laurentian Highlands, Canada.

Can. J. For. Res. 15(1): 252–261. doi: https://doi-org.services.lib.mtu.edu/10.1139/x85-043.

Drobyshev, I., A. Granström, H.W. Linderholm, E. Hellberg, Y. Bergeron, et al. 2014. Multi-century reconstruction of fire activity in northern European boreal forest suggests differences in regional fire regimes and their sensitivity to climate. J. Ecol. 102(3): 738–748. doi: 10.1111/1365-2745.12235.

Fenton, N.J., and Y. Bergeron. 2008. Does time or habitat make old-growth forests species rich? Bryophyte richness in boreal Picea mariana forests. Biol. Conserv. 141(5): 1389–1399. doi: 10.1016/j.biocon.2008.03.019.

Flanagan, N.E., H. Wang, S. Winton, and C.J. Richardson. 2020. Low-severity fire as a mechanism of organic matter protection in global peatlands: Thermal alteration slows decomposition. Glob. Chang. Biol. 26(March): 3930–3946. doi: 10.1111/gcb.15102.

Fujiwara, A., T. Hirawake, K. Suzuki, I. Imai, and S.I. Saitoh. 2014. Timing of sea ice retreat can alter phytoplankton community structure in the western Arctic Ocean. Biogeosciences 11(7): 1705–1716. doi: 10.5194/bg-11-1705-2014.

Gaffney, J.S., N.A. Marley, and K.J. Smith. 2015. Characterization of fine mode atmospheric aerosols by Raman microscopy and diffuse reflectance FTIR. J. Phys. Chem. A 119(19): 4524–4532. doi: 10.1021/jp510361s.

Gardegaront, M., D. Farlay, O. Peyruchaud, and H. Follet. 2018. Automation of the Peak Fitting Method in Bone FTIR Microspectroscopy Spectrum Analysis: Human and Mice Bone Study. J. Spectrosc. 2018(Figure 1). doi: 10.1155/2018/4131029.

Giorgi, F. 2006. Climate change hot-spots. Geophys. Res. Lett. 33(8): 1–4. doi: 10.1029/2006GL025734.

Goldstein, A., W.R. Turner, S.A. Spawn, K.J. Anderson-teixeira, S. Cook-patton, et al. 2020. Protecting irrecoverable carbon in Earth's ecosystems. Nat. Clim. Chang. 10(April): 287–295. doi: 10.1038/s41558-020-0738-8.

Hodgkins, S.B., C.J. Richardson, R. Dommain, H. Wang, P.H. Glaser, et al. 2018. Tropical peatland carbon storage linked to global latitudinal trends in peat recalcitrance. Nat. Commun. 9(1): 1–13. doi: 10.1038/s41467-018-06050-2.

Hribljan, J.A., E.S. Kane, and R.A. Chimner. 2017. Implications of Altered Hydrology for Substrate Quality and Trace Gas Production in a Poor Fen Peatland. Soil Sci. Soc. Am. J. 81(3): 633. doi: 10.2136/sssaj2016.10.0322.

Johnstone, J.F., T.N. Hollingsworth, F.S. Chapin, and M.C. Mack. 2010. Changes in fire regime break the legacy lock on successional trajectories in Alaskan boreal forest. Glob. Chang. Biol. 16(4): 1281–1295. doi: 10.1111/j.1365-2486.2009.02051.x.

Jules, A.N., H. Asselin, Y. Bergeron, and A.A. Ali. 2018. Are marginal balsam fir and eastern white cedar stands relics from once more extensive populations in north-eastern North America? Holocene 28(10): 1672–1679. doi: 10.1177/0959683618782601.

Kalbitz, K., W. Geyer, and S. Geyer. 1999. Spectroscopic properties of dissolved humic substances - A reflection of land use history in a fen area. Biogeochemistry 47(2): 219–238. doi: 10.1023/A:1006134214244.

Kane, E.S., E.S. Kasischke, D.W. Valentine, M.R. Turetsky, and A.D. McGuire. 2007.

Topographic influences on wildfire consumption of soil organic carbon in interior Alaska: Implications for black carbon accumulation. J. Geophys. Res. Biogeosciences 112(3): 1–11. doi: 10.1029/2007JG000458.

Keller, J.K., A.K. Bauers, S.D. Bridgham, L.E. Kellogg, and C.M. Iversen. 2006. Nutrient control of microbial carbon cycling along an ombrotrophic-minerotrophic peatland gradient. J. Geophys. Res. Biogeosciences 111(3): 1–14. doi: 10.1029/2005JG000152.

Keller, J.K.., J.R. White, S.D. Bridgeham, and J. Paster. 2004. Climate change effects on carbon and nitrogen mineralization in peatlands through changes in soil quality. Glob. Chang. Biol.: 1053–1064. doi: 10.1111/j.1365-2486.2004.00785.x.

Kim, S., R.W. Kramer, and P.G. Hatcher. 2003. Graphical Method for Analysis of Ultrahigh-Resolution Broadband Mass Spectra of Natural Organic Matter, the Van Krevelen Diagram. Anal. Chem. 75(20): 5336–5344. doi: 10.1021/ac034415p.

Kolka, R., S.D. Bridgham, and C.L. Ping. 2016. Soils of peatlands: histosols and gelisols. In: Vepraskas, M.J. and Craft, C.L., editors, Wetlands soils: genesis, hydrology, landscapes and classification. Press/Lewis Publishing, Boca Raton, FL. p. 277–309

Kost, M.A., D.A. Albert, J.G. Cohen, B.S. Slaughter, R.K. Schillo, et al. 2007. Natural Communities of Michigan: Classification and Description. Michigan Nat. Featur. Invent. Rep. No. 2007-21. https://mnfi.anr.msu.edu/communities/community.cfm?id=10652 (accessed 20 September 2016).

Kudray, G. 2019. Field Guide Hiawatha National Forest Ecological Classification

System.

Kuhry, P. 1994. The role of fire in the development of Sphagnum-dominated peatlands in western boreal Canada. J. Ecol. 82(4): 899–910.

Laiho, R. 2006. Decomposition in peatlands: Reconciling seemingly contrasting results on the impacts of lowered water levels. Soil Biol. Biochem. 38(8): 2011–2024. doi: 10.1016/j.soilbio.2006.02.017.

Langor, D.W., E.K. Cameron, C.J.K. Macquarrie, A. Mcbeath, A. Mcclay, et al. 2014. Non-native species in Canada's boreal zone: diversity, impacts, and risk. Environ. Rev. 22(4): 372–420.

Larson, E.R., and M.A. Green. 2017. Fire History at the Confluence of the Driftless Area and Central Sand Plains of Wisconsin: A Case Study from Castle Mound Pine Forest State Natural Area. Nat. Areas J. 37(3): 309–321. doi: 10.3375/043.037.0306.

Loisel, J., A. V. Gallego-Sala, M.J. Amesbury, G. Magnan, G. Anshari, et al. 2021. Expert assessment of future vulnerability of the global peatland carbon sink. Nat. Clim. Chang. 11(1): 70–77. doi: 10.1038/s41558-020-00944-0.

Malmer, N., and B. Wallén. 1993. Accumulation and release of organic matter in ombrotrophic bog hummocks - processes and regional variation. Ecography (Cop.). 16(3): 193–211.

Marcott, S.A., J.D. Shakun, P.U. Clark, and A.C. Mix. 2013. A reconstruction of regional and global temperature for the past 11,300 years. Science (80-.). 339(6124): 1198–1201. doi: 10.1126/science.1228026.

Nichols, J.E., and D.M. Peteet. 2019. Rapid expansion of northern peatlands and doubled

estimate of carbon storage. Nat. Geosci. 12(November): 917–922. doi: 10.1038/s41561-019-0454-z.

Nolte, C.G., J.J. Schauer, G.R. Cass, and B.R.T. Simoneit. 2001. Highly polar organic compounds present in wood smoke and in the ambient atmosphere. Environ. Sci. Technol. 35(10): 1912–1919. doi: 10.1021/es001420r.

Pitkänen, A., J. Turunen, and K. Tolonen. 1999. The role of fire in the carbon dynamics of a mire, eastern Finland. Holocene 9(4): 453–462. doi: 10.1191/095968399674919303.

Potvin, L.R., E.S. Kane, R.A. Chimner, R.K. Kolka, and E.A. Lilleskov. 2015. Effects of water table position and plant functional group on plant community, aboveground production, and peat properties in a peatland mesocosm experiment (PEATcosm). Plant Soil 387(1–2): 277–294. doi: 10.1007/s11104-014-2301-8.

Rayfield, B., V. Paul, F. Tremblay, M.J. Fortin, C. Hély, et al. 2021. Influence of habitat availability and fire disturbance on a northern range boundary. J. Biogeogr. 48(2): 394–404. doi: 10.1111/jbi.14004.

Robinson, S.D., and T.R. Moore. 1999. Carbon and peat accumulation over the past 1200 years in a landscape with discontinuous permafrost, Northwestern Canada. Global Biogeochem. Cycles 13(2): 591–601. doi: 10.1002/(ISSN)1944-9224.

Robinson, S.D., and T.R. Moore. 2000. The influence of permafrost and fire upon carbon accumulation in high boreal peatlands, Northwest Territories, Canada. Arct. Antarct. Alp. Res. 32(2): 155–166. doi: 10.2307/1552447.

Sadat, A., and I.J. Joye. 2020. Peak fitting applied to fourier transform infrared and

raman spectroscopic analysis of proteins. Appl. Sci. 10(17). doi: 10.3390/app10175918.

Sazawa, K., T. Wakimoto, M. Fukushima, Y. Yustiawati, M.S. Syawal, et al. 2018. Impact of Peat Fire on the Soil and Export of Dissolved Organic Carbon in Tropical Peat Soil, Central Kalimantan, Indonesia. ACS Earth Sp. Chem. 2(7): 692–701. doi: 10.1021/acsearthspacechem.8b00018.

Šeparović, L., A. Alexandru, R. Laprise, A. Martynov, L. Sushama, et al. 2013. Present climate and climate change over North America as simulated by the fifth-generation Canadian regional climate model.

Simoneit, B.R.T., J.J. Schauer, C.G. Nolte, D.R. Oros, V.O. Elias, et al. 1999. Levoglucosan, a tracer for cellulose in biomass burning and atmospheric particles. Atmos. Environ. 33(2): 173–182. papers3://publication/uuid/3E935E2F-ED96-40DC-8374-344125150073.

Skoog, D.A. 2014. Fundamentals of analytical chemistry. 9th ed. Thomson-Brooks/Cole, Belmont, California.

Stuiver, M., and H.A. Polach. 1977. Discussion of Reporting of 14C Data. Radiocarbon 19(3): 355–363.

Taylor, A.R., and H.Y.H. Chen. 2011. Multiple successional pathways of boreal forest stands in central Canada. Ecography (Cop.). 34(2): 208–219. doi: 10.1111/j.1600-0587.2010.06455.x.

Turetsky, M.R., B. Benscoter, S. Page, G. Rein, G.R. van der Werf, et al. 2015. Global vulnerability of peatlands to fire and carbon loss. Nat. Geosci. 8(1): 11–14. doi:

10.1038/NGEO2325.

Turetsky, M.R., E.S. Kane, J.W. Harden, R.D. Ottmar, K.L. Manies, et al. 2011. Recent acceleration of biomass burning and carbon losses in Alaskan forests and peatlands. Nat. Geosci. 4(1): 27–31. doi: 10.1038/ngeo1027.

U.S. Environmental Protection Agency. 2013. Level III and IV Ecoregions of the Continental United States. https://www.epa.gov/eco-research/level-iii-and-iv-ecoregions-continental-united-states%0Ahttp://www.epa.gov/wed/pages/ecoregions/level_iii_iv.htm.

Updegraff, K., S.D. Bridgham, J. Pastor, P. Weishampel, and C. Harth. 2001. Response of CO2 and CH4 emissions from peatlands to warming and water table manipulation. Ecol. Appl. 11(2): 311–326. doi: 10.1890/1051-0761(2001)011[0311:rocace]2.0.co;2.

Updegraff, K., J. Pastor, S.D.. Bridgham, and C.A.. Johnston. 1995. Environmental and Substrate Controls over Carbon and Nitrogen Mineralization in Northern Wetlands. Ecol. Appl. 5(1): 151–163.

Verbeke, B. 2018. Peatland Organic Matter Chemistry Trends Over A Global Latitudinal Gradient. Thesis. http://purl.flvc.org/fsu/fd/2018_Sp_Verbeke_fsu_0071N_14561.

Vetrita, Y., and M.A. Cochrane. 2020. Fire frequency and related land-use and land-cover changes in Indonesia's Peatlands. Remote Sens. 12(1). doi: 10.3390/RS12010005.

Viau, A.E., K. Gajewski, M.C. Sawada, and P. Fines. 2006. Millennial-scale temperature variations in North America during the Holocene. doi: 10.1029/2005JD006031.

Vogel, J.S., J.R. Southon, and D.E. Nelson. 1987. Catalyst and binder effects in the use of filamentous graphite for AMS. Nucl. Inst. Methods Phys. Res. B 29(1–2): 50–56. doi: 10.1016/0168-583X(87)90202-3.

Walker, X.J., J.L. Baltzer, L. Bourgeau-Chavez, N.J. Day, C.M. Dieleman, et al. 2020. Patterns of Ecosystem Structure and Wildfire Carbon Combustion Across Six Ecoregions of the North American Boreal Forest. Front. For. Glob. Chang. 3(July): 1–12. doi: 10.3389/ffgc.2020.00087.

Walker, X.J., J.L. Baltzer, S.G. Cumming, N.J. Day, C. Ebert, et al. 2019. Increasing wildfires threaten historic carbon sink of boreal forest soils. Nature 572(7770): 520–523. doi: 10.1038/s41586-019-1474-y.

Wieder, R.K., and D.H. Vitt, editors. 2010. Boreal Peatland Ecosystems. Springer.

Wiken, E., F.J. Nava, and G. Griffith. 2011. North American Terrestrial Ecoregions—Level III. (April): 1–149.

Young, D.M., A.J. Baird, A. V. Gallego-Sala, and J. Loisel. 2021. A cautionary tale about using the apparent carbon accumulation rate (aCAR) obtained from peat cores. Sci. Rep. 11(1): 1–12. doi: 10.1038/s41598-021-88766-8.

Yu, Z.C. 2012. Northern peatland carbon stocks and dynamics: A review. Biogeosciences 9(10): 4071–4085. doi: 10.5194/bg-9-4071-2012.

Zackrisson, O. 1977. Influence of Forest Fires on the North Swedish Boreal Forest. Oikos 29: 22–32. https://www.jstor.org/stable/3543289.

Zhang, Y., J. Maxted, A. Barber, C. Lowe, and R. Smith. 2013. The durability of clear polyurethane coil coatings studied by FTIR peak fitting. Polym. Degrad. Stab. 98(2):

527–534. doi: 10.1016/j.polymdegradstab.2012.12.003.

Zoppi, U., J. Crye, Q. Song, and A. Arjomand. 2007. Performance evaluation of the new AMS system at Accium Biosciences. Radiocarbon 49(1): 173–182. doi: 10.1017/S0033822200041990.

5 Dissertation Conclusion

In chapter 1 we pioneered a novel method of peatland charcoal detection and quantification. The speed and cost efficiency of this method allows more extensive, intensive, and/or numerous studies of peatland fire history. This should enable a marked increase in the productivity of peatland fire history research.

In chapter 2 we exercised this novel method to analyze the fire histories of 29 peatland sites and correlate them with carbon storage and accumulation data. We established the fire frequency for hemi-boreal poor fens and the negative relationship between fire frequency and long-term apparent rate of carbon accumulation. The natural fire regimes of peatlands need to be understood if managers desire to take informed action for the conservation of these ecosystems. Further, we have shown that fire has substantial impacts on the carbon cycling and storage of peatland ecosystems, emphasizing the importance of fire to modeling scenarios, and making the required data available for the purpose of ecosystem and global modeling.

In chapter 3 we leveraged the spectral data already gathered for char quantification in chapter 2 to describe the trends in peat properties throughout entire peat profile for 3 different hemi-boreal peatland ecotypes. This research has implications for peatland resilience to the rapidly changing climate at northern latitudes. With both climate change and direct anthropogenic modifications affecting water tables, and increasing will to act in response, this depth spanning information comes at a pivotal time.

With climate change altering temperature and precipitation patterns, and wildfire patterns changing, data on normal fire regimes is more important than ever. The vast stores of carbon present in peatland soils needs to be understood to be protected.

Knowledge of the disturbance regimes and peat properties are crucial to promoting peatland resilience. Future work to adapt our charcoal quantification method to different peat matrices to replicate and expand on the success of chapter 2 would be beneficial. In particular, gathering fire history data in understudied peatland ecotypes such as mountain and tropical peatlands would greatly assist in the advancement of the field. Being able to consider other peat properties, as we did in chapter 3, with the same spectral data should also bolster our understanding of peatlands.

A Appendix

A.1 Supplementary Radiocarbon Data

Site Name	Profile Name	Sample ID	Year of sampling	Layer Top	Layer Bottom	Bulk Density	Organic Matter	Radiocarbon Analysis Year	Bulk Layer $\Delta^{14}C$	Bulk Layer $\Delta^{14}C$ Standard Deviation (AMS analytical)	Bulk Layer Fraction Modern	Bulk Layer Fraction Modern Standard Deviation (AMS analytical)
			yyyy	cm	cm	g cm^{-3}	%	YYYY	‰	‰		
Bete Grise	1	310	2011-2012	40.3	42.3	0.091	93.671	2021	-56.5348	1.244128241	0.951602919	0.001244128
Bete Grise	1	323	2011-2012	69.9	71.9	0.206	93.478	2020	-165.21	1.393032942	0.841888582	0.001393033
Bete Grise	2	334	2011-2012	48.9	50.9	0.068	91.209	2021	-56.5839	1.244026528	0.9515534	0.001244027
Bete Grise	2	349	2011-2012	83.4	85.4	0.212	92.121	2020	-130.235	1.519975696	0.877161316	0.001519976
Sleeper Lake	3	282	2011-2012	22	24	0.216	91.241	2019	-178.039	2.8	0.82885	0.0028
Sleeper Lake	3	287	2011-2012	33.5	35.5	0.217	75.159	2019	-228.516	2.6	0.77795	0.0026
Sleeper Lake	3	291	2011-2012	42.7	44.7	0.223	82.775	2019	-199.856	2.9	0.80685	0.0029
Sleeper Lake	3	295	2011-2012	51.9	53.9	0.212	91.818	2019	-217.013	1.4	0.78955	0.0014
Sleeper Lake	4	560	2011-2012	49.6	51.6	0.216	79.412	2020	-269.966	1.247286993	0.736241333	0.001247287
Eagle harbor	10	436	2011-2012	138.6	140.6	0.189	84.483	2013			0.736212283	
Painesdale	11	456	2011-2012	66.5	68.5	0.049	100.000	2019	-22.1458	2.9	0.98605	0.0029
Painesdale	11	491	2011-2012	142.4	144.4	0.056	97.561	2019	-47.4338	2.6	0.96055	0.0026
Painesdale	11	507	2011-2012	193	195	0.046	94.872	2019	-94.539	3.4	0.91305	0.0034
Painesdale	11	523	2011-2012	241.3	243.3	0.133	93.103	2019	-115.662	3.3	0.89175	0.0033

Painesdale	12	169	2011-2012	89.7	91.7	0.230	94.118	2020	-385.798	1.148212535	0.619424438	0.001148213
Painesdale	12	185	2011-2012	126.5	128.5	0.190	94.915	2020	-351.201	1.196619038	0.654316005	0.001196619
Painesdale	12	199	2011-2012	158.7	160.7	0.230	95.890	2020	-474.851	1.035987768	0.529614864	0.001035988
Painesdale	12	233	2011-2012	236.9	238.9	0.230	91.489	2020	-559.439	1.135982176	0.444307385	0.001135982
Bete Grise	14	573	2011-2012	48.3	50.3	0.147	93.636	2021	-139.689	1.141244287	0.86773186	0.001141244
Bete Grise	14	592	2011-2012	92	94	0.185	94.000	2020	-237.31	1.492858537	0.76917543	0.001492859
Seney	16	46	2011-2012	34.3	36.3	0.051	91.667	2021	-21.1448	1.286801449	0.987298188	0.001286801
Seney	16	47	2011-2012	36.6	38.6	0.047	91.667	2021	-20.6232	1.366520805	0.987824271	0.001366521
Seney	16	49	2011-2012	41.2	43.2	0.114	88.889	2019	-27.7984	2.7	0.98035	0.0027
Seney	16	50	2011-2012	43.5	45.5	0.164	85.897	2021	-17.9643	1.413910195	0.990506146	0.00141391
Seney	16	52	2011-2012	48.1	50.1	0.199	91.000	2021	-40.4176	1.532222021	0.967859167	0.001532222
Seney	16	53	2011-2012	50.4	52.4	0.305	91.000	2019	-82.2421	2.7	0.92545	0.0027
Seney	16	54	2011-2012	52.7	54.7	0.323	86.875	2021	-97.0718	1.351690825	0.91071625	0.001351691
Seney	16	57	2011-2012	59.6	61.6	0.300	87.912	2019	-157.214	1.9	0.84985	0.0019
Seney	16	58	2011-2012	61.9	63.9	0.273	89.362	2021	-164.876	1.231586362	0.8423275	0.001231586
Seney	16	59	2011-2012	64.2	66.2	0.300	89.362	2021	-176.226	1.125912303	0.830879271	0.001125912
Seney	16	60	2011-2012	66.5	68.5	0.322	84.977	2019	-199.658	2.7	0.80705	0.0027
Seney	16	61	2011-2012	68.8	70.8	0.307	84.977	2021	-210.067	1.082764463	0.79674625	0.001082764
Seney	16	63	2011-2012	73.4	75.4	0.265	91.837	2021	-234.514	1.355706642	0.772088854	0.001355707
Seney	16	64	2011-2012	75.7	77.7	0.255	94.611	2019	-243.986	2.1	0.76235	0.0021
Seney	16	67	2011-2012	82.6	84.6	0.256	91.111	2021	-256.03	1.149388116	0.750387083	0.001149388
Seney	16	68	2011-2012	84.9	86.9	0.164	91.111	2019	-265.804	2.2	0.74035	0.0022

Marsin	19	354	2011-2012	24.3	26.3	0.090	77.670	2021	-69.5051	1.225635285	0.93852077	0.001225635
Marsin	19	375	2011-2012	72.6	74.6	0.351	85.385	2013			0.480955475	
Bob's Lake	21	250	2011-2012	44.3	46.3	0.106	85.106	2021	-150.399	1.30068114	0.85692935	0.001300681
Bob's Lake	21	271	2011-2012	92.6	94.6	0.325	72.254	2013			0.416803643	
Whitney	22	376	2011-2012	49.3	51.3	0.126	83.217	2021	-262.43	0.998449416	0.74393162	0.000998449
Whitney	22	397	2011-2012	97.6	99.6	0.329	96.909	2021	-579.4	0.7	0.4243	0.0007
Eagle Harbor	26	104	2011-2012	48.3	50.3	0.148	86.667	2021	-130.72	1.149510241	0.876777755	0.00114951
Eagle Harbor	26	145	2011-2012	142.6	144.6	0.199	88.618	2013			0.698708883	
Elmer, MN	1001	1152	2018	146	148	0.068	88.985	2020	-243.649	1.238801863	0.76278269	0.001238802
Betchler Lake	2001	1223	2018	70	72	0.107	91.187	2020	-149.609	1.717693896	0.857621989	0.001717694
Betchler Lake	2011	1331	2018	246	248	0.056	86.462	2020	-446	1.085603506	0.558711059	0.001085604
Betchler Lake	2021	1339	2018	54	56	0.052	85.599	2020	-59.6627	3.7	0.948333333	0.0037
Betchler Lake	2031	1412	2018	148	150	No Data	No Data	2020	-276.816	1.2	0.729333333	0.0012
Betchler Lake	2041	1457	2018	90	92	0.124	88.567	2020	-250.143	2.2	0.756233333	0.0022
Ramsey Lake	3001	1562	2018	248	250	0.147	87.871	2020	-447.168	2.3	0.557533333	0.0023
Ramsey Lake	3011	1664	2018	246	248	0.094	88.879	2020	-444.193	2.2	0.560533333	0.0022
Ramsey Lake	3021	1692	2018	94	96	0.137	80.093	2020	-254.308	1.6	0.752033333	0.0016
Ramsey Lake	3031	1712	2018	72	74	0.094	91.705	2020	-111.353	1.571759466	0.896203654	0.001571759
Ramsey Lake	3031	1717	2018	82	84	0.115	93.440	2020	-161.143	1.490053626	0.845989684	0.001490054
Ramsey Lake	3031	1725	2018	98	100	0.103	91.373	2020	-268.487	1.6	0.737733333	0.0016
Hedmark Pines, WI	4001	1957	2018	446	448	0.031	93.874	2020	-274.337	2.3	0.731833333	0.0023
Hedmark Pines, WI	4011	1989	2018	104	106	0.061	93.637	2020	-128.235	1.659454183	0.879177604	0.001659454
Hedmark Pines, WI	4011	1994	2018	114	116	0.063	91.777	2020	-115.217	1.891354954	0.892306756	0.001891355
Hedmark Pines, WI	4011	2118	2018	372	374	0.060	93.019	2020	-267.921	1.319278931	0.738303957	0.001319279
Hedmark Pines, WI	4011	2124	2018	384	386	0.065	95.643	2020	-268.318	1.122734157	0.737903515	0.001122734

Hedmark Pines, WI	4011	2138	2018	1412	1414	0.070	92.698	2020	-264.818	3.2	0.741433333	0.0032
Hedmark Pines, WI	4021	2259	2018	144	146	0.184	68.474	2020	-520.022	0.905704486	0.484059882	0.000905704
Hedmark Pines, WI	4021	2288	2018	202	204	0.113	91.521	2021	-654.051	0.794861482	0.348932927	0.000794861
Hedmark Pines, WI	4021	2298	2018	222	224	0.098	94.507	2021	-676.819	0.755177467	0.325968333	0.000755177
Rexton	5001	3022	2019	48	50	0.143	68.380	2021	-290.987	1.02668589	0.715128229	0.001026686
Seney Forested	7001	3069	2019	92	94	0.063	89.166	2021	-416.657	0.972758764	0.588374266	0.000972759
Seney Forested	7001	3120	2019	183	185	0.066	86.505	2021	-472.112	0.774449481	0.532441563	0.000774449
Alt Sph Lake	8001	897	2018	112	114	0.086	96.924	2021	-323.738	1.103168932	0.682095301	0.001103169
Alt Sph Lake	8001	993	2018	304	306	0.057	96.671	2021	-375.469	0.933726173	0.62991745	0.000933726
Alt Sph Lake	8001	1085	2018	488	490	0.059	80.067	2020	-550.662	1.025421746	0.453158575	0.001025422
Peck Lake	8002	1096	2018	14	16	0.076	98.194	2021	35.10312	1.405986335	1.04403125	0.001405986
Peck Lake	8002	742	2018	50	52	0.006	95.475	2021	21.53773	1.397436567	1.030348854	0.001397437
Peck Lake	8002	755	2018	76	78	0.048	97.395	2021	281.9934	1.757012202	1.293051042	0.001757012
Peck Lake	8002	757	2018	80	82	0.051	96.536	2021	36.26704	1.417742023	1.045205208	0.001417742
Peck Lake	8002	761	2018	88	90	0.049	96.740	2021	-10.6329	1.355007185	0.997900729	0.001355007
Peck Lake	8002	763	2018	92	94	0.080	96.529	2021	-26.9801	1.330816974	0.9814125	0.001330817
Peck Lake	8002	767	2018	100	102	0.061	96.408	2021	-29.6498	1.334068079	0.978719792	0.001334068
Peck Lake	8002	772	2018	110	112	0.096	95.266	2021	-83.9247	1.300696444	0.923976771	0.001300696
Peck Lake	8002	774	2018	115	117	0.101	94.450	2021	-106.524	1.244081929	0.901182188	0.001244082
Peck Lake	8002	775	2018	117	119	0.105	94.497	2021	-110.422	1.22022699	0.897251146	0.001220227
Peck Lake	8002	780	2018	127.5	129.5	0.104	94.772	2021	-150.562	1.540331137	0.856764792	0.001540331
Peck Lake	8002	781	2018	130	132	0.102	93.770	2021	-163.626	1.152725224	0.843588333	0.001152725
Peck Lake	8002	783	2018	134	136	0.113	87.643	2021	-174.506	1.139171696	0.832614583	0.001139172
Peck Lake	8002	796	2018	160	162	0.088	96.082	2021	-247.213	1.044900695	0.759280208	0.001044901
Peck Lake	8002	800	2018	168	170	0.084	97.704	2021	-258.131	1.120296032	0.748267708	0.001120296
Peck Lake	8002	799	2018	166	168	0.095	94.385	2020	-254.979	1.225056409	0.751355744	0.001225056

A.2 Char Concentration Profiles

These charts indicate the model-predicted char concentrations throughout the depth profile for each of our 29 cores. Locations and ecotypes are included for reference purposes. Listed in ascending numerical order by core ID.

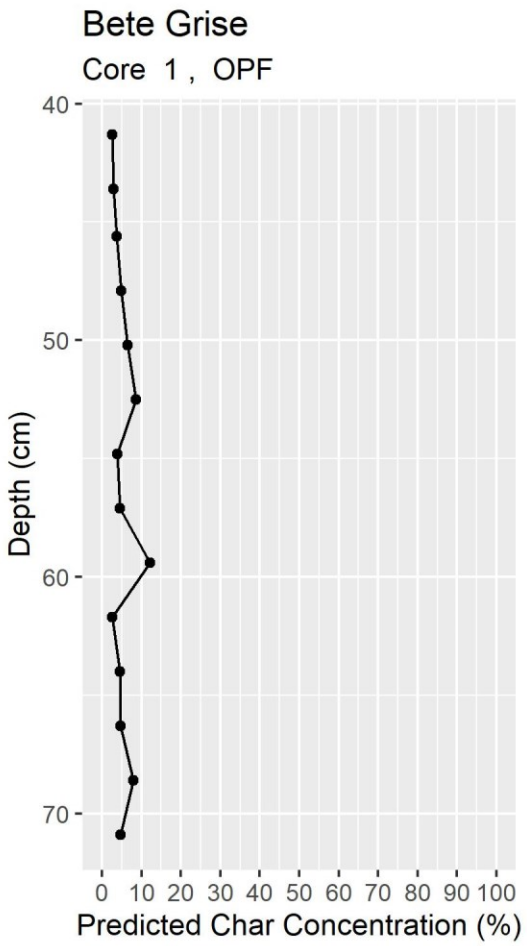
Bete Grise
Core 1 , OPF
Depth (cm)
40
50
60
70
0 10 20 30 40 50 60 70 80 90 100
Predicted Char Concentration (%)

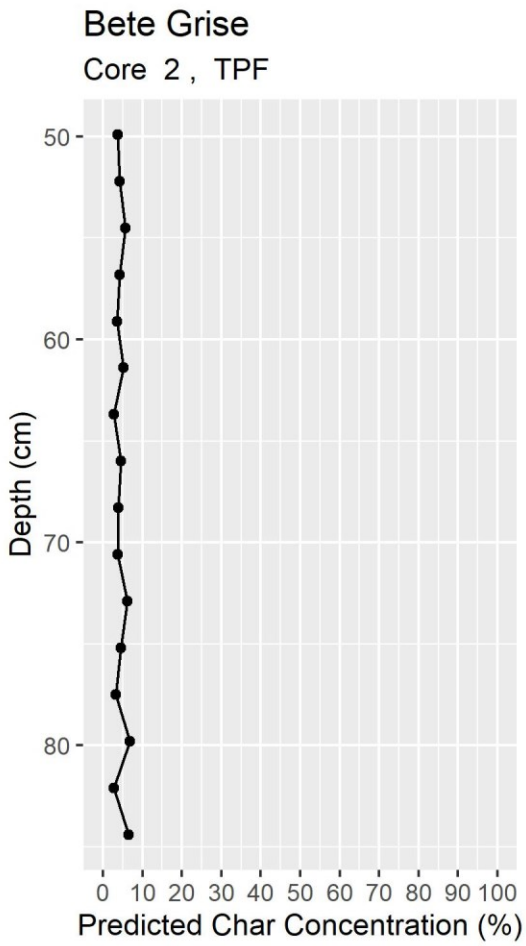
Bete Grise
Core 2 , TPF
Depth (cm)
50
60
70
80
0 10 20 30 40 50 60 70 80 90 100
Predicted Char Concentration (%)

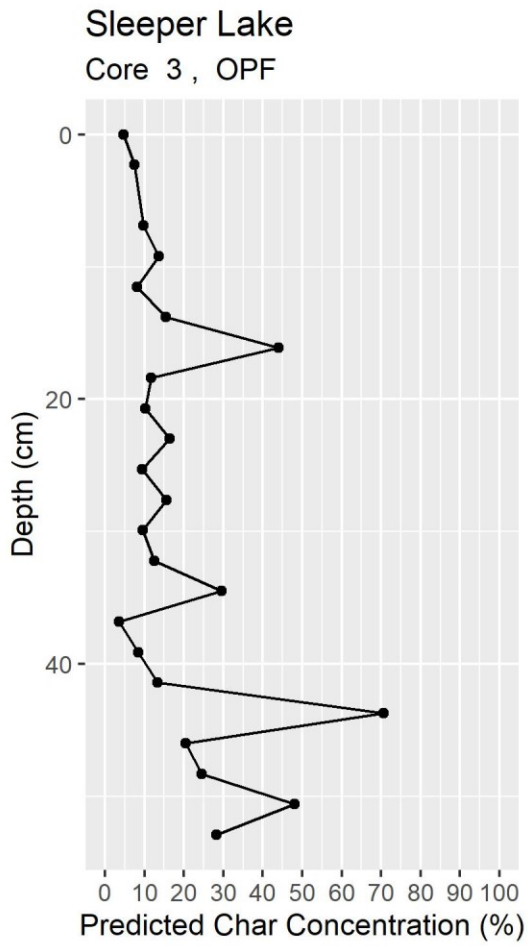
Sleeper Lake
Core 3 , OPF
Depth (cm)
0
20
40
0 10 20 30 40 50 60 70 80 90 100
Predicted Char Concentration (%)

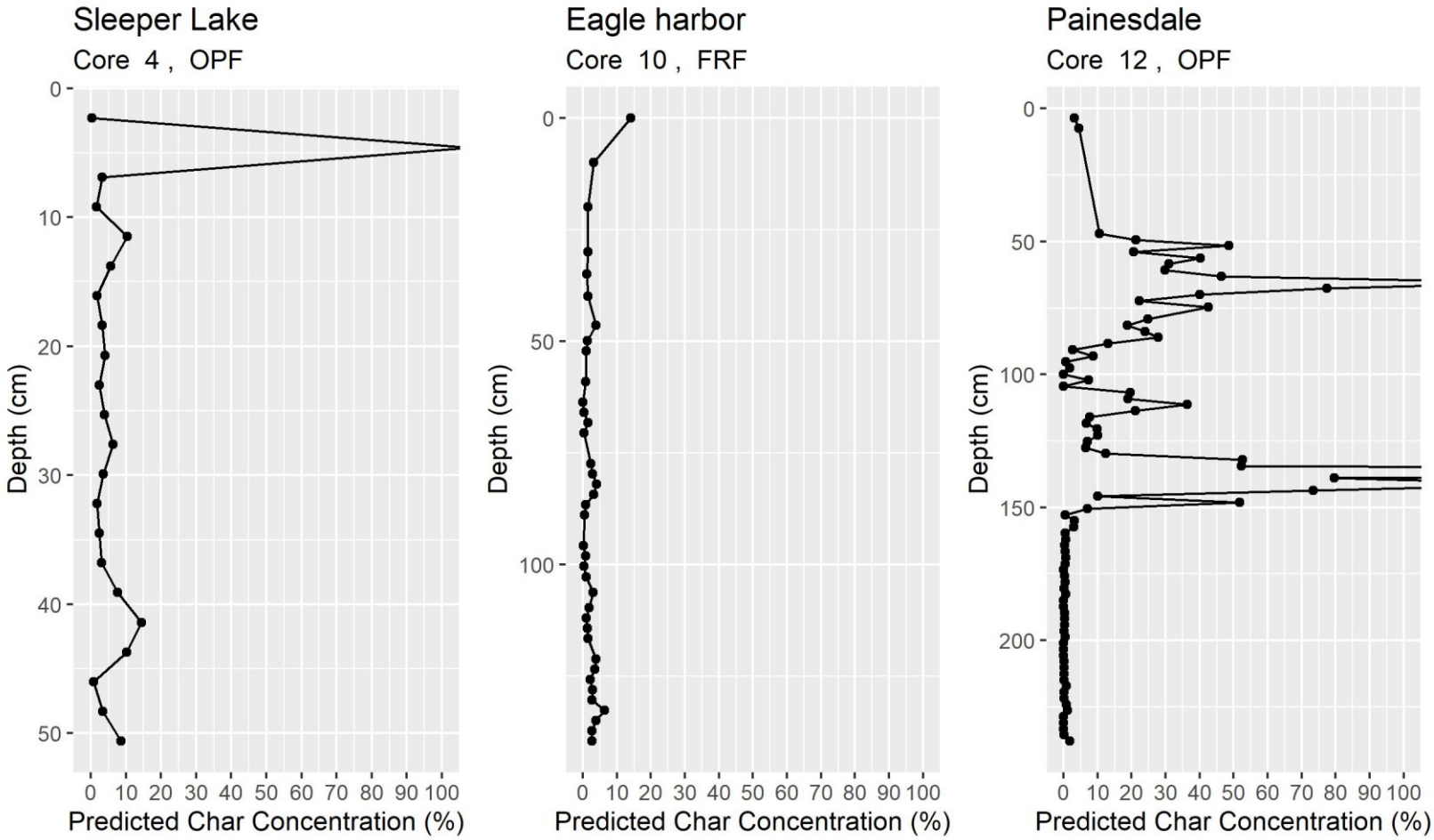
Sleeper Lake
Core 4 , OPF
Depth (cm)
0
10
20
30
40
50
0 10 20 30 40 50 60 70 80 90 100
Predicted Char Concentration (%)
Eagle harbor
Core 10 , FRF
Depth (cm)
0
50
100
0 10 20 30 40 50 60 70 80 90 100
Predicted Char Concentration (%)
Painesdale
Core 12 , OPF
Depth (cm)
0
50
100
150
200
0 10 20 30 40 50 60 70 80 90 100
Predicted Char Concentration (%)

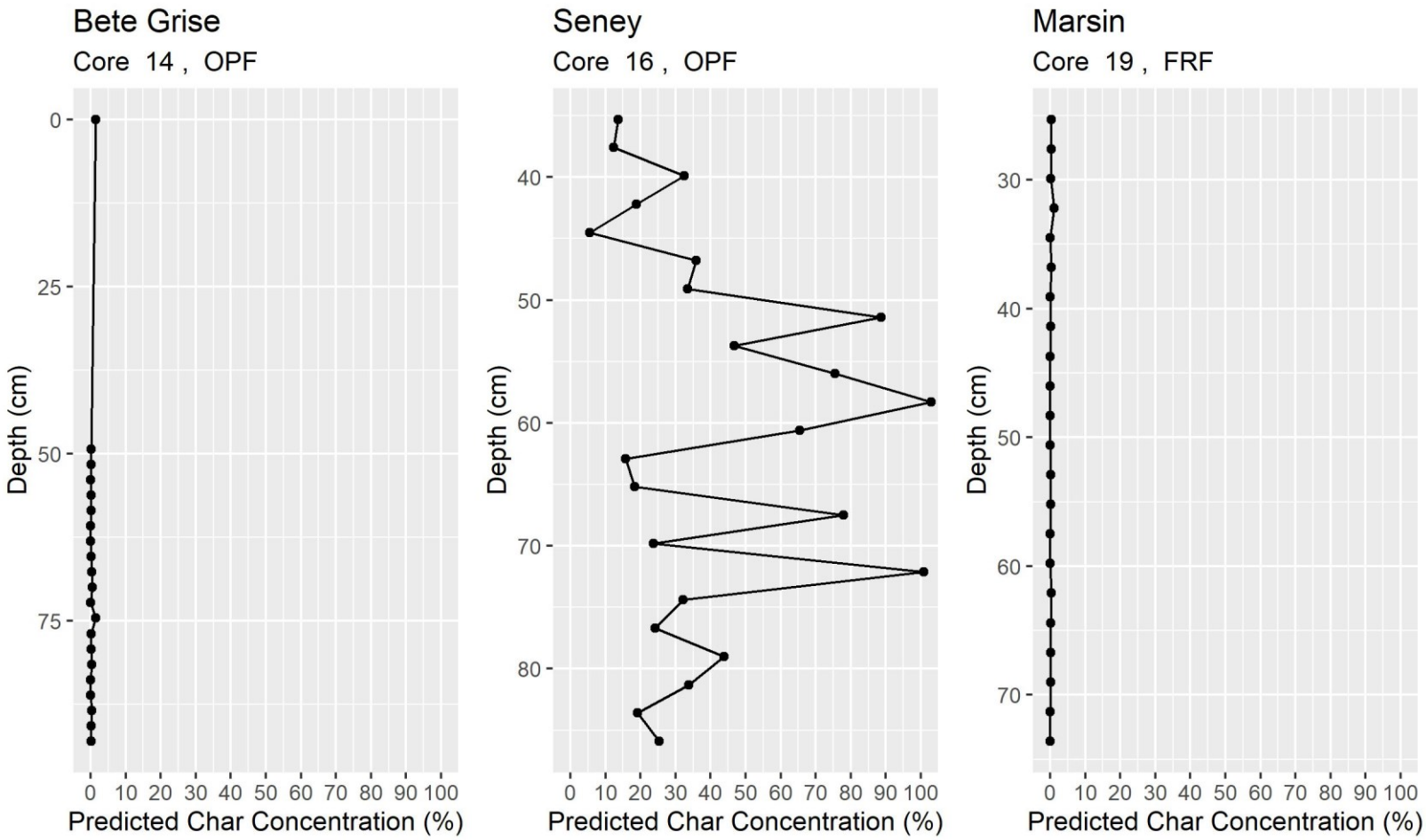
Bete Grise
Core 14 , OPF
Depth (cm)
0
25
50
75
0 10 20 30 40 50 60 70 80 90 100
Predicted Char Concentration (%)
Seney
Core 16 , OPF
Depth (cm)
40
50
60
70
80
0 10 20 30 40 50 60 70 80 90 100
Predicted Char Concentration (%)
Marsin
Core 19 , FRF
Depth (cm)
30
40
50
60
70
0 10 20 30 40 50 60 70 80 90 100
Predicted Char Concentration (%)

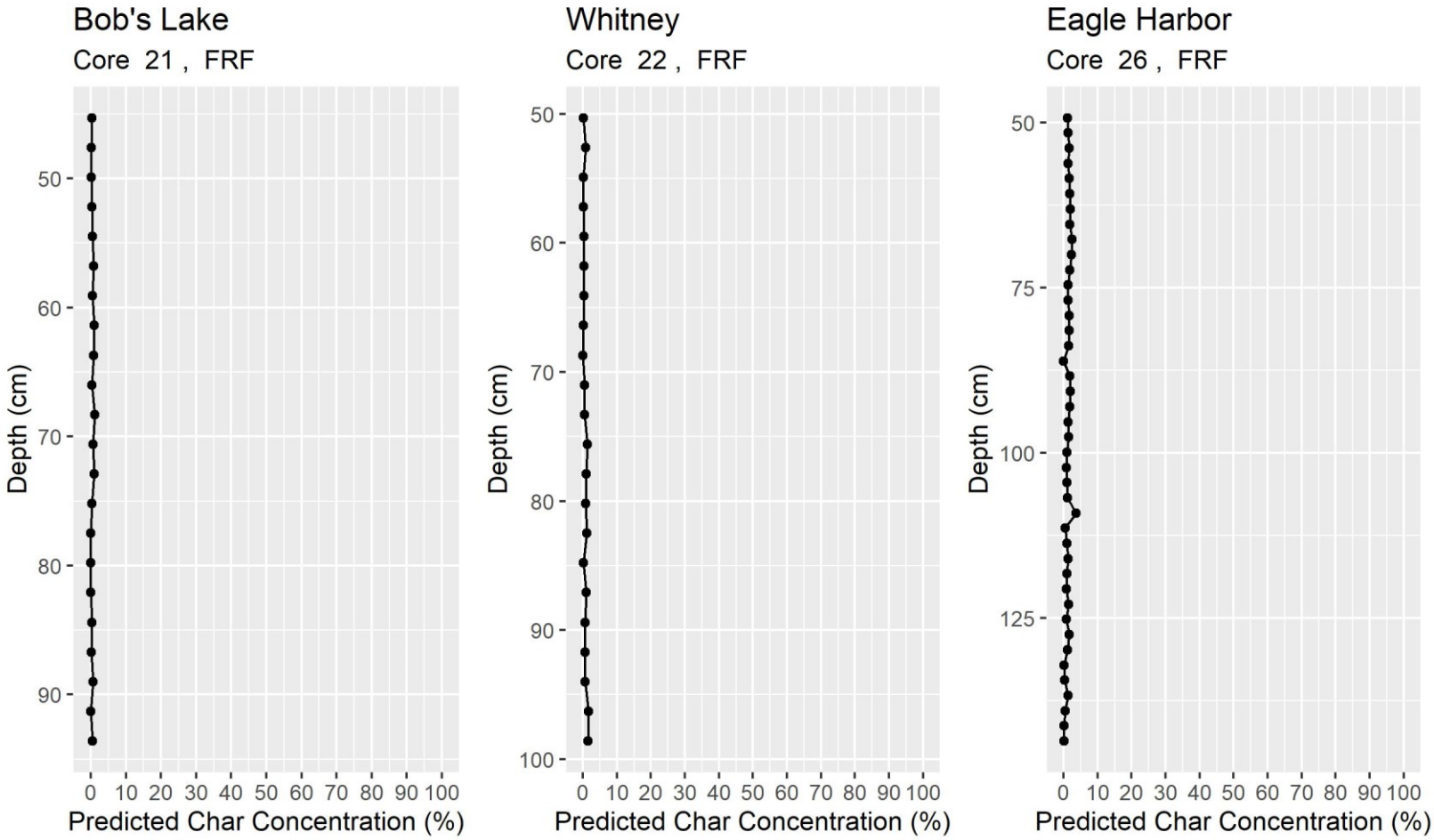
Bob's Lake
Core 21 , FRF
Depth (cm)
50
60
70
80
90
0 10 20 30 40 50 60 70 80 90 100
Predicted Char Concentration (%)
Whitney
Core 22 , FRF
Depth (cm)
50
60
70
80
90
100
0 10 20 30 40 50 60 70 80 90 100
Predicted Char Concentration (%)
Eagle Harbor
Core 26 , FRF
Depth (cm)
50
75
100
125
0 10 20 30 40 50 60 70 80 90 100
Predicted Char Concentration (%)

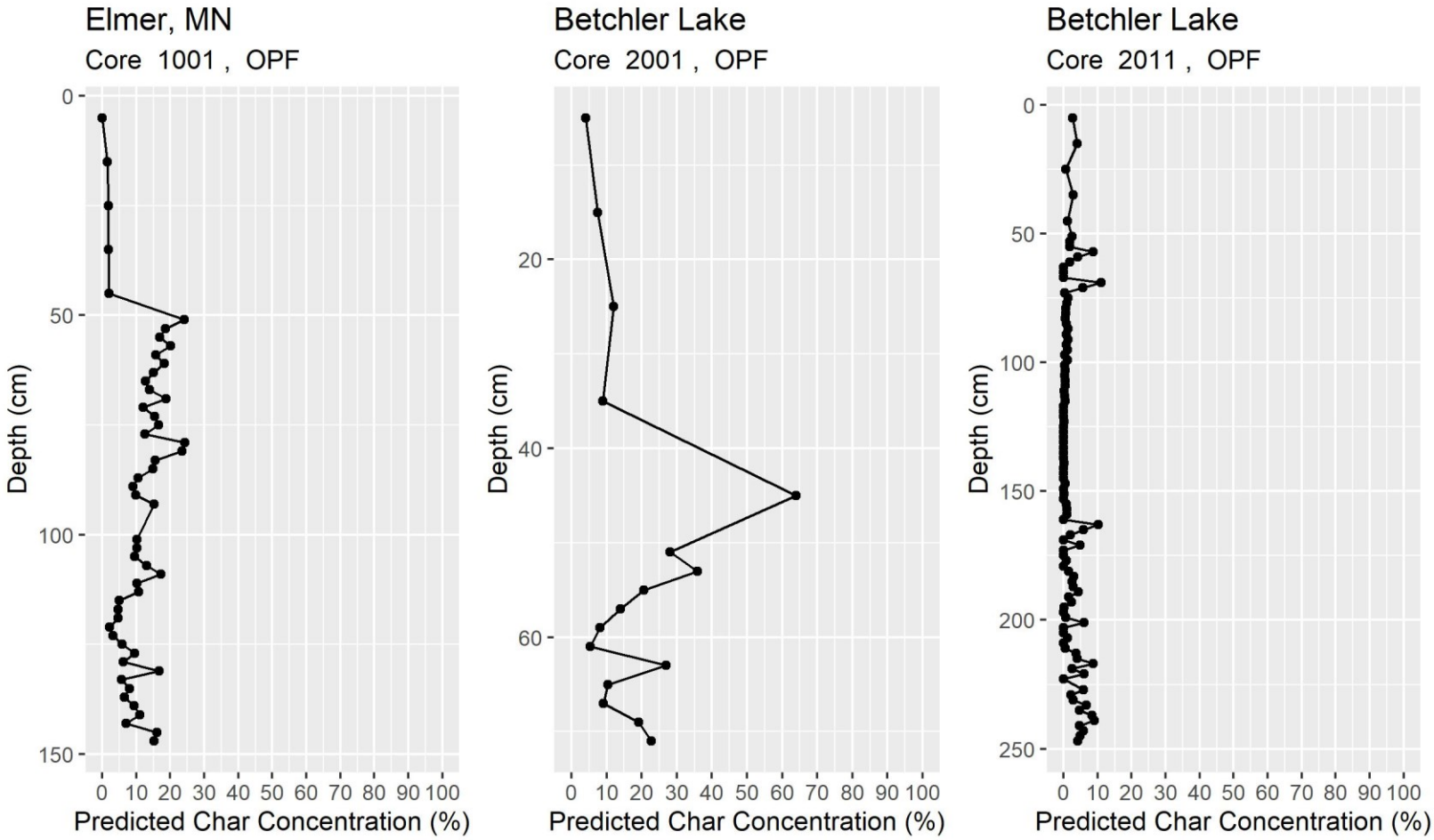
Elmer, MN
Core 1001 , OPF
Depth (cm)
0
50
100
150
0 10 20 30 40 50 60 70 80 90 100
Predicted Char Concentration (%)
Betchler Lake
Core 2001 , OPF
Depth (cm)
20
40
60
0 10 20 30 40 50 60 70 80 90 100
Predicted Char Concentration (%)
Betchler Lake
Core 2011 , OPF
Depth (cm)
0
50
100
150
200
250
0 10 20 30 40 50 60 70 80 90 100
Predicted Char Concentration (%)

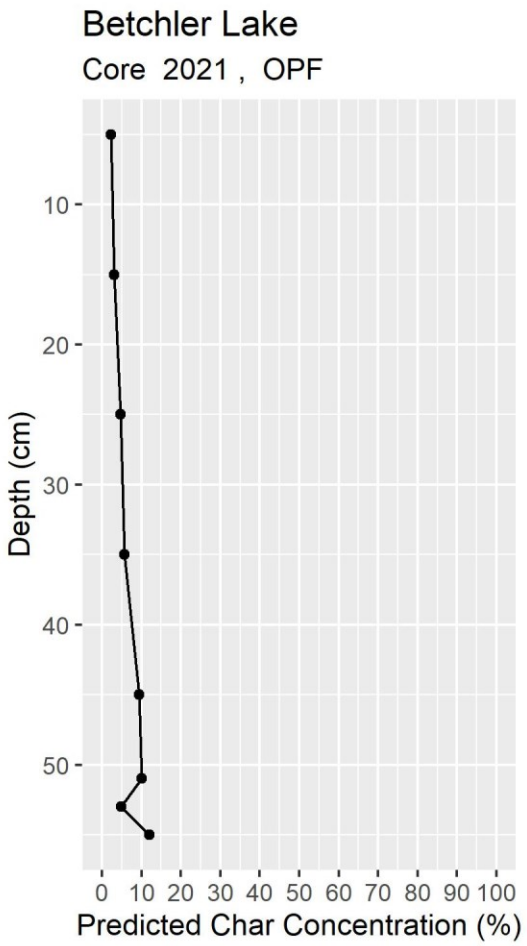
Betchler Lake
Core 2021 , OPF
Depth (cm)
10
20
30
40
50
0 10 20 30 40 50 60 70 80 90 100
Predicted Char Concentration (%)

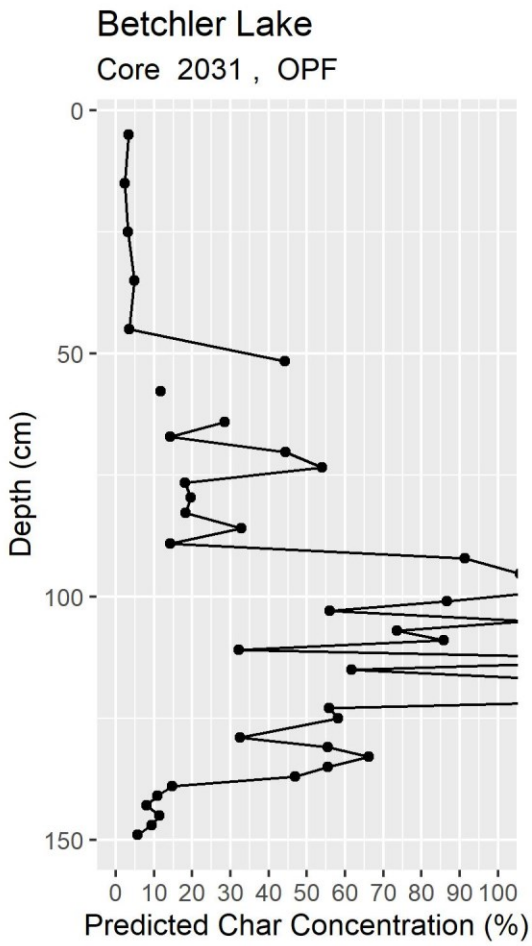
Betchler Lake
Core 2031 , OPF
Depth (cm)
0
50
100
150
0 10 20 30 40 50 60 70 80 90 100
Predicted Char Concentration (%)

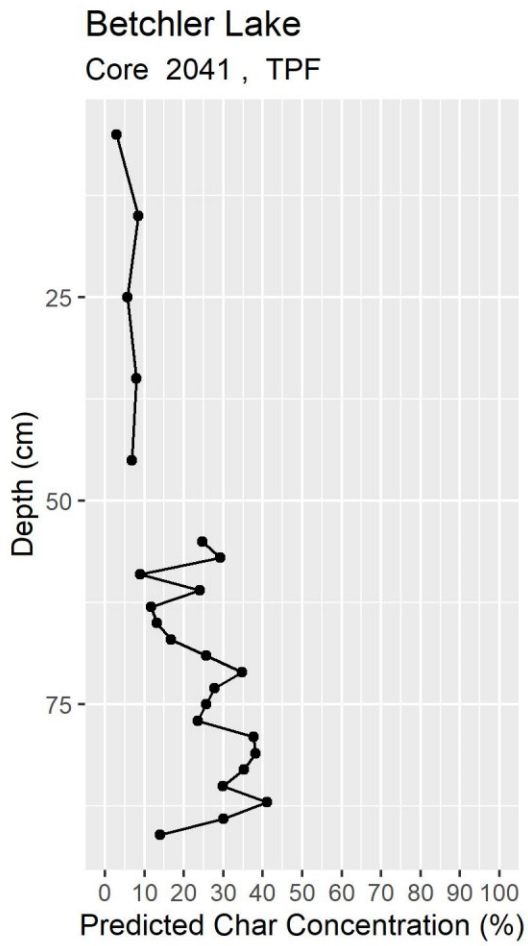
Betchler Lake
Core 2041 , TPF
Depth (cm)
25
50
75
0 10 20 30 40 50 60 70 80 90 100
Predicted Char Concentration (%)

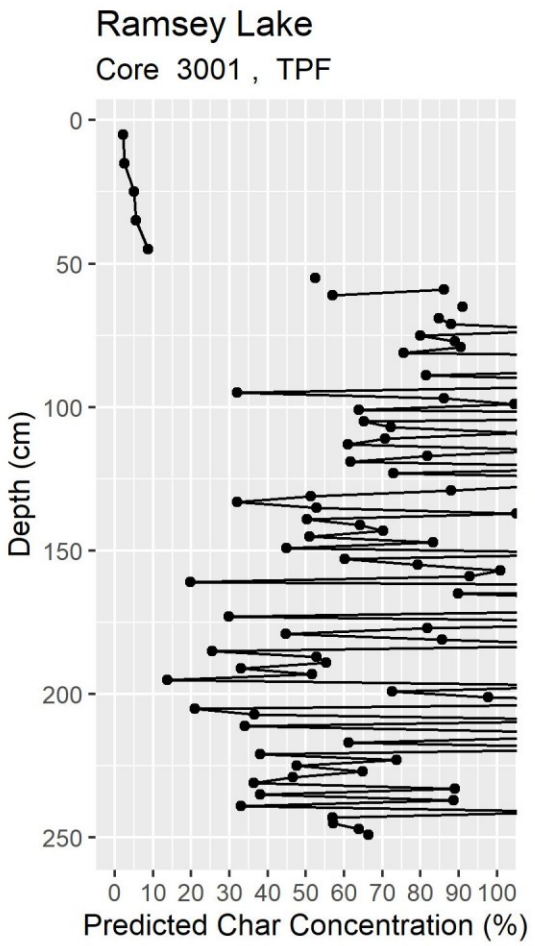
Ramsey Lake
Core 3001 , TPF
Depth (cm)
0
50
100
150
200
250
0 10 20 30 40 50 60 70 80 90 100
Predicted Char Concentration (%)

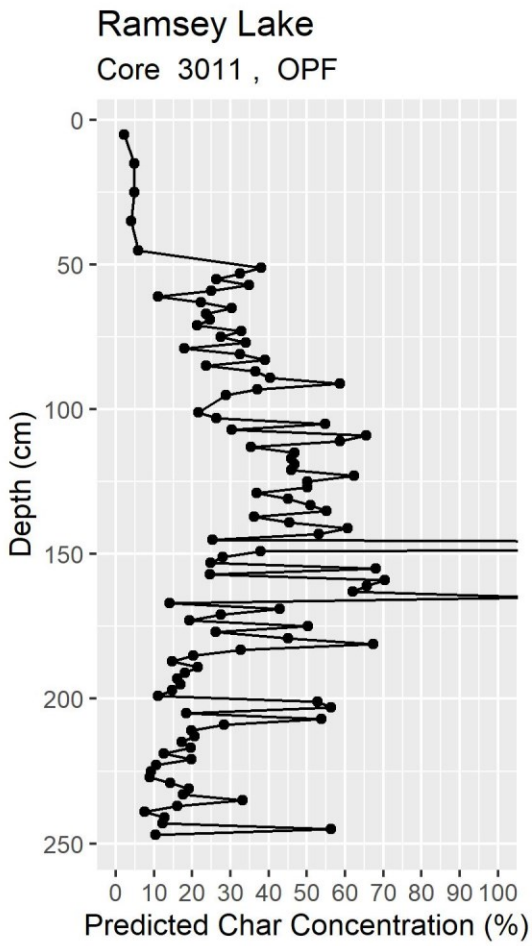
Ramsey Lake
Core 3011 , OPF
Depth (cm)
0
50
100
150
200
250
0 10 20 30 40 50 60 70 80 90 100
Predicted Char Concentration (%)

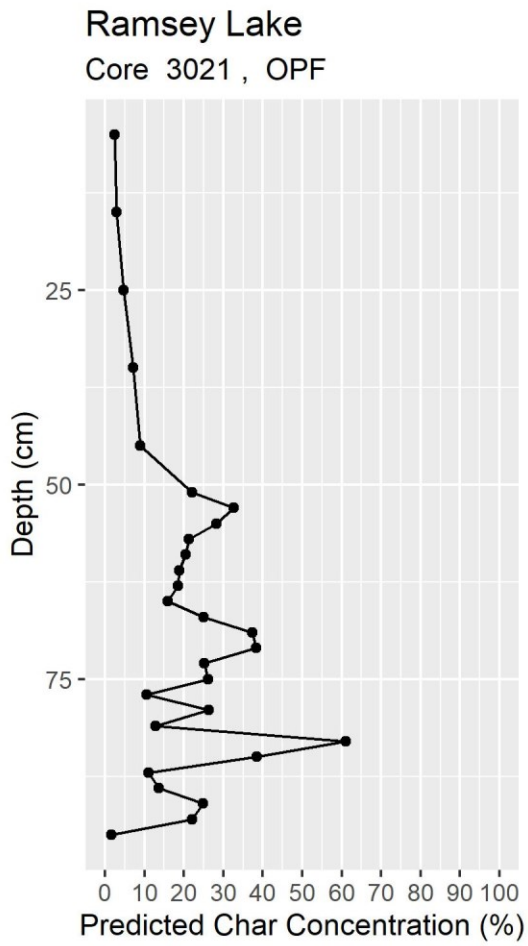
Ramsey Lake
Core 3021 , OPF
Depth (cm)
25
50
75
0 10 20 30 40 50 60 70 80 90 100
Predicted Char Concentration (%)

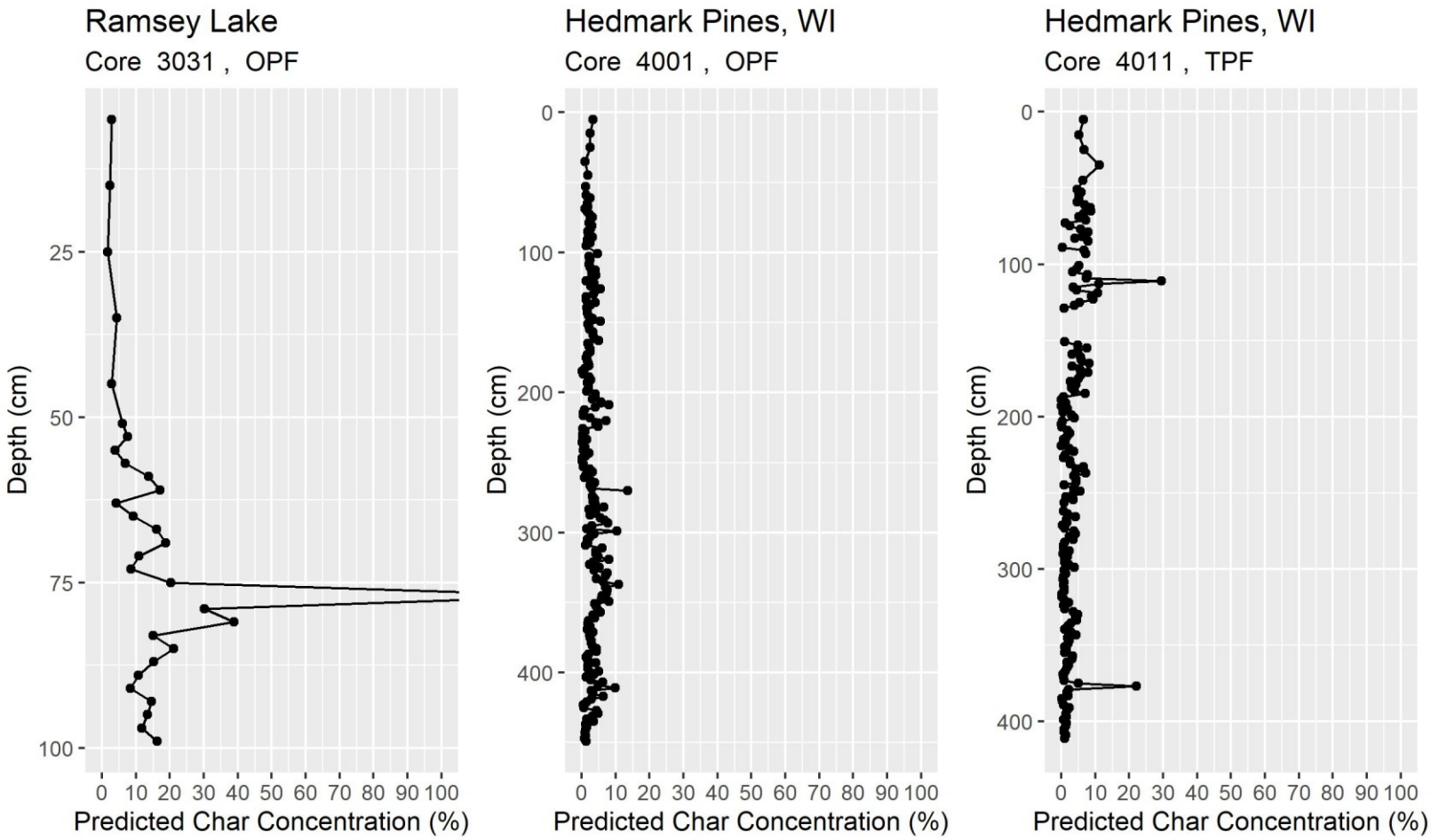
Ramsey Lake
Core 3031 , OPF
Depth (cm)
25
50
75
100
0 10 20 30 40 50 60 70 80 90 100
Predicted Char Concentration (%)
Hedmark Pines, WI
Core 4001 , OPF
Depth (cm)
0
100
200
300
400
0 10 20 30 40 50 60 70 80 90 100
Predicted Char Concentration (%)
Hedmark Pines, WI
Core 4011 , TPF
Depth (cm)
0
100
200
300
400
0 10 20 30 40 50 60 70 80 90 100
Predicted Char Concentration (%)

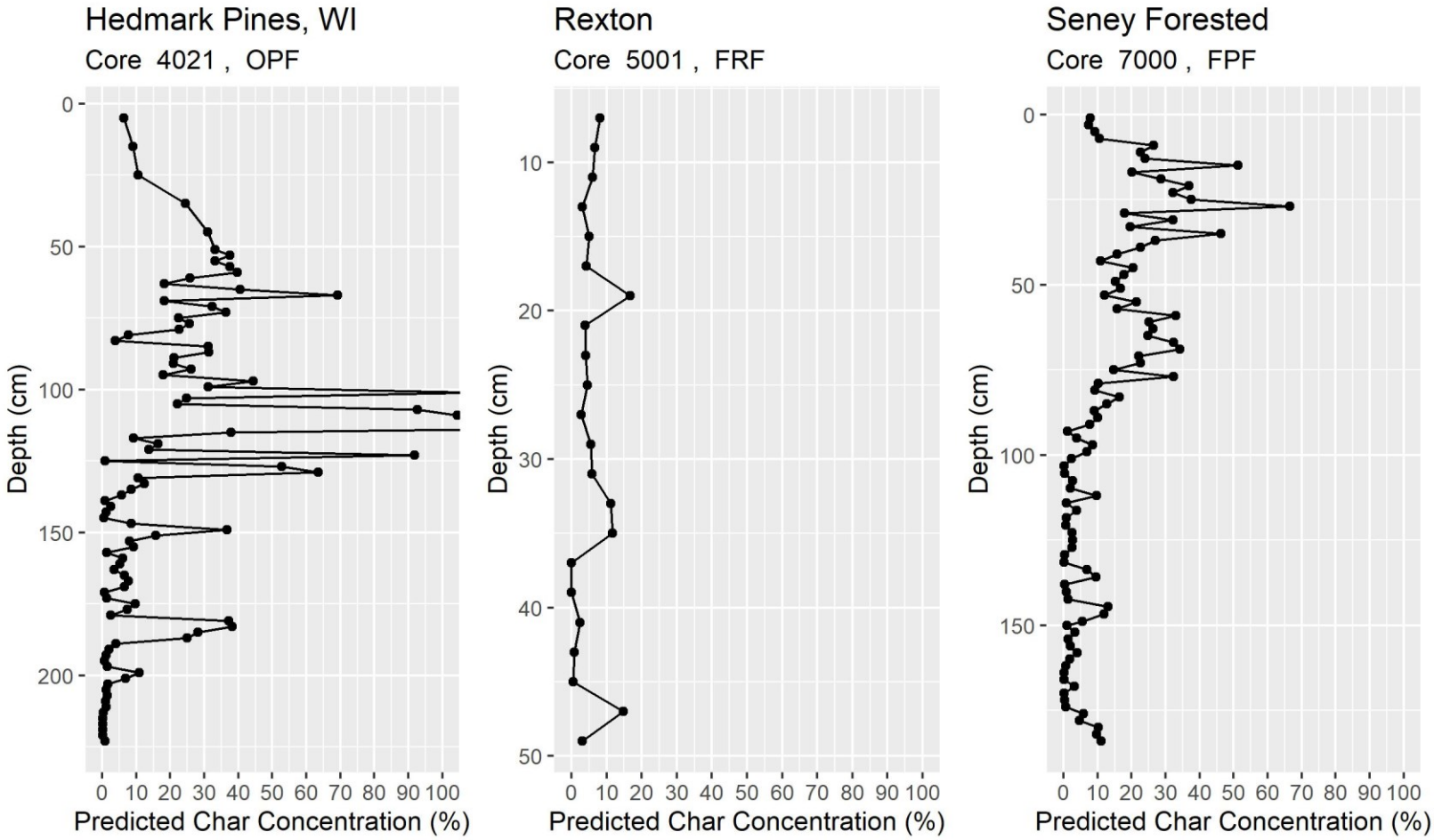
Hedmark Pines, WI
Core 4021 , OPF
Depth (cm)
0
50
100
150
200
0 10 20 30 40 50 60 70 80 90 100
Predicted Char Concentration (%)
Rexton
Core 5001 , FRF
Depth (cm)
10
20
30
40
50
0 10 20 30 40 50 60 70 80 90 100
Predicted Char Concentration (%)
Seney Forested
Core 7000 , FPF
Depth (cm)
0
50
100
150
0 10 20 30 40 50 60 70 80 90 100
Predicted Char Concentration (%)

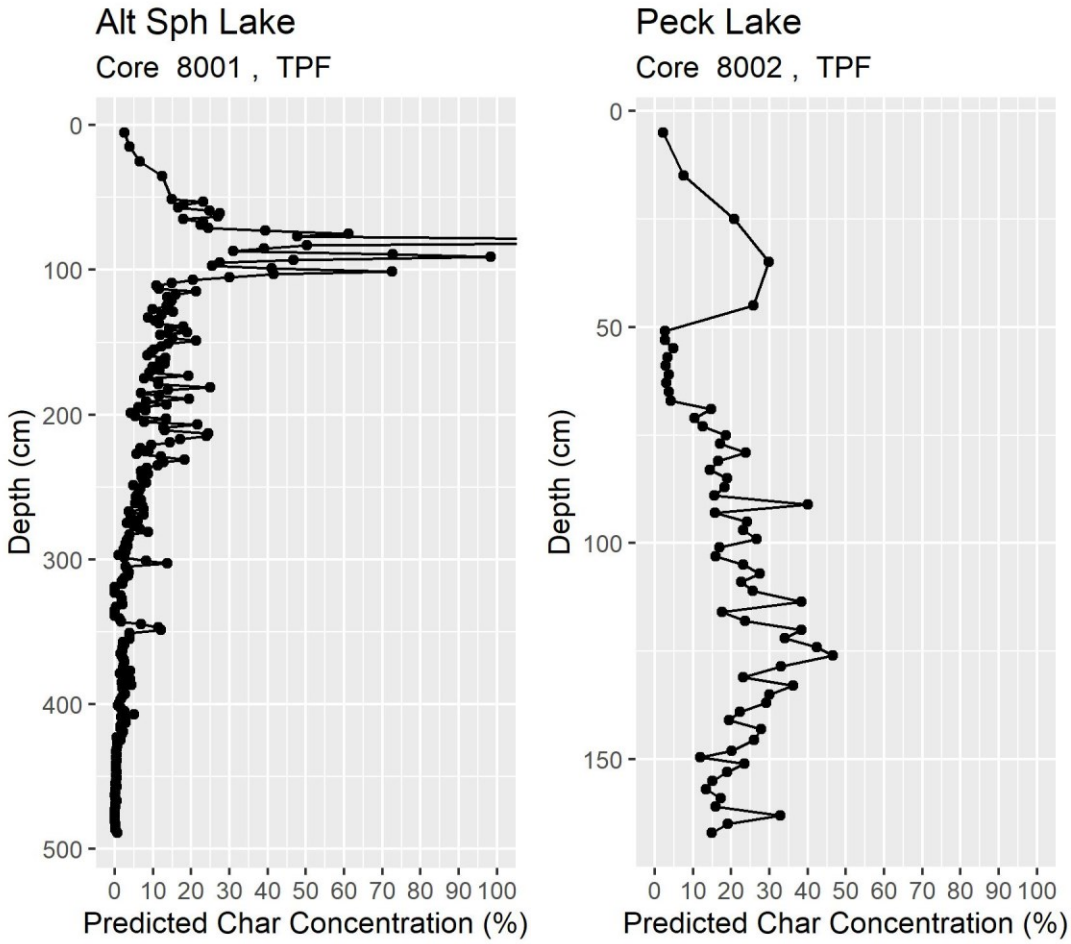
Alt Sph Lake
Core 8001 , TPF
Depth (cm)
0
100
200
300
400
500
0 10 20 30 40 50 60 70 80 90 100
Predicted Char Concentration (%)
Peck Lake
Core 8002 , TPF
Depth (cm)
0
50
100
150
0 10 20 30 40 50 60 70 80 90 100
Predicted Char Concentration (%)